

62-72346

N 63 20537

162-1

TECHNICAL MEMORANDUM

X-522

HEAT-TRANSFER AND PRESSURE MEASUREMENTS OF A
1/7-SCALE MODEL OF A MERCURY CAPSULE AT ANGLES OF ATTACK
FROM 0° TO $\pm 20^{\circ}$ AT MACH NUMBERS OF 3.50 AND 4.44

By Nancy L. Taylor, Ward F. Hodge,
and Paige B. Burbank

Langley Research Center
Langley Field, Va.

CLASSIFICATION CHANGED FROM
CONFIDENTIAL TO UNCLASSIFIED--
AUTHORITY NASA CON 5-EFFECTIVE
17 JULY 63, JIM CARROLL
DOC. INC.

OTS PRICE

XEROX \$
MICROFILM \$

NATIONAL AERONAUTICS AND SPACE ADMINISTRATION
WASHINGTON

June 1961

DECLASSIFIED**NATIONAL AERONAUTICS AND SPACE ADMINISTRATION****TECHNICAL MEMORANDUM X-522****HEAT-TRANSFER AND PRESSURE MEASUREMENTS OF A****1/7-SCALE MODEL OF A MERCURY CAPSULE AT ANGLES OF ATTACK****FROM 0° TO $\pm 20^\circ$ AT MACH NUMBERS OF 3.50 AND 4.44***

L
1
0
2
2
By Nancy L. Taylor, Ward F. Hodge,
and Paige B. Burbank

SUMMARY

Heat-transfer and pressure coefficients were obtained on the reentry, exit, and escape configurations of a 1/7-scale model of a Mercury capsule. The model was tested through an angle-of-attack (α) range of 0° to $\pm 20^\circ$ at Mach numbers (M) of 3.50 and 4.44 and a Reynolds number range, based on maximum diameter, of 2.0×10^6 to 4.0×10^6 .

In the reentry configuration the Stanton numbers on the hemispherical heat shield could be predicted by Lees' theory by using measured pressures. At $\alpha = 0^\circ$ the separated flow from the shoulder of the hemispherical heat shield reattaches on the parachute canister and the resultant Stanton numbers are approximately 85 percent of the maximum measured Stanton numbers on the hemispherical heat shield at $M = 3.50$ and approximately 60 percent at $M = 4.44$. On the windward side of the parachute canister at an angle of attack of 15° , the maximum Stanton numbers at $M = 3.50$ are approximately 90 percent of the maximum Stanton numbers on the hemispherical heat shield and approximately 80 percent at $M = 4.44$.

In the exit configuration the measured Stanton numbers on the conical portion of the capsule (for $\alpha = 0^\circ$ and on the leeward side when $\alpha \neq 0^\circ$) agreed with Van Driest's turbulent theory for a flat plate based on local pressures. These Stanton numbers are of the same magnitude as those measured on the hemispherical heat shield of the reentry configuration. At angle of attack the multiple shocks of the front face, of the step between the canisters, and of the reattached flow coalesce on the windward side, and the resultant flow field with multiple vortices limits mathematical definition of the flow.

*Title, Unclassified.

0313122A1030

The tower of the escape configuration creates extreme turbulence over the entire capsule; however, the heating rates are of the same magnitude as for the exit configuration except at 15° angle of attack at $M = 4.44$. At this test condition, the maximum Stanton numbers are approximately 3 times as large as Stanton numbers on the hemispherical heat shield of the reentry configuration.

INTRODUCTION

Project Mercury is a National Aeronautics and Space Administration program for placing a manned earth satellite into orbit and subsequently retrieving it. A Mercury space capsule, evolved from a basic blunted-nose cone shape, was modified to achieve minimum weight without seriously affecting its stability and other aerodynamic characteristics. The prerequisite of minimum weight necessitates definition of the local heat transfer to the capsule shell in all configurations: reentry, exit, and escape. The prediction of heat transfer by theoretical means is limited by the irregular capsule shape and the resultant undefined flow field. Consequently heat-transfer coefficients and corresponding pressure coefficients were experimentally obtained in Langley Unitary Plan wind tunnel for an angle-of-attack range of 0° to $\pm 20^\circ$ at Mach numbers of 3.50 and 4.44 and a Reynolds number range, based on maximum diameter, of 2.0×10^6 to 4.0×10^6 .

SYMBOLS

b wall thickness, in.

C_p pressure coefficient based on free-stream conditions,

$$C_p = \frac{P_l - P_\infty}{q_\infty}$$

c_p specific heat of air, Btu/lb-°R

c_w specific heat of skin, Btu/lb-°R (0.100 for Inconel, 0.105 for nickel)

g acceleration due to gravity, ft/sec²

h heat-transfer coefficient, Btu/sq ft-sec-°R (eq. (2))

L
1
0
2
2

DECLASSIFIED

3

h_c	heat-transfer coefficient considering conduction, Btu/sq ft-sec-°R (eq. (3))
K	thermal conductivity of Inconel, 0.00241 Btu/ft-sec-°R
M	free-stream Mach number
n	time limit of integration, sec
N_{St}	Stanton number based on free-stream conditions, $h/\rho_\infty V_\infty c_p g$
p_l	local static pressure, lb/sq ft abs
p_∞	free-stream static pressure, lb/sq ft abs
q_∞	free-stream dynamic pressure, lb/sq ft abs
r	radial distance, in. (fig. 3)
R	free-stream Reynolds number based on capsule maximum diameter (10.64 in.)
t	time, sec
T_e	equilibrium temperature, °R
T_t	stagnation temperature, °R
T_w	wall temperature, °R
$T_{w,n}$	wall temperature at time greater than zero, °R
$T_{w,0}$	wall temperature at zero time, °R
V_∞	free-stream velocity, ft/sec
W	specific weight for Inconel skin, 530.5 lb/cu ft
w	weight per unit area, $w = Wb/12$, lb/sq ft
x	longitudinal distance, in. (fig. 3)
x_1	surface distance measured in a plane perpendicular to the body central axis, ft

0319122A1030

4

- y_1 surface distance measured in a plane containing the body central axis, ft
- α angle of attack, deg
- ϕ meridian angle, deg
- ρ_∞ density of air based on free-stream conditions, slugs/cu ft
- λ Newtonian flow angle (included angle of surface with a plane perpendicular to flow), deg

L
1
0
2
2

APPARATUS AND MODEL

Tests were conducted in the high Mach number test section of the Langley Unitary Plan wind tunnel. This test section has an asymmetrical sliding-block nozzle which permits continuous variation of Mach number from 2.29 to 4.65 and is described in reference 1. The maximum deviation for the Mach numbers over the entire 4-foot by 4-foot test section is ± 0.05 for a Mach number of 3.50 and ± 0.06 for a Mach number of 4.44. The procedure for conducting heat-transfer tests is described in reference 2.

A 1/7-scale model of a Mercury capsule was constructed with interchangeable components to permit testing of the reentry, exit, and escape configurations. Evaluation of the heat-transfer coefficient from transient wall-temperature measurements necessitates thin-walled construction; therefore, with the exception of the flow diverter and the camera fairings on the parachute canister, the capsule shell was constructed by spinning a 0.030-inch Inconel sheet on a form mandrel. The camera fairings were formed from 0.030-inch Inconel and silver soldered to the capsule shell; the flow diverter was electroplated nickel with a 0.015-inch nominal skin thickness. Internal conduction was minimized by the use of only two internal bulkheads constructed of Transite; the bulkheads were relieved in the vicinity of the thermocouples. Internal convection was minimized by venting the shell interior to free-stream static pressure. Radiation losses were minimized by polishing the model to a 10-microinch-rms finish. A sketch of the model configuration is shown in figure 1 and photographs in figure 2. In the exit-configuration photograph the model has been rotated 90° to illustrate the shape of the flow diverter.

The capsule model was instrumented with both thermocouples and static pressure orifices. The thermocouples were located along 3 meridian lines

DECLASSIFIED

5

L
1
0
2
2

of 0° , 45° , and 90° as illustrated in figure 3, and to prevent interference of pressure instrumentation on thermocouples, the pressure orifices were located in the diametrically opposite quadrant along 3 meridian lines of 180° , 225° , and 270° . The locations of the 55 30-gage iron-constantan thermocouples and the 49 static pressure orifices are shown in figure 3. The wall thickness for each thermocouple is listed in table I. The capsule was symmetrical except for the presence of the flow diverter on the flat face of the exit configuration and the tower in the escape configuration. The model was tested at both positive and negative angles of attack to obtain both windward and leeward heat-transfer and pressure distributions.

The thermocouple output was recorded on the multichannel sequential analog to digital converter discussed in reference 2. Pressure measurements were made by connecting the orifices to valves which sample 48 pressures in sequence on a single transducer. The transducer output is recorded on digitized self-balancing potentiometers for machine calculations. The free-stream and stagnation pressures were measured on precision manometers.

TEST CONDITIONS

Heat-transfer coefficients and pressure coefficients were determined for a natural boundary-layer transition for the following test conditions:

Configuration	α , deg	$M = 3.50$		$M = 4.44$	
		Stagnation pressure, lb/sq in. abs	Reynolds number, R	Stagnation pressure, lb/sq in. abs	Reynolds number, R
Reentry	0, ± 5 , ± 10 , ± 15	36	2.5×10^6	57	2.7×10^6
Exit	0, ± 5 , ± 10 , ± 15 , ± 20	57	4.0	40	2.0
Escape	0, ± 5 , ± 10 , ± 15	57	4.0	40	2.0

Schlieren photographs and shadowgraphs were taken at several of the test conditions.

A comparison of a typical Mercury capsule trajectory and the tunnel test conditions is shown in figure 4 for the reentry and exit configurations.

ACCURACY

The accuracy of the temperature measurements including recorder resolution, thermocouple wire calibration, and cold junction is $\pm 2^\circ F$; however, this error will occur in temperature level rather than random temperature fluctuations. A temperature error of $\pm 2^\circ F$ could result in ratios of equilibrium temperature to stagnation temperature (T_e/T_t) greater than 1 in stagnation regions of the model. In regions of low heat transfer (h less than 0.001) the ratio T_e/T_t may be questionable, because the wall temperature has not reached equilibrium from the preceding test point.

An estimated accuracy of heat-transfer coefficient determined by the repeatability of data is dependent upon the magnitude of the heat-transfer coefficient. For heat-transfer coefficients greater than 0.0150 the accuracy is within 10 percent; for heat-transfer coefficients from 0.0010 to 0.0150, within 15 percent; and for heat-transfer coefficients less than 0.0010, within 20 percent. Although heat-transfer coefficients from 0.0003 to 0.0010 are within the accuracy of data reduction, no significance is attached to their magnitude other than to indicate the low-heat-transfer regions. Heat-transfer coefficients less than 0.0003 have been deleted and denoted as LOW to indicate that these values were measured but were of small magnitude.

The accuracy of the precision manometers is within 0.5 lb/sq ft. Therefore, the accuracy of the pressure measurement is limited to that of the electrical transducer which is 0.5 percent of full-scale deflection. In order to increase the accuracy of the pressure data both 5- and 15-lb/sq in. electrical transducers were used. The regions of the model where each transducer was used and the corresponding maximum error in the pressure coefficient is listed in the following table:

Configuration	Transducer used, lb/sq in.	$M = 3.50$		$M = 4.44$	
		R	ΔC_p	R	ΔC_p
Reentry: Hemispherical heat shield	15	2.5×10^6	± 0.0185	2.7×10^6	± 0.0256
	5		$\pm .0062$		$\pm .0085$
Exit and escape: Hemispherical heat shield	5	4.0	$\pm .0039$	2.0	$\pm .0122$
	15		$\pm .0117$		$\pm .0365$

REF ID: A6572
DECLASSIFIED

7

METHOD OF HEAT-TRANSFER DATA REDUCTION

The heat-transfer coefficients were obtained from transient skin-temperature measurements resulting from a stepwise increase in stagnation temperature as shown in reference 2. The following relation, which assumes constant temperature through the skin, negligible lateral heat flow, negligible heat flow to the model interior, and no losses due to radiation, was used:

L
1
0
2
2

$$h = \frac{wc_w(dT_w/dt)}{T_e - T_w} \quad (1)$$

Equation (1) is written in the following form for complete machine calculation:

$$h = \frac{wc_w(T_{w,n} - T_{w,0})}{\frac{T_e}{T_t} \sum_{t=0}^{t=n} T_t - \sum_{t=0}^{t=n} T_w} \quad (2)$$

The summations are evaluated over increments of time according to the trapezoidal rule and the ratio T_e/T_t is experimentally determined.

The location of thermocouples prevented the evaluation of lateral conduction losses for some thermocouples. However, where possible the heat-transfer coefficients were also calculated from the following relation:

$$h_c = \frac{\frac{wc_w(T_{w,n} - T_{w,0})}{Kb} - \sum_{t=0}^{t=n} \left(\frac{\partial^2 T_w}{\partial x_1^2} + \frac{\partial^2 T_w}{\partial y_1^2} \right)}{\frac{T_e}{T_t} \sum_{t=0}^{t=n} T_t - \sum_{t=0}^{t=n} T_w} \quad (3)$$

A statistical comparison of the results of equations (2) and (3) for three angles of attack on the three model configurations indicated the standard deviation was less than 3.5 percent for $M = 3.50$ and less than 6.7 percent for $M = 4.44$; therefore, the results of equation (3) are not presented.

PRESENTATION OF RESULTS

The results of the pressure and heat-transfer measurements are presented in tabular form for each configuration. The heat-transfer measurements obtained at positive angles of attack will be denoted as leeward and those obtained at negative angles of attack will be denoted as windward. The pressure measurements obtained at positive angles of attack will be denoted as windward and those obtained at negative angles of attack will be denoted as leeward. In order to show the location of the orifices and thermocouples on the hemispherical heat shield, on the step between the parachute and radar canisters, and on the flat face of the exit configuration, the radial distance is presented in the tables and is illustrated in figure 3. Typical pressure and Stanton number distribution plots are presented for the reentry, exit, and escape configurations with the flow direction from left to right.

Results of this investigation are presented as follows:

Table

Pressure coefficients measured on reentry configuration	II
Pressure coefficients measured on exit configuration	III
Pressure coefficients measured on escape configuration	IV
Heat-transfer measurements on reentry configuration	V
Heat-transfer measurements on exit configuration	VI
Heat-transfer measurements on escape configuration	VII

Figure

Shadowgraphs of a Mercury capsule model	5
Schlieren photographs of a Mercury capsule model	6
Effect of Mach number on pressure distribution. $\phi = 180^\circ$; $\alpha = 0^\circ$	7
Variation of Stanton numbers on the hemispherical heat shield of the reentry configuration for Newtonian flow angle	8
Effect of Mach number on Stanton number distribution at $\phi = 0^\circ$ and angles of attack of 0° and $\pm 15^\circ$	9
Effect of tower on Stanton number distribution at $\phi = 0^\circ$ and angles of attack of 0° and $\pm 15^\circ$	10

DISCUSSION

Shadowgraphs and Schlieren Photographs

In the analysis of the distribution of local heat-transfer coefficients on any body a pressure distribution and a knowledge of the flow

DECLASSIFIED

9

L
1
0
2

field are desirable. The flow field of a Mercury capsule with regions of multiple intersecting shocks, unsteady flow, and regions of flow separation deviates from the normal flow field of axisymmetric bodies and makes questionable the application of any existent theories to the prediction of local heat-transfer coefficient. Typical shadowgraphs of the three configurations are presented in figure 5 and schlieren photographs in figure 6.

In the reentry configuration at an angle of attack of 0° , the separated flow from the shoulder of the hemispherical heat shield reattaches on the parachute canister (fig. 6(a)) and the resultant wavy shock is indicative of unsteady flow. As the angle of attack is increased the region of separated flow on the windward side decreases, stable reattachment occurs on the conical portion of the capsule, and a second shock occurs at the junction of the conical surface and the parachute canister. The flow on the leeward side of the model is separated for all angles of attack.

In the exit configuration the forward-facing step between the radar and parachute canisters causes a large unstable region of flow separation and very thick turbulent boundary layer on the conical portion of the body. The shoulder of the hemispherical heat shield also produces separated flow on the conical section. An overlay of the shock pattern for both the 20° and the -20° angle of attack at $M = 4.44$ (illustrated in figs. 5(h) and 5(i)) indicates that the visible effect of the flow diverter is confined to the front face and the remaining flow field is essentially similar. At an angle of attack of 20° (with the flow diverter on the windward portion of the surface) a high-density separation occurs on the leeward portion of the front face. The multiple shocks of the front face, of the step between the canisters, and of the reattached flow coalesce, and the resultant flow field with multiple vortices limits mathematical definition of the flow.

The tower of the escape configuration creates extreme turbulence and unstable flow over the entire capsule at low angles of attack and further complicates the flow field as discussed for the exit configuration.

Pressure Distribution

The variation of pressure coefficient along the 180° meridian line for each configuration at $\alpha = 0^\circ$ and $M = 3.50$ and 4.44 is illustrated in figure 7. The pressures on the hemispherical heat shield of the reentry configuration were only measured at $M = 3.50$. These pressures are in fair agreement with modified Newtonian pressure distribution. Pressures measured on the hemispherical heat shield of the reentry

configuration were directly applicable to heat-transfer calculations. For theoretical heat-transfer calculations, the assumption is made that the asymmetry of the flow in the exit configuration (due to the flow diverter) has a negligible effect on the pressures, and the pressures obtained on the conical portion of the exit configuration at $\phi = 180^\circ$, 225° , and 270° for positive angles of attack can be considered as pressures at $\phi = 0^\circ$, 45° , and 90° at negative angles of attack and thereby can be applied to heat-transfer calculation.

Heat Transfer

Windward and leeward Stanton numbers (obtained at negative and positive angles of attack) are presented for the 0° meridian line.

Reentry configuration.- The measured Stanton numbers on the zero meridian line of the hemispherical heat shield are compared in figure 8 with the theory of Lees (ref. 3) evaluated with a Sibulkin stagnation Stanton number (ref. 4). The use of a Newtonian pressure distribution in Lees' theory underestimates the measured Stanton numbers by approximately 24 percent at $M = 3.50$ and by approximately 34 percent at $M = 4.44$. Correlation, within the range of data repeatability, of measured Stanton numbers with Lees' theory is obtained by using measured pressures and these results are shown as solid symbols.

The conical portion of the body is in a region of separated flow at $\alpha = 0^\circ$ and, as shown in figure 9(a) has very low heat transfer. As determined from the schlieren photographs in figure 6(a) the separated flow reattaches on the parachute canister and the resultant Stanton numbers at $M = 3.50$ are approximately 85 percent of the Stanton numbers on the hemispherical heat shield. Stanton numbers on the radar canister are of the same magnitude as on the parachute canister; however, it is to be pointed out that the effects of the model sting support system have not been isolated and, for this reason, there is some question as to whether the heat-transfer data for the radar canister is representative of the actual Mercury configuration. At $\alpha = -15^\circ$, the overall heating along the windward meridian line of the model is generally higher than at $\alpha = 0^\circ$. The flow reattachment (as illustrated in fig. 5(d)) occurs on the conical portion of the body; however, the Stanton numbers do not exhibit a sudden increase in the region of flow reattachment. Stanton numbers on the parachute canister increase to approximately 90 percent of those on the hemispherical heat shield at $M = 3.50$.

The flow field and distribution of Stanton numbers at $M = 3.50$ and 4.44 are similar; at $M = 4.44$ the regions of high heating on the parachute canister are approximately 60 percent of the stagnation heating at $\alpha = 0^\circ$ and approximately 80 percent at $\alpha = -15^\circ$.

~~DECLASSIFIED~~

11

L
1 Exit configuration.- As previously discussed the flow field around
0 the capsule in the exit configuration is so complex that the validity
2 of applying any known theory for the prediction of local pressure or
2 heat-transfer coefficient appears questionable. However, comparison of
heat-transfer measurements on the flat face of this configuration with
the results of reference 5 indicates the effect of the flow diverter.
Also, comparison of Stanton numbers on the conical portion of the cap-
sule with flat-plate theory indicates the limitations imposed on that
theory by the strong shocks and resultant turbulence on the conical
surface.

L
1 At $\alpha = 0^\circ$ the three thermocouples on the flat face indicate that
0 the effect of the flow diverter at these locations is within the accu-
2 racy of the data. A comparison of the results of this investigation
2 with a corresponding location on the model in reference 5 indicates, as
shown in figure 9(b), that the deviation due to the flow diverter is
less than 20 percent for $M = 3.50$. At positive angles of attack the
thermocouples on the flat face are leeward of the flow diverter; how-
ever, as shadowgraphs (fig. 5(h)) indicate, a high-density separation
blankets the location of these thermocouples and the maximum Stanton
number at $\alpha = 15^\circ$ is twice as large as the value at $\alpha = 0^\circ$.

The Stanton number distribution on the conical surface (at $\alpha = 0^\circ$
and on the leeward side at $\alpha = 15^\circ$) is in good agreement with the Van
Driest turbulent theory for a flat plate (ref. 6) based on the exposed
conical length and the measured local static pressure (as discussed in
the section entitled "Pressure Distribution") and assuming a local total
head pressure corresponding to a normal shock at free-stream Mach number.
At $\alpha = -15^\circ$ the flow field on the windward side of the conical surface
cannot be theoretically duplicated, and the measured data are much
greater than predicted by theory.

Another region of localized high heat transfer occurs on the flat
face between the radar and parachute canisters (in a region of high-
density flow separation). At $\alpha = 0^\circ$ the Stanton number on this flat
face is approximately 2 times the maximum value measured on the hemi-
spherical heat shield in the reentry configuration for both Mach numbers.
At an angle of attack of -15° the maximum Stanton number is increased
to $2\frac{1}{2}$ times the maximum for the hemispherical heat shield at $M = 3.50$
and to 3 times the maximum at $M = 4.44$. Flow separation also occurs
upstream of the junction of the conical surface with the hemispherical
heat shield (see figs. 5(e) to 5(i)); however, the effect of this sepa-
ration on the Stanton number was only experimentally indicated at
 $M = 4.44$.

A comparison of the heat transfer on the hemispherical heat shield
of the reentry configuration with the heat transfer on the cone of the

0317122A1030

12

exit configuration shows that the measured Stanton numbers are of the same magnitude at $\alpha = 0^\circ$ for both Mach numbers. Angle of attack has a negligible effect on the magnitude of the Stanton number measured on the hemispherical heat shield, but has a marked effect on the windward side of the cone where the measured Stanton numbers are equal to or greater than the values measured on the hemispherical heat shield. At $\alpha = -15^\circ$ the maximum Stanton number on the cone is at least 2 times the maximum values measured on the hemispherical heat shield at both Mach numbers.

Escape configuration.- Despite the extreme turbulence generated by the escape tower, the overall Stanton number distribution is very similar to that for the exit configuration at $M = 3.50$ as illustrated in figure 10(a). However, at $M = 4.44$ an increase of Stanton number occurs on the windward conical portion of the escape configuration at $\alpha = -15^\circ$ as illustrated in figure 10(b), and the maximum Stanton number is approximately 3 times as large as the maximum Stanton number on the hemispherical heat shield in the reentry configuration.

L
1
0
2
2

SUMMARY OF RESULTS

Heat-transfer and pressure measurements were obtained on a 1/7-scale model of a Mercury capsule. Tests were made with the reentry, exit, and escape configurations of the model at angles of attack (α) from 0° to $\pm 20^\circ$ and at Mach numbers (M) of 3.50 and 4.44.

In the reentry configuration the Stanton numbers on the hemispherical heat shield could be predicted by Lees' theory by using measured pressures. At $\alpha = 0^\circ$ the separated flow from the shoulder of the hemispherical heat shield reattaches on the parachute canister and the resultant Stanton numbers are approximately 85 percent of the maximum measured Stanton numbers on the hemispherical heat shield at $M = 3.50$ and approximately 60 percent at $M = 4.44$. On the windward side of the parachute canister at an angle of attack of 15° the maximum Stanton numbers at $M = 3.50$ are approximately 90 percent of the maximum Stanton numbers on the hemispherical heat shield and approximately 80 percent at $M = 4.44$.

In the exit configuration the measured Stanton numbers on the conical portion of the capsule (for $\alpha = 0^\circ$ and on the leeward side when $\alpha \neq 0^\circ$) agreed with Van Driest's turbulent theory for a flat plate based on local pressures. These Stanton numbers are of the same magnitude as those measured on the hemispherical heat shield of the reentry configuration. At angle of attack the multiple shocks of the front face, of the step between the canisters, and of the reattached flow coalesce on the

DECLASSIFIED

13

windward side, and the resultant flow field with multiple vortices limits mathematical definition of the flow.

The tower of the escape configuration creates extreme turbulence over the entire capsule; however, the heating rates are of the same magnitude as the exit configuration except at 15° angle of attack at $M = 4.44$. At this test condition, the maximum Stanton numbers are approximately 3 times as large as Stanton numbers on the hemispherical heat shield of the reentry configuration.

L
1 Langley Research Center,
0 National Aeronautics and Space Administration,
2 Langley Field, Va., February 7, 1961.
2

REFERENCES

1. Anon.: Manual for Users of the Unitary Plan Wind Tunnel Facilities of the National Advisory Committee for Aeronautics. NACA, 1956.
2. Burbank, Paige B., and Hodge, B. Leon: Distribution of Heat Transfer on a 10° Cone at Angles of Attack From 0° to 15° for Mach Numbers of 2.49 to 4.65 and a Solution to the Heat-Transfer Equation That Permits Complete Machine Calculations. NASA MEMO 6-4-59L, 1959.
3. Lees, Lester: Laminar Heat Transfer Over Blunt-Nosed Bodies at Hypersonic Flight Speeds. Jet Propulsion, vol. 26, no. 4, Apr. 1956, pp. 259-269.
4. Sibulkin, M.: Heat Transfer Near the Forward Stagnation Point of a Body of Revolution. Jour. Aero. Sci. (Readers' Forum), vol. 19, no. 8, Aug. 1952, pp. 570-571.
5. Burbank, Paige B., and Stallings, Robert L., Jr.: Heat-Transfer and Pressure Measurements on a Flat-Face Cylinder at a Mach Number Range of 2.49 to 4.44. NASA TM X-19, 1959.
6. Van Driest, E. R.: The Problem of Aerodynamic Heating. Aero. Eng. Rev., vol. 15, no. 10, Oct. 1956, pp. 26-41.

0319122A1030

14

TABLE I.- WALL THICKNESS FOR REENTRY, EXIT, AND ESCAPE CONFIGURATION

Thermo-couple	x, in.	Thickness, in.*		
		Reentry	Exit	Escape
1	-0.98	0.0290	0.0300	0.0300
2	-.62	.0280	.0300	.0300
3	-.11	.0290	.0300	.0300
4	.45	.0330		
5	1.69	.0320		
6	2.93	.0330		
7	4.36	.0330		
8	5.78	.0330		
9	7.13	.0330		
10	8.49	.0330		
11	9.27	.0305		
12	10.84	.0305		
13	11.30	.0305		
14	11.59	.0310	.0300	----
15	12.32	.0310	.0315	
16	13.82	.0310		.0305
17	-.98	.0300		
18	-.62	.0290	.0300	.0300
19	-.11	.0290	.0310	.0310
20	.45	.0335		
21	1.69	.0335		
22	2.93	.0325		
23	4.36	.0325		
24	5.78	.0320		
25	7.13	.0325		
26	8.49	.0320		
27	9.27	.0325		
28	10.84	.0325		
29	11.30	.0300		----
30	11.59	.0310		----
31	12.32	.0310		.0305
32	13.82	.0310		.0305
33	-1.28	.0310	----	----
34	-.98	.0310		
35	-.62	.0290	.0310	.0310
36	-.11	.0280	.0310	.0310
37	.45	.0320		
38	1.69	.0320		
39	2.93	.0320		
40	4.36	.0320		
41	5.78	.0325		
42	7.13	.0325		
43	8.49	.0325		
44	9.27	.0305		
45	10.84	.0305		
46	11.30	.0305		
47	11.59	.0310		----
48	12.32	.0305	.0300	.0315
49	13.82	.0305	.0300	.0310
50	15.02		.0310	
51	15.02		.0305	
52	15.02		.0300	
53	15.36		.0150	
54	15.51		.0150	
55	15.12		.0130	

*Thermocouples on exit and escape have same thickness as reentry unless otherwise noted.

L-1022

DECLASSIFIED

19

TABLE IV. - PRESSURE COEFFICIENTS MEASURED ON ESCAPE CONFIGURATION

(a) M = 3.50

x, in.	r, in.	Windward			Leeward			
		C _p at θ of:						
		180°	225°	270°	270°	225°	180°	
		$\alpha = 0^\circ$						
		$\alpha = 0^\circ$						
		$\alpha = 5^\circ$						
		$\alpha = -5^\circ$						
		$\alpha = 10^\circ$						
		$\alpha = -10^\circ$						
		$\alpha = 150^\circ$						
		$\alpha = -150^\circ$						

*Radius is listed only for hemispherical heat shield.

L-1022

TABLE V. - HEAT-TRANSFER MEASUREMENTS ON REENTRY CONFIGURATION - Continued

(a) $M = 3.50$ - Concluded

x, in.	r, in. (a)	$\alpha = 15^\circ$						$\alpha = -15^\circ$					
		Leeward ($T_t = 719.2^\circ$)				Windward ($T_t = 717.2^\circ$)							
		θ , deg	T_e/T_t	T_w , deg	h (b)	N_{St}	θ , deg	T_e/T_t	T_w , deg	h (b)	N_{St}		
-1.28	.53	0	.99499	635.8	.00685	.001852	0	.99720	635.8	.00699	.001896		
-.98	2.66	0 45 90	.98998 .99499 .99499	630.1 633.5 650.1	.00647 .00630 .00640	.001749 .001703 .001730	90 45 0	.99664 1.00167 1.00000	634.5 639.8 642.8	.00621 .00706 .00777	.001685 .001915 .002108		
-.62	3.86	0 45 90	.98331 .98442 .98887	624.1 626.1 632.1	.00569 .00587 .00626	.001538 .001587 .001692	90 45 0	.98936 .99496 .99720	629.1 637.5 641.5	.00605 .00711 .00752	.001641 .001929 .002040		
-.11	5.05	0 45 90	.97608 .96662 .96996	617.1 613.8 619.8	.00459 .00523 .00606	.001241 .001424 .001638	90 45 0	.97032 .97592 .98880	617.5 627.5 644.1	.00582 .00697 .00716	.001579 .001891 .001942		
.45		0 45 90	.97886 .97941 .98108	586.8 586.1 587.1	.00048 .00037 .00032	.000130 .000100 .000087	90 45 0	.98432 — —	584.5 583.1 581.1	.00038 LOW LOW	.000103 LOW LOW		
1.69		0 45 90	1.00389 — —	601.5 600.5 600.1	.00039 LOW LOW	.000105 LOW LOW	90 45 0	— — .97928	597.5 580.8	LOW — .00044	LOW LOW .000119		
2.93		0 45 90	.99610 — —	596.5 602.8 599.8	.00039 LOW LOW	.000105 LOW LOW	90 45 0	.96528 .95856	596.5 578.1 580.1	LOW — .00095	LOW LOW .000258 .000353		
4.36		0 45 90	1.00055 — —	599.1 600.8 592.1	.00036 LOW LOW	.000097 LOW LOW	90 45 0	.95408 .96136	594.5 581.8 587.8	LOW — .00191	LOW LOW .000518 .000534		
5.78		0 45 90	.98831 — .95049	592.5 597.1 573.8	.00047 LOW .00105	.000127 LOW .000284	90 45 0	.95352 .94904 .95800	572.5 580.5 586.8	.00146 .00254 .00247	.000396 .000689 .000670		
7.13		0 45 90	.96662 — .92323	581.8 587.8 563.5	.00081 LOW .00184	.000219 LOW .000497	90 45 0	.92440 .95016 .95072	560.1 582.5 585.5	.00195 .00291 .00322	.000529 .000789 .000873		
8.49		0 45 90	.96217 .95438 .92935	582.8 572.5 567.8	.00109 .00061 .00202	.000295 .000165 .000546	90 45 0	.93224 .95576 .95632	565.5 589.8 599.1	.00213 .00376 .00483	.000578 .001020 .001310		
9.27		0 45 90	.96106 .93269 .91378	586.8 563.5 571.5	.00146 .00104 .00395	.000395 .000281 .001068	90 45 0	.91488 .92832 .93560	567.8 593.1 615.5	.00354 .00710 .00725	.000960 .001926 .001967		
10.84		0 45 90	.93213 .92546 .90933	578.5 559.8 560.5	.00317 .00116 .00268	.000857 .000314 .000724	90 45 0	.91432 .92832 .93504	560.1 586.5 593.1	.00274 .00612 .00588	.000743 .001660 .001595		
11.30		0 45 90	.91266 .90448 .91211	567.8 568.1 555.5	.00283 .00099 .00175	.000765 .000268 .000473	90 45 0	.92048 .94680 .92160	557.8 593.8 571.8	.00192 .00483 .00403	.000521 .001310 .001093		
11.59	1.90	0 45 90	.91878 .92546 .94938	556.5 558.1 569.8	.00120 .00083 .00057	.000324 .000224 .000154	90 45 0	.96024 .94680 .95352	572.8 571.8 575.1	.00062 .00145 .00110	.000168 .000393 .000298		
12.32		0 45 90	.91044 .92379 .94548	579.5 561.8 572.1	.00440 .00153 .000351	.001189 .000414 .000351	90 45 0	.94792 .95744 .93784	569.8 589.5 600.5	.00134 .00310 .00498	.000363 .000841 .001321		
13.82		0 45 90	.90988 .91767 .92212	581.1 564.8 565.1	.00492 .00254 .00229	.001330 .000687 .000619	90 45 0	.92384 .90928 .91376	563.5 569.8 580.1	.00231 .00487 .00609	.000627 .001321 .001652		

^aRadius is listed only for hemispherical heat shield and the step between parachute and radar canisters.^bAccuracy depends on magnitude: $h > 0.015$, accuracy 10 percent; $0.001 \leq h \leq 0.015$, accuracy 15 percent; $h < 0.001$, accuracy 20 percent. (h measured in $\text{Btu}/\text{sq ft}\cdot\text{sec}^{-0.5}\text{R}$.)

DECLASSIFIED

25

TABLE V. - HEAT-TRANSFER MEASUREMENTS ON REENTRY CONFIGURATION - Continued

(b) M = 4.44

x, in.	r, in. (a)	$\alpha = 0^\circ$					$\alpha = 0^\circ$				
		Leeward ($T_t = 687.8^\circ$)					Windward ($T_t = 678.5^\circ$)				
		θ , deg	Te/Tt	T _w , deg	h (b)	N _{St}	θ , deg	Te/Tt	T _w , deg	h (b)	N _{St}
-1.28	.53	0	1.00055	638.8	.00675	.002553	0	.99944	632.8	.00681	.002577
-.98	2.66	0 45 90	.99889 1.00000	637.1 637.8	.00677 .00642	.002561 .002429	90 45 0	1.00000 1.00000 .99833	632.5 631.8 631.1	.00632 .00638 .00672	.002392 .002414 .002543
-.62	3.86	0 45 90	.99336 .99391 .99336	632.8 633.1 632.5	.00630 .00620 .00587	.002383 .002345 .002221	90 45 0	.99166 .99277 .99277	626.5 627.1 627.1	.00603 .00635 .00607	.002282 .002403 .002297
-.11	5.05	0 45 90	.98507 .97180 .97180	625.5 618.1 617.8	.00520 .00557 .00553	.001967 .002107 .002092	90 45 0	.97109 .97053 .98498	616.1 612.5 620.8	.00572 .00556 .00511	.002165 .002104 .001934
.45		0 45 90	.97235 .96738 .97125	584.5 580.8 583.8	.00039 .00041 .00040	.000148 .000155 .000151	90 45 0	.97720 .97275 .97498	582.8 579.1 581.8	.00038 .00037 .00034	.000144 .000140 .000129
4.36		0 45 90	— — —	597.1 593.5 592.8	LOW LOW LOW	LOW LOW LOW	90 45 0	— — —	— — —	— — —	— — —
5.78		0 45 90	— — —	596.5 596.1 593.1	LOW LOW LOW	LOW LOW LOW	90 45 0	— — —	594.1 595.5 595.1	LOW LOW LOW	LOW LOW LOW
7.13		0 45 90	1.00939 1.01105 .99944	607.5 609.8 603.5	.00051 .00046 .00051	.000193 .000174 .000193	90 45 0	1.01000 1.02112 1.01723	603.1 608.5 606.1	.00055 .00045 .00044	.000208 .000170 .000167
8.49		0 45 90	1.00884 1.01271 .99336	613.1 617.8 606.1	.00172 .00169 .00193	.000651 .000639 .000730	90 45 0	.99555 1.01501 1.01000	602.5 612.5 608.8	.00187 .00154 .00155	.000708 .000583 .000587
9.27		0 45 90	.95134 .94471 .93752	591.5 590.1 586.5	.00369 .00429 .00394	.001396 .001623 .001490	90 45 0	.93662 .94440 .94996	584.5 585.5 586.1	.00417 .00426 .00352	.001578 .001612 .001332
10.84		0 45 90	.90988 .91098 .90711	572.1 576.1 570.5	.00427 .00512 .00400	.001615 .001937 .001513	90 45 0	.90548 .90993 .90882	564.8 570.8 566.8	.00403 .00524 .00390	.001525 .001983 .001476
11.30		0 45 90	.90214 .92480 .90601	561.1 582.1 562.1	.00311 .00383 .00268	.001176 .001449 .001014	90 45 0	.90493 .92383 .90326	556.8 576.1 556.8	.00279 .00393 .00283	.001056 .001487 .001071
11.59	1.90	0 45 90	.93807 .92702 .93918	570.1 567.5 571.5	.00089 .00162 .00110	.000337 .000613 .000416	90 45 0	.93884 .92717 .93439	566.1 562.5 563.5	.00107 .00155 .00090	.000405 .000587 .000341
12.32		0 45 90	.93144 .93642 .93365	584.1 583.1 586.5	.00343 .00271 .00280	.001298 .001025 .001437	90 45 0	.93384 .93662 .92772	580.8 577.8 577.5	.00374 .00282 .00323	.001415 .001067 .001222
13.82		0 45 90	.91209 .90822 .91596	577.5 572.8 580.1	.00505 .00464 .00529	.001910 .001755 .002001	90 45 0	.91382 .90660 .90882	574.5 567.1 570.8	.00539 .00475 .00505	.002040 .001798 .001911

^aRadius is listed only for hemispherical heat shield and the step between parachute and radar canisters.^bAccuracy depends on magnitude: $h > 0.015$, accuracy 10 percent; $0.001 \leq h \leq 0.015$, accuracy 15 percent; $h < 0.001$, accuracy 20 percent. (h measured in Btu/sq ft-sec.^{0.5}R.)

L-1022

03131232A1030

TABLE V. - HEAT-TRANSFER MEASUREMENTS ON REENTRY CONFIGURATION - Continued

(b) $M = 4.44$ - Continued

x , in.	r , in. (a)	$\alpha = 5^\circ$ Leeward ($T_t = 685.5^\circ$)						$\alpha = -5^\circ$ Windward ($T_t = 680.5^\circ$)					
		θ , deg	T_e/T_t	T_w , deg	h (b)	N_{St}	θ , deg	T_e/T_t	T_w , deg	h (b)	N_{St}		
-1.28	.53	0	.99944	631.1	.00637	.002406	0	1.00055	637.1	.00656	.002469		
-.98	2.66	0 45 90	.99612 .99778 .99889	632.8 634.5 630.8	.00631 .00633 .00608	.002383 .002391 .002296	90 45 0	1.00055 1.00167 1.00000	633.5 633.5 633.5	.00631 .00668 .00692	.002375 .002514 .002604		
-.62	3.86	0 45 90	.98947 .99168 .99335	628.1 624.5 626.5	.00587 .00559 .00563	.002217 .002111 .002126	90 45 0	.99275 .99498 .99498	628.1 629.5 630.1	.00585 .00652 .00644	.002202 .002454 .002424		
-.11	5.05	0 45 90	.98503 .97229 .97284	618.5 610.8 612.8	.00468 .00485 .00530	.001767 .001832 .002002	90 45 0	.97324 .97379 .98773	617.5 615.5 627.5	.00550 .00580 .00552	.002070 .002183 .002078		
.45		0 45 90	1.00055 .99279 .99113	601.5 595.8 595.1	.00053 .00046 .00042	.000200 .000174 .000159	90 45 0	.99052 .97881 .97491	592.8 584.1 582.5	.00046 .00042 .00044	.000173 .000158 .000166		
1.69		0 45 90	1.03601 — —	622.1 614.8 611.1	.00031 LOW LOW	.000117 LOW LOW	90 45 0	— — —	608.8 — —	LOW — —	LOW — —		
2.93		0 45 90	1.02770 — —	617.1 619.5 614.5	.00031 LOW LOW	.000117 LOW LOW	90 45 0	— — —	— — —	— — —	— — —		
4.36		0 45 90	1.03989 — —	623.1 622.8 614.8	.00030 LOW LOW	.000113 LOW LOW	90 45 0	— — —	585.8 580.5	LOW LOW	LOW LOW		
5.78		0 45 90	1.03878 1.04488 —	622.1 626.8 614.8	.00037 .00030 LOW	.000140 .000113 LOW	90 45 0	.98494 .97101	605.5 591.1 583.1	LOW LOW LOW	LOW LOW LOW		
7.13		0 45 90	1.03102 1.04488 1.01883	618.8 627.1 613.1	.00056 .00039 .00073	.000211 .000147 .000276	90 45 0	1.01282 .99275 .97993	608.5 598.5 590.1	.00083 .00112 .00103	.000312 .000422 .000388		
8.49		0 45 90	1.01496 1.01329 .96342	613.8 611.8 585.5	.00086 .00085 .00184	.000325 .000321 .000695	90 45 0	.95986 .96933 .96822	584.1 590.8 592.5	.00216 .00227 .00258	.000813 .000854 .000971		
9.27		0 45 90	1.00609 .97617 .91577	607.5 591.5 567.1	.00079 .00153 .00303	.000298 .000578 .001144	90 45 0	.91135 .92250 .92529	569.5 580.1 584.1	.00354 .00574 .00463	.001332 .002160 .001743		
10.84		0 45 90	.98171 .91134 .88696	599.8 562.5 555.1	.00202 .00310 .00370	.000763 .001171 .001397	90 45 0	.89128 .91526 .91972	559.1 574.1 573.5	.00389 .00557 .00419	.001464 .002096 .001577		
11.30		0 45 90	.97451 .92021 .88807	595.8 570.5 546.1	.00216 .00273 .00238	.000816 .001031 .000899	90 45 0	.89128 .92808 .91637	548.8 578.1 562.5	.00272 .00369 .00292	.001024 .001389 .001099		
11.59	1.90	0 45 90	.96398 .92907 .92796	587.1 565.8 561.1	.00176 .00177 .00102	.000665 .000668 .000385	90 45 0	.92696 .92641 .94313	559.1 560.8 565.5	.00110 .00150 .00067	.000414 .000565 .000252		
12.32		0 45 90	.96564 .93849 .92076	599.1 575.1 564.8	.00339 .00217 .00212	.001280 .000820 .000801	90 45 0	.91749 .94202 .95205	566.5 576.8 588.5	.00277 .00233 .00255	.001043 .000877 .000960		
13.82		0 45 90	.95068 .90968 .90414	596.8 567.1 558.5	.00423 .00387 .00305	.001598 .001462 .001152	90 45 0	.90020 .89965 .90243	560.1 561.5 567.8	.00398 .00435 .00462	.001498 .001637 .001739		

^aRadius is listed only for hemispherical heat shield and the step between parachute and radar canisters.^bAccuracy depends on magnitude: $h > 0.015$, accuracy 10 percent; $0.001 \leq h \leq 0.015$, accuracy 15 percent; $h < 0.001$, accuracy 20 percent. (h measured in $\text{Btu}/\text{sq ft}\cdot\text{sec}^{-0.5}\text{R}$.)

DECLASSIFIED

27

TABLE V. - HEAT-TRANSFER MEASUREMENTS ON REENTRY CONFIGURATION - Continued

(b) M = 4.44 - Continued

L-1022

x, in.	r, in. (a)	Leeward ($T_t = 687.8^{\circ}$)						$\alpha = -10^{\circ}$					
		β , deg	T_e/T_t	T_w , deg	h (b)	N_{St}	β , deg	T_e/T_t	T_w , deg	h (b)	N_{St}		
-1.28	.53	0	.99500	633.5	.00623	.002364	0	.99611	633.5	.00734	.002775		
-0.98	2.66	0 45 90	.99056 .99500 .99556	629.5 632.1 634.8	.00591 .00571 .00605	.002243 .002167 .002296	90 45 0	.99500 .99777 .99722	639.5 634.5 634.5	.00680 .00715 .00815	.002571 .002704 .003082		
-0.62	3.86	0 45 90	.98446 .98668 .99001	624.5 626.1 630.5	.00532 .00539 .00561	.002019 .002046 .002129	90 45 0	.98778 .99222 .99278	627.5 631.5 632.8	.00649 .00739 .00757	.002454 .002794 .002862		
-0.11	5.05	0 45 90	.98058 .96838 .97004	619.1 615.1 616.5	.00421 .00447 .00513	.001598 .001696 .001947	90 45 0	.96780 .97002 .98501	613.8 621.1 630.5	.00656 .00716 .00680	.002480 .002707 .002571		
.45		0 45 90	.99667 .99001 .99112	599.5 594.1 595.5	.00050 .00055 .00050	.000190 .000209 .000190	90 45 0	.98501 .97224 .96891	591.8 582.1 580.5	.00047 .00048 .00038	.000178 .000181 .000144		
1.69		0 45 90	— — —	621.1 614.1 —	LOW LOW —	LOW LOW —	90 45 0	— — —	606.1 586.8 —	LOW LOW —	LOW LOW —		
2.93		0 45 90	— — —	618.5 619.8 —	LOW LOW —	LOW LOW —	90 45 0	— — —	604.1 579.5 575.8	LOW LOW —	LOW LOW —		
4.36		0 45 90	— — —	625.8 621.5 604.8	LOW LOW LOW	LOW LOW LOW	90 45 0	— — —	595.1 577.8 579.5	LOW LOW —	LOW LOW —		
5.78		0 45 90	— — —	621.1 618.5 594.5	LOW LOW LOW	LOW LOW LOW	90 45 0	.97890 .95948 .95726	590.1 581.8 580.1	.00056 .00138 .00112	.000212 .000522 .000423		
7.13		0 45 90	1.01553 — .96061	609.5 609.8 583.8	.00041 LOW .00120	.000156 LOW .000455	90 45 0	.96170 .95726 .95837	580.5 581.8 582.1	.00127 .00162 .00142	.000480 .000613 .000537		
8.49		0 45 90	.99278 .96782 .93731	599.1 582.5 572.5	.00062 .00061 .00176	.000235 .000232 .000668	90 45 0	.93561 .96003 .96059	571.5 589.5 592.1	.00210 .00266 .00305	.000794 .001006 .001153		
9.27		0 45 90	.98113 .93010 .91568	593.1 563.1 572.8	.00068 .00101 .00304	.000258 .000383 .001154	90 45 0	.91119 .92451 .92562	571.8 586.8 586.5	.00362 .00620 .00666	.001369 .002344 .002518		
10.84		0 45 90	.95506 .90348 .90625	588.5 553.8 560.8	.00189 .00175 .00248	.000717 .000664 .000941	90 45 0	.90342 .92007 .92340	561.8 577.1 578.5	.00314 .00519 .00487	.001187 .001962 .001841		
11.30		0 45 90	.94674 .92012 .90680	583.1 562.1 556.1	.00207 .00183 .00174	.000786 .000695 .000660	90 45 0	.90509 .93506 .91785	554.8 582.1 567.8	.00216 .00414 .00314	.000817 .001565 .001187		
11.59	1.90	0 45 90	.93565 .92178 .93898	571.8 558.8 566.8	.00163 .00119 .00063	.000619 .000452 .000239	90 45 0	.94116 .93839 .94893	567.8 568.8 571.5	.00078 .00133 .00072	.000295 .000503 .000272		
12.32		0 45 90	.93288 .93898 .94619	585.5 572.1 574.8	.00325 .00150 .00124	.001233 .000569 .000471	90 45 0	.94227 .96003 .95337	572.5 586.1 592.1	.00152 .00188 .00301	.000575 .000711 .001138		
13.82		0 45 90	.92123 .92677 .92400	583.1 574.1 566.1	.00419 .00266 .00197	.001590 .001010 .000748	90 45 0	.90897 .90287 .90231	556.8 563.5 569.1	.00221 .00415 .00504	.000836 .001569 .001906		

^aRadius is listed only for hemispherical heat shield and the step between parachute and radar canisters.^bAccuracy depends on magnitude: $h > 0.015$, accuracy 10 percent; $0.001 \leq h \leq 0.015$, accuracy 15 percent; $h < 0.001$, accuracy 20 percent. (h measured in Btu/sq ft-sec^{0.8}R.)

L-1022

TABLE V. - HEAT-TRANSFER MEASUREMENTS ON REENTRY CONFIGURATION - Concluded
(b) M = 4.44 - Concluded

x, in.	r, in. (a)	$\alpha = 15^\circ$						$\alpha = -15^\circ$					
		Leeward ($T_t = 687.8^\circ$)						Windward ($T_t = 680.8^\circ$)					
		θ , deg	T_e/T_t	T_w , deg	h (b)	N_{St}	θ , deg	T_e/T_t	T_w , deg	h (b)	N_{St}		
-1.28	.53	0	.99554	629.1	.00605	.002289	0	.99610	628.1	.00631	.002383		
-0.98	2.66	0 45 90	.98942 .99387 .99610	623.5 626.1 629.5	.00569 .00555 .00586	.002152 .002099 .002217	90 45 0	.99610 1.00000 .99944	628.1 631.5 639.8	.00576 .00630 .00672	.002175 .002379 .002537		
-0.62	3.86	0 45 90	.98163 .98497 .98886	616.5 619.1 624.5	.00490 .00498 .00550	.001854 .001884 .002081	90 45 0	.98886 .99387 .99610	629.8 628.8 631.1	.00535 .00632 .00666	.002020 .002386 .002515		
-0.11	5.05	0 45 90	.97885 .98660 .96938	611.1 605.5 611.1	.00371 .00418 .00501	.001403 .001581 .001895	90 45 0	.96937 .97327 .98830	609.8 615.5 626.1	.00503 .00581 .00593	.001899 .002194 .002239		
.45		0 45 90	.99165 .98608 .98831	593.8 589.5 591.5	.00044 .00041 .00040	.000166 .000155 .000151	90 45 0	.98663 .96491 .96380	589.5 573.8 574.8	.00038 .00033 .00046	.000143 .000125 .000174		
1.69		0 45 90	---	615.5 608.5 605.8	LOW LOW LOW	LOW LOW LOW	90 45 0	---	573.8 581.1	LOW LOW			
2.93		0 45 90	---	611.1 612.5 601.1	LOW LOW LOW	LOW LOW LOW	90 45 0	.95879 .95767	572.1 576.1	.00049 .00090	.000185 .000340		
4.36		0 45 90	---	613.1 609.5 584.8	LOW LOW LOW	LOW LOW LOW	90 45 0	---	575.8 572.1 578.5	LOW .00083 .00105	.000313 .000396		
5.78		0 45 90	1.01001 -	603.5 602.1 571.1	.00044 LOW .00082	.000166 LOW .000310	90 45 0	.94821 .95377 .95545	570.1 576.1 577.8	.00088 .00122 .00118	.000332 .000461 .000446		
7.13		0 45 90	.99053 -	592.8 594.5 568.8	.00054 LOW .00099	.000204 LOW .000374	90 45 0	.94988 .95934 .95656	570.8 580.1 581.1	.00087 .00144 .00150	.000329 .000544 .000566		
8.49		0 45 90	.97996 .97551 .94211	588.5 582.8 570.8	.00061 .00031 .00116	.000231 .000117 .000439	90 45 0	.94876 .96268 .96157	572.1 587.5 591.5	.00123 .00233 .00277	.000464 .000880 .001046		
9.27		0 45 90	.97662 .95157 .92375	588.1 571.5 573.8	.00077 .00069 .00227	.000291 .000261 .000859	90 45 0	.92872 .92816 .92983	569.8 582.8 587.5	.00251 .00559 .00571	.000948 .002111 .002156		
10.84		0 45 90	.95046 .93766 .90872	580.1 563.8 554.5	.00168 .00078 .00190	.000636 .000295 .000719	90 45 0	.91368 .92426 .92872	557.1 575.5 578.8	.00196 .00441 .00417	.000740 .001665 .001575		
11.30		0 45 90	.93766 .94935 .91206	570.8 569.5 551.8	.00166 .00047 .00130	.000628 .000178 .000492	90 45 0	.91702 .93818 .92426	555.1 582.1 567.5	.00142 .00308 .00277	.000536 .001163 .001046		
11.59	1.90	0 45 90	.94378 .94044 -	565.5 562.5 569.8	.00045 .00040 LOW	.000170 .000151 0	90 45 0	.95600 .93985 .94431	571.1 566.5 569.5	.00039 .00118 .00083	.000147 .000446 .000313		
12.32		0 45 90	.91373 .93265 .95213	561.1 561.1 572.1	.00206 .00078 .00081	.000779 .000295 .000306	90 45 0	.95155 .95656 .94041	573.5 582.8 581.8	.00085 .00180 .00322	.000321 .000680 .001216		
13.82		0 45 90	.89926 .92041 .92709	556.1 559.1 562.5	.00278 .00140 .00146	.001052 .000530 .000552	90 45 0	.92649 .91201 .90755	560.8 563.5 565.5	.00148 .00335 .00429	.000559 .001265 .001620		

^aRadius is listed only for hemispherical heat shield and the step between parachute and radar canisters.

^bAccuracy depends on magnitude: $h > 0.015$, accuracy 10 percent; $0.001 \leq h \leq 0.015$, accuracy 15 percent; $h < 0.001$, accuracy 20 percent. (h measured in Btu/sq ft-sec^{-0.5}R.)

DECLASSIFIED

29

TABLE VI. - HEAT-TRANSFER MEASUREMENTS ON EXIT CONFIGURATION

(a) $M = 3.50$

x , in.	r , in. (a)	$\alpha = 0^\circ$ Leeward ($T_t = 715.8^\circ$)					$\alpha = 0^\circ$ Windward ($T_t = 721.8^\circ$)				
		θ , deg	T_e/T_t	T_w , deg	h (b)	N_{St}	θ , deg	T_e/T_t	T_w , deg	h (b)	N_{St}
-.98	2.66	0	.96608	586.5	.00168	.000286	90	.96748	595.1	.00185	.000316
		45	.97553	593.1	.00167	.000284	45	.97906	602.1	.00187	.000320
		90	.96275	585.8	.00177	.000301	0	.97410	598.8	.00180	.000308
-.62	3.86	0	.96553	583.8	.00128	.000218	90	.97189	591.8	.00113	.000193
		45	.96886	586.1	.00126	.000214	45	.97244	596.5	.00163	.000279
		90	.96775	583.8	.00104	.000177	0	.97189	593.8	.00138	.000236
-.11	5.05	0	.95385	582.5	.00242	.000412	90	.95261	591.8	.00243	.000416
		45	.94885	583.8	.00252	.000429	45	.95867	599.1	.00308	.000527
		90	.95274	585.1	.00235	.000400	0	.94875	634.1	.01218	.002083
+.45		0	.94774	624.8	.01152	.001959	90	.95205	641.8	.01214	.002076
		45	.95385	636.1	.01218	.002071	45	.94875	634.1	.01218	.002083
		90	.95385	634.8	.01174	.001996	0	.94875	634.1	.01218	.002083
1.69		0	.94885	621.1	.01148	.001952	90	.94158	622.8	.01164	.001991
		45	.94440	618.1	.01227	.002087	45	.94379	625.1	.01248	.002134
		90	.94384	615.8	.01118	.001901	0	.95040	629.8	.01180	.002018
2.93		0	.93940	614.5	.01147	.001951	90	.93828	619.1	.01152	.001970
		45	.94162	615.8	.01173	.001995	45	.93993	622.8	.01215	.002078
		90	.94162	613.1	.01110	.001888	0	.93938	622.5	.01178	.002015
4.36		0	.94162	615.8	.01143	.001944	90	.93497	617.5	.01156	.001977
		45	.94440	617.1	.01138	.001935	45	.94324	624.5	.01189	.002034
		90	.93662	610.8	.01128	.001918	0	.94103	623.8	.01194	.002042
5.78		0	.93439	611.5	.01167	.001985	90	.93001	615.5	.01203	.002057
		45	.93439	610.8	.01134	.001928	45	.93277	617.8	.01180	.002018
		90	.93328	609.5	.01153	.001961	0	.93277	618.8	.01226	.002097
7.13		0	.93439	613.8	.01233	.002097	90	.92450	613.8	.01269	.002170
		45	.93328	610.5	.01161	.001974	45	.93167	617.8	.01222	.002090
		90	.92717	607.1	.01208	.002054	0	.93222	620.8	.01305	.002232
8.49		0	.93551	621.8	.01135	.001930	90	.93607	627.5	.01122	.001919
		45	.93717	627.5	.01243	.002114	45	.93663	626.8	.01329	.002273
		90	.93829	620.8	.01081	.001838	0	.93442	621.5	.01227	.002099
9.27		0	.93829	592.1	.00542	.000922	90	.92946	588.8	.00546	.000934
		45	.92828	587.1	.00641	.001090	45	.92726	593.5	.00644	.001101
		90	.93106	582.8	.00442	.000752	0	.93663	597.5	.00532	.000910
10.84		0	.92272	600.5	.01054	.001792	90	.91018	584.8	.00717	.001226
		45	.92439	594.5	.00904	.001537	45	.92671	606.1	.00949	.001623
		90	.91549	589.5	.00714	.001214	0	.92065	607.1	.01084	.001854
11.30		0	.96108	655.5	.01620	.002755	90	.92781	624.5	.01508	.002579
		45	.92327	610.8	.01377	.002342	45	.95812	662.1	.01701	.002909
		90	—	—	—	0	—	—	—	—	—
11.59	1.90	0	.97776	677.5	.02155	.003665	90	.97244	671.1	.02183	.003734
		45	.96441	665.5	.02039	.003467	45	.96252	663.8	.02181	.003730
		90	.97553	672.8	.01987	.003379	0	.97685	685.1	.02224	.003804
12.32		0	.96775	639.5	.01318	.002241	90	.97024	646.8	.01386	.002370
		45	.97109	639.8	.01324	.002252	45	.96859	647.1	.01381	.002362
		90	.97164	639.5	.01332	.002265	0	.96473	645.8	.01367	.002338
13.82		0	.94607	587.8	.00363	.000617	90	.94654	603.1	.00548	.000937
		45	.95330	592.8	.00384	.000653	45	.95095	597.8	.00389	.000665
		90	.94940	597.8	.00540	.000918	0	.94379	592.8	.00371	.000635
15.02	1.15	0	.99277	656.1	.01269	.002158	90	.98291	664.1	.01479	.002530
		45	.96108	655.1	.01614	.002745	45	.95701	660.8	.01688	.002887
		90	.98498	658.5	.01469	.002498	0	.99008	662.5	.01318	.002254
15.12		180	.97943	684.5	.00813	.001383	180	.98897	708.5	.02232	.003817
15.51		180	.99054	706.8	.02091	.003556	180	—	—	—	—

^aRadius is listed only for hemispherical heat shield, step between parachute and radar canisters, and exit flat face.^bAccuracy depends on magnitude: $h > 0.015$, accuracy 10 percent; $0.001 \leq h \leq 0.015$, accuracy 15 percent; $h < 0.001$, accuracy 20 percent. (h measured in $\text{Btu}/\text{sq ft}\cdot\text{sec}^{-0.5}\text{R}^2$.)

031718201030

TABLE VI. - HEAT-TRANSFER MEASUREMENTS ON EXIT CONFIGURATION - Continued

(a) $M = 3.50$ - Continued

x, in.	r, in. (a)	$\alpha = 5^\circ$					$\alpha = -5^\circ$				
		θ , deg	T _e /T _t	T _w , deg	h (b)	N _{St}	θ , deg	T _e /T _t	T _w , deg	h (b)	N _{St}
-•.98	2.66	0	.94865	575.1	.00165	.000280	90	.95862	588.5	.00178	.000305
		45	.95479	579.1	.00155	.000263	45	.97021	596.1	.00177	.000304
		90	.94363	575.5	.00207	.000351	0	.97352	594.8	.00143	.000245
-•.62	3.86	0	.94865	572.5	.00122	.000207	90	.95917	585.1	.00130	.000223
		45	.94921	572.5	.00118	.000200	45	.96579	595.5	.00205	.000352
		90	.94865	574.5	.00129	.000219	0	.97186	593.8	.00143	.000245
-•.11	5.05	0	.93023	565.5	.00199	.000338	90	.94318	580.5	.00215	.000369
		45	.93135	567.5	.00262	.000445	45	.94759	600.5	.00583	.001000
		90	.93637	576.1	.00248	.000421	0	.95697	593.8	.00314	.000539
•.45		0	.91070	592.8	.00952	.001616	90	.95310	629.8	.01133	.001943
		45	.94586	627.1	.01146	.001945	45	.96193	650.1	.01679	.002880
		90	.94195	632.8	.01116	.001894	0	.95752	648.5	.01536	.002635
1.69		0	.91628	590.1	.00886	.001504	90	.94924	625.1	.01104	.001894
		45	.94028	612.1	.01169	.001984	45	.95200	635.1	.01426	.002446
		90	.94251	615.1	.01101	.001869	0	.96083	646.5	.01511	.002592
2.93		0	.91125	585.5	.00860	.001460	90	.94759	623.8	.01142	.001959
		45	.93693	610.5	.01147	.001947	45	.95035	634.1	.01398	.002398
		90	.94697	614.8	.01054	.001789	0	.95200	639.8	.01501	.002575
4.36		0	.92186	591.8	.00848	.001439	90	.94428	622.5	.01162	.001993
		45	.93860	611.8	.01137	.001930	45	.95586	636.8	.01349	.002314
		90	.94809	617.5	.01110	.001884	0	.95421	641.1	.01509	.002588
5.78		0	.92856	596.1	.00852	.001446	90	.93766	619.1	.01190	.002041
		45	.92577	605.1	.01173	.001991	45	.94649	631.5	.01349	.002314
		90	.94474	618.1	.01194	.002026	0	.94593	635.1	.01505	.002581
7.13		0	.94195	604.5	.00850	.001443	90	.92883	616.1	.01264	.002168
		45	.92465	606.1	.01224	.002077	45	.94538	631.8	.01397	.002396
		90	.93637	618.5	.01365	.002317	0	.94428	636.5	.01577	.002705
8.49		0	.93358	602.5	.00822	.001395	90	.94207	630.5	.01109	.001902
		45	.92465	617.5	.01207	.002049	45	.94814	646.5	.01434	.002460
		90	.94642	624.5	.01230	.002088	0	.94593	642.1	.01340	.002298
9.27		0	.93023	581.1	.00426	.000723	90	.93656	591.1	.00416	.000714
		45	.90902	572.5	.00604	.001025	45	.93987	605.8	.00753	.001292
		90	.93470	584.8	.00435	.000738	0	.95035	612.5	.00669	.001147
10.84		0	.93358	599.5	.00821	.001393	90	.91339	592.5	.00677	.001161
		45	.90400	579.5	.00871	.001478	45	.93987	620.5	.01154	.001979
		90	.91349	583.5	.00759	.001288	0	.93269	621.1	.01278	.002192
11.30		0	.96483	646.1	.01564	.002654	90	.93325	630.8	.01663	.002852
		45	.90456	592.1	.01175	.001994	45	.96910	669.1	.01670	.002864
		90					0				
11.59	1.90	0	.97544	639.1	.01112	.001887	90	.96083	669.8	.02033	.003487
		45	.94195	630.5	.01565	.002656	45	.96028	674.8	.02395	.004108
		90	.96260	661.1	.02342	.003975	0	.97572	688.1	.02509	.004304
12.32		0	.95758	618.1	.00875	.001485	90	.94924	631.1	.01332	.002285
		45	.92856	602.1	.01017	.001726	45	.96524	645.8	.01421	.002437
		90	.93581	623.1	.01515	.002571	0	.96690	648.1	.01399	.002400
13.82		0	.94642	600.1	.00616	.001045	90	.94428	606.1	.00620	.001063
		45	.92856	585.5	.00591	.001003	45	.95697	614.5	.00607	.001041
		90	.91851	593.1	.00888	.001507	0	.94979	617.1	.00760	.001304
15.02	1.15	0	.99051	668.1	.01795	.003047	90	.98234	654.1	.01164	.001997
		45	.96260	647.8	.01658	.002814	45	.96303	666.1	.01738	.002981
		90	.98381	677.1	.02297	.003899	0	.99282	663.1	.01254	.002151
15.12		180	.97488	682.8	.00726	.001232	180				
15.51		180	.98995	704.5	.02459	.004173	180	.98841	712.8	.02073	.003556

^aRadius is listed only for hemispherical heat shield, step between parachute and radar canisters, and exit flat face.^bAccuracy depends on magnitude: $h > 0.015$, accuracy 10 percent; $0.001 \leq h \leq 0.015$, accuracy 15 percent; $h < 0.001$, accuracy 20 percent. (h measured in Btu/sq ft-sec⁻²R.)

DECCLASSIFIED

31

TABLE VI. - HEAT-TRANSFER MEASUREMENTS ON EXIT CONFIGURATION - Continued

(a) $M = 3.50$ - Continued

x, in.	r, in. (a)	$\alpha = 10^\circ$						$\alpha = -10^\circ$					
		Leeward ($T_f = 721.2^\circ$)						Windward ($T_f = 723.2^\circ$)					
		θ , deg	T_e/T_t	T_w , deg	h (b)	N_{St}	θ , deg	T_e/T_t	T_w , deg	h (b)	N_{St}		
-.98	2.66	0	.95104	574.5	.00110	.000189	90	.94916	578.1	.00139	.000238		
		45	.95383	576.8	.00120	.000206	45	.95690	583.5	.00137	.000234		
		90	.94548	574.5	.00151	.000259	0	.96905	587.1	.00099	.000169		
-.62	3.86	0	.95049	573.5	.00106	.000182	90	.94640	575.5	.00125	.000214		
		45	.94715	576.5	.00166	.000285	45	.95579	585.8	.00179	.000306		
		90	.95049	575.5	.00116	.000199	0	.96905	590.8	.00113	.000193		
-.11	5.05	0	.93769	570.1	.00174	.000299	90	.92871	573.1	.00207	.000354		
		45	.92879	571.8	.00237	.000407	45	.93811	594.8	.00607	.001037		
		90	.93825	581.1	.00243	.000417	0	.95026	591.1	.00362	.000619		
+.45		0	.92768	598.1	.00772	.001326	90	.94142	618.1	.01072	.001832		
		45	.93046	601.8	.00863	.001482	45	.96132	651.5	.01869	.003194		
		90	.95049	621.8	.01112	.001909	0	.95413	655.1	.02033	.003475		
1.69		0	.93269	595.8	.00728	.001250	90	.94308	618.8	.01094	.001870		
		45	.92101	593.5	.00900	.001545	45	.95579	641.5	.01641	.002805		
		90	.94938	621.1	.01123	.001928	0	.95855	653.8	.01935	.003307		
2.93		0	.92713	591.5	.00716	.001229	90	.94198	617.5	.01101	.001882		
		45	.92156	594.1	.00865	.001485	45	.95413	641.5	.01625	.002777		
		90	.94882	619.1	.01115	.001915	0	.95358	648.8	.01869	.003194		
4.36		0	.93491	597.1	.00729	.001252	90	.94087	617.5	.01128	.001928		
		45	.92935	599.5	.00881	.001513	45	.95911	644.1	.01600	.002735		
		90	.94659	619.1	.01142	.001961	0	.96021	652.8	.01858	.003176		
5.78		0	.93825	599.5	.00758	.001302	90	.93700	615.5	.01128	.001928		
		45	.92879	603.8	.00979	.001681	45	.95082	638.5	.01578	.002697		
		90	.94437	619.1	.01184	.002033	0	.95303	647.1	.01853	.003167		
7.13		0	.94381	602.8	.00747	.001283	90	.92650	610.1	.01158	.001979		
		45	.93881	615.1	.01132	.001944	45	.94971	638.5	.01610	.002752		
		90	.93324	612.5	.01184	.002033	0	.95137	647.5	.01909	.003263		
8.49		0	.93158	600.8	.00817	.001403	90	.92595	607.5	.00991	.001694		
		45	.92935	608.8	.01086	.001865	45	.94861	640.8	.01602	.002738		
		90	.92101	608.1	.00970	.001666	0	.95082	643.1	.01648	.002817		
9.27		0	.92101	577.5	.00423	.000726	90	.93258	586.8	.00385	.000658		
		45	.91266	570.5	.00457	.000785	45	.93921	609.8	.00876	.001497		
		90	.91489	572.8	.00406	.000697	0	.95468	621.8	.00852	.001456		
10.84		0	.93046	597.1	.00748	.001284	90	.91048	589.5	.00671	.001147		
		45	.89820	573.5	.00738	.001267	45	.93700	622.8	.01406	.002403		
		90	.90710	579.1	.00755	.001296	0	.93866	630.5	.01526	.002608		
11.30		0	.96328	646.5	.01589	.002728	90	.92650	628.5	.01798	.003073		
		45	.89208	580.1	.01002	.001721	45	.96905	665.5	.01942	.003319		
		90	—	—	—	—	0	—	—	—	—		
11.59	1.90	0	.96439	631.5	.01023	.001757	90	.94750	656.8	.01934	.003305		
		45	.92045	613.5	.01419	.002437	45	.95579	663.1	.02465	.004213		
		90	.95828	667.5	.02119	.003639	0	.97900	688.1	.03160	.005401		
12.32		0	.92601	598.1	.00811	.001393	90	.94087	620.8	.01207	.002063		
		45	.90710	580.5	.00757	.001300	45	.95634	642.5	.01535	.002623		
		90	.93658	621.5	.01433	.002461	0	.96353	654.8	.01736	.002967		
13.82		0	.91600	576.1	.00495	.000850	90	.94363	598.1	.00484	.000827		
		45	.91934	572.1	.00402	.000690	45	.95468	622.1	.00645	.001102		
		90	.93491	610.5	.01022	.001755	0	.94805	614.1	.00671	.001147		
15.02	1.15	0	.99221	679.5	.02116	.003633	90	.98066	649.5	.01081	.001848		
		45	.96161	649.1	.01709	.002935	45	.96684	661.5	.01877	.003208		
		90	.98776	700.8	.03045	.005229	0	.99226	661.5	.01251	.002138		
15.12		180	.97496	680.1	.00764	.001312	180	—	—	—	—		
15.51		180	.99109	705.5	.02270	.003898	180	.97789	700.8	.01966	.003360		

^aRadius is listed only for hemispherical heat shield, step between parachute and radar canisters, and exit flat face.^bAccuracy depends on magnitude: $h > 0.015$, accuracy 10 percent; $0.001 \leq h \leq 0.015$, accuracy 15 percent; $h < 0.001$, accuracy 20 percent. (h measured in Btu/sq ft-sec.⁻²R.)

L-1022

REF ID: A6577
CLASSIFIED

33

TABLE VI. - HEAT-TRANSFER MEASUREMENTS ON EXIT CONFIGURATION - Continued

(a) M = 3.50 - Concluded

$\alpha = 20^\circ$

		Leeward ($T_t = 723.2^\circ$)						Windward ($T_t = 720.5^\circ$)					
x, in.	r, in. (a)	θ , deg	T_e/T_t	T_w , deg	h (b)	N _{St}	θ , deg	T_e/T_t	T_w , deg	h (b)	N _{St}		
-.98	2.66	0	.94888	572.5	.00084	.000144	90	.94283	572.1	.00106	.000181		
		45	.94777	571.8	.00077	.000132	45	.96336	583.8	.00101	.000173		
		90	.94443	569.5	.00081	.000139	0	.95781	584.5	.00159	.000272		
-.62	3.86	0	.93888	568.1	.00109	.000187	90	.94061	570.5	.00108	.000185		
		45	.94110	569.8	.00107	.000184	45	.96947	589.8	.00129	.000220		
		90	.94777	571.8	.00079	.000136	0	.96281	585.5	.00137	.000234		
-.11	5.05	0	.94276	572.8	.00151	.000259	90	.92285	574.8	.00255	.000436		
		45	.91887	560.1	.00166	.000285	45	.94005	584.5	.00403	.000688		
		90	.92832	567.5	.00212	.000364	0	.94782	594.5	.00509	.000870		
.45		0	.94665	600.5	.00553	.000949	90	.93062	623.1	.01137	.001942		
		45	.91998	580.8	.00557	.000956	45	.94283	654.1	.01922	.003284		
		90	.93665	620.8	.01338	.002296	0	.95337	664.8	.01945	.003323		
1.69		0	.94221	593.1	.00525	.000901	90	.92729	613.5	.01168	.001995		
		45	.92498	581.1	.00527	.000904	45	.94005	651.5	.02057	.003514		
		90	.93387	617.8	.01315	.002257	0	.95282	665.1	.02197	.003753		
2.93		0	.93054	587.1	.00552	.000947	90	.92784	612.8	.01174	.002006		
		45	.91887	576.8	.00501	.000860	45	.94671	657.1	.02061	.003521		
		90	.93221	616.5	.01365	.002342	0	.94394	659.5	.02250	.003844		
4.36		0	.93110	589.5	.00600	.001030	90	.92618	611.1	.01161	.001983		
		45	.92554	580.5	.00502	.000861	45	.95837	662.8	.01998	.003413		
		90	.93165	615.5	.01336	.002293	0	.94893	664.1	.02302	.003933		
5.78		0	.91943	584.5	.00668	.001146	90	.92729	608.5	.01091	.001864		
		45	.91721	577.1	.00529	.000908	45	.95282	660.8	.02053	.003507		
		90	.93332	612.8	.01235	.002119	0	.94394	659.1	.02263	.003866		
7.13		0	.91554	585.5	.00748	.001284	90	.92451	602.1	.00980	.001674		
		45	.90943	573.5	.00569	.000976	45	.95393	660.5	.02043	.003490		
		90	.92943	605.1	.01083	.001858	0	.94838	662.8	.02297	.003924		
8.49		0	.89887	581.5	.00830	.001424	90	.91397	583.5	.00643	.001098		
		45	.90720	578.1	.00607	.001042	45	.95171	655.5	.01643	.002807		
		90	.91554	583.8	.00695	.001193	0	.95892	661.5	.01745	.002981		
9.27		0	.88831	554.1	.00373	.000640	90	.92396	572.8	.00310	.000530		
		45	.89276	548.1	.00253	.000434	45	.94949	626.5	.01176	.002009		
		90	—	—	—	—	0	.96114	645.1	.01151	.001966		
10.84		0	.87942	563.1	.00559	.000959	90	.89998	574.1	.00634	.001083		
		45	.84997	533.1	.00475	.000815	45	.95226	638.8	.01581	.002701		
		90	.90832	589.5	.00755	.001296	0	.95282	659.8	.01983	.003388		
11.30		0	.93499	634.8	.01342	.002303	90	—	—	.01834	.003133		
		45	.84720	541.1	.00721	.001237	45	—	—	.01521	.002598		
		90	—	—	—	—	0	.93506	644.8	—	—		
11.59	1.90	0	.90554	589.5	.00927	.001591	90	.90897	613.5	.01183	.002021		
		45	.87164	586.1	.01240	.002128	45	.95504	665.1	.02052	.003506		
		90	.91054	611.5	.01591	.002730	0	.98889	696.5	.02559	.004372		
12.32		0	.87664	565.1	.00758	.001301	90	.90731	592.8	.00981	.001676		
		45	.88053	565.1	.00767	.001316	45	.95004	650.5	.01630	.002785		
		90	.90887	594.1	.01133	.001944	0	.97169	675.5	.02023	.003456		
13.82		0	.91721	579.8	.00545	.000935	90	.94560	607.8	.00690	.001179		
		45	.93832	587.1	.00453	.000777	45	.96503	642.5	.01250	.002135		
		90	.95054	617.1	.00959	.001646	0	.96503	655.1	.01350	.002306		
15.02	1.15	0	.99888	704.8	.02724	.004674	90	.97779	640.1	.00919	.001570		
		45	.93776	639.8	.01413	.002425	45	.97557	672.8	.01592	.002720		
		90	.98610	695.8	.02589	.004443	0	.99389	669.8	.01270	.002170		
15.12		180	.97221	666.1	.00824	.001414	180	—	—	—	—		
15.51		180	.98999	703.5	.01561	.002679	180	.96059	676.8	.01202	.002053		

^aRadius is listed only for hemispherical heat shield, step between parachute and radar canisters, and exit flat face.^bAccuracy depends on magnitude: h > 0.015, accuracy 10 percent; 0.001 ≤ h ≤ 0.015, accuracy 15 percent; h < 0.001, accuracy 20 percent. (h measured in Btu/sq ft-sec^{0.5}R.)

L-1022

03191220.1030

34

TABLE VI. - HEAT-TRANSFER MEASUREMENTS ON EXIT CONFIGURATION - Continued

(b) $M = 4.44$

I-1021

x, in.	r, in. (a)	$\alpha = 0^\circ$						$\alpha = 0^\circ$					
		Leeward ($T_e = 684.2^\circ$)						Windward ($T_e = 678.2^\circ$)					
		β , deg	T_e/T_t	T_w , deg	h (b)	N_{St}	β , deg	T_e/T_t	T_w , deg	h (b)	N_{St}		
-.98	2.66	0	.98393	591.5	.00058	.000311	90	.97073	574.1	.00051	.000272		
		45	.98836	593.5	.00053	.000284	45	.97467	576.5	.00062	.000331		
		90	.98171	589.8	.00053	.000284	0	.97017	573.8	.00062	.000331		
-6.62	3.86	0	—	586.8	LOW	LOW	90	—	573.5	LOW	LOW	LOW	
		45	—	587.1	LOW	LOW	45	—	572.1	LOW	LOW	LOW	
		90	—	588.5	LOW	LOW	0	—	571.5	LOW	LOW	LOW	
-11	5.05	0	.96176	583.5	.00153	.000820	90	.95553	571.8	.00140	.000748		
		45	.95013	578.1	.00149	.000799	45	.94653	565.5	.00135	.000721		
		90	.95567	579.1	.00108	.000579	0	.95441	571.5	.00147	.000785		
+4.5		0	.94736	591.8	.00522	.002798	90	.95272	588.1	.00583	.003114		
		45	.95290	596.8	.00588	.003152	45	.95047	587.1	.00591	.003157		
		90	.95234	593.8	.00505	.002707	0	.94371	581.8	.00527	.002815		
1.69		0	.94791	587.1	.00390	.002091	90	.94259	575.5	.00401	.002142		
		45	.93849	582.1	.00439	.002353	45	.93640	572.5	.00436	.002329		
		90	.94459	585.1	.00412	.002208	0	.94371	576.5	.00400	.002137		
2.93		0	.93627	579.5	.00383	.002053	90	.93640	571.8	.00418	.002233		
		45	.93517	579.8	.00410	.002198	45	.93471	571.1	.00412	.002201		
		90	.93904	581.5	.00403	.002160	0	.93246	572.5	.00389	.002078		
4.36		0	.93406	578.1	.00389	.002085	90	.93640	572.1	.00417	.002227		
		45	.93794	580.8	.00395	.002117	45	.93414	575.5	.00407	.002174		
		90	.93295	577.8	.00405	.002171	0	.93020	570.8	.00375	.002003		
5.78		0	.92464	572.5	.00396	.002123	90	.92120	563.1	.00422	.002254		
		45	.92408	572.1	.00387	.002074	45	.92233	569.1	.00394	.002104		
		90	.92298	572.5	.00437	.002342	0	.92458	564.8	.00405	.002163		
7.13		0	.92575	575.5	.00475	.002546	90	.92176	565.8	.00504	.002692		
		45	.92464	574.5	.00457	.002450	45	.92176	571.1	.00461	.002462		
		90	.91633	570.5	.00492	.002637	0	.92401	566.5	.00469	.002505		
8.49		0	.94015	582.8	.00402	.002155	90	.93977	574.1	.00405	.002163		
		45	.94126	587.1	.00494	.002648	45	.93696	575.8	.00480	.002564		
		90	.94182	584.1	.00418	.002241	0	.93865	579.1	.00396	.002115		
9.27		0	.94459	572.1	.00120	.000643	90	.93527	559.8	.00109	.000582		
		45	.92408	564.8	.00214	.001147	45	.91726	553.1	.00191	.001020		
		90	.93794	568.1	.00107	.000574	0	.93527	557.5	.00098	.000523		
10.84		0	.91965	568.8	.00376	.002015	90	.90657	547.8	.00242	.001293		
		45	.91356	565.1	.00386	.002069	45	.91107	553.8	.00339	.001811		
		90	.91079	561.8	.00270	.001447	0	.90994	552.8	.00231	.001234		
11.30		0	—	—	—	—	90	.91895	568.8	.00566	.003023		
		45	.92076	578.1	.00598	.003205	45	.92401	568.8	.00571	.003050		
		90	—	—	—	—	0	—	—	—	—		
11.59	1.90	0	.97063	617.5	.00896	.004803	90	.96116	602.8	.00878	.004690		
		45	.95511	608.8	.00926	.004964	45	.95609	601.5	.00918	.004903		
		90	.96287	612.1	.00896	.004803	0	.96960	607.5	.00824	.004401		
12.32		0	.96287	602.5	.00547	.002932	90	.95947	603.1	.00667	.003563		
		45	.96232	602.8	.00578	.003098	45	.96229	594.8	.00581	.003103		
		90	.96065	603.5	.00668	.003581	0	.96229	593.8	.00548	.002927		
13.82		0	.97007	589.1	.00131	.000702	90	.95947	575.1	.00147	.000785		
		45	.97839	591.8	.00114	.000611	45	.97748	584.8	.00123	.000657		
		90	.96121	583.8	.00155	.000831	0	.97017	578.1	.00110	.000588		
15.02	1.15	0	.99279	626.5	.00737	.003951	90	.98255	616.8	.00900	.004807		
		45	.95511	605.1	.00803	.004304	45	—	—	.00741	.003958		
		90	.98393	625.8	.00883	.004733	0	.99155	617.1	.00741	.003958		
15.12		180		—	—	—	180	.97748	624.8	.00524	.002799		
		180		.98891	648.5	.01079	.005784	180	—	—	—		
15.51		180		—	—	—	—	—	—	—	—		

^aRadius is listed only for hemispherical heat shield, step between parachute and radar canisters, and exit flat face.

^bAccuracy depends on magnitude: $h > 0.015$, accuracy 10 percent; $0.001 \leq h \leq 0.015$, accuracy 15 percent; $h < 0.001$, accuracy 20 percent. (h measured in $\text{Btu}/\text{sq ft}\cdot\text{sec}^{-0.5}$.)

DECLASSIFIED

35

TABLE VI. - HEAT-TRANSFER MEASUREMENTS ON EXIT CONFIGURATION - Continued

(b) M = 4.44 - Continued

x, in.	r, in. (a)	$\alpha = 50^\circ$						$\alpha = -50^\circ$					
		θ , deg	T_e/T_t	T_w , deg	h (b)	N_{St}	θ , deg	T_e/T_t	T_w , deg	h (b)	N_{St}		
-.98	2.66	0	.97996	587.5	.00063	.000339	90	.97753	577.8	.00038	.000202		
		45	.98330	589.8	.00066	.000366	45	.98483	583.1	.00045	.000239		
		90	.97606	585.8	.00067	.000361	0	—	582.1	LOW	LOW		
-.62	3.86	0	—	581.1	LOW	LOW	90	—	579.1	LOW	LOW		
		45	—	581.8	LOW	LOW	45	—	581.1	LOW	LOW		
		90	—	583.5	LOW	LOW	0	—	582.5	LOW	LOW		
-.11	5.05	0	.95547	578.5	.00144	.000775	90	.95675	571.1	.00094	.000500		
		45	.94712	574.1	.00147	.000791	45	.95226	569.5	.00132	.000702		
		90	.95046	576.5	.00129	.000694	0	.96069	574.1	.00130	.000691		
.45		0	.93655	583.1	.00365	.001964	90	.95282	585.8	.00501	.002665		
		45	.95213	597.5	.00488	.002626	45	.95395	591.5	.00704	.003744		
		90	.94657	593.5	.00454	.002443	0	.95002	590.8	.00745	.003962		
1.69		0	.94100	580.5	.00281	.001512	90	.94721	580.5	.00355	.001888		
		45	.94100	584.8	.00379	.002040	45	.94722	579.1	.00538	.002861		
		90	.94211	588.8	.00396	.002131	0	.95170	590.1	.00528	.002808		
2.93		0	.93098	574.1	.00284	.001528	90	.94159	585.8	.00369	.001963		
		45	.93822	583.1	.00374	.002013	45	.94159	585.8	.00517	.002750		
		90	.93989	585.1	.00399	.002147	0	.94215	587.8	.00558	.002968		
4.36		0	.93376	576.1	.00292	.001571	90	.94103	574.5	.00405	.002154		
		45	.93989	584.1	.00368	.001980	45	.94215	581.8	.00475	.002526		
		90	.93989	585.5	.00423	.002276	0	.94047	582.8	.00514	.002734		
5.78		0	.92987	574.8	.00308	.001657	90	.92418	570.5	.00404	.002149		
		45	.92319	574.8	.00383	.002061	45	.92980	570.5	.00430	.002287		
		90	.93376	582.8	.00440	.002368	0	.93373	578.1	.00506	.002691		
7.13		0	.93432	579.1	.00336	.001808	90	.92306	565.8	.00475	.002526		
		45	.91929	574.5	.00454	.002443	45	.92475	568.8	.00531	.002824		
		90	.92597	582.1	.00533	.002868	0	.92812	572.8	.00597	.003175		
8.49		0	.93432	579.5	.00306	.001647	90	.94103	574.5	.00395	.002101		
		45	.93376	582.5	.00381	.002050	45	.93766	578.8	.00548	.002915		
		90	.95102	593.1	.00391	.002104	0	.94159	578.8	.00492	.002617		
9.27		0	.93655	568.1	.00128	.000689	90	.93373	557.8	.00104	.000553		
		45	.91317	557.1	.00192	.001033	45	—	562.1	.00115	.000612		
		90	.94267	570.5	.00113	.000608	0	.93991	562.1	—	—		
10.84		0	.92709	573.1	.00297	.001598	90	.90397	546.5	.00219	.001165		
		45	.89692	555.1	.00322	.001733	45	.91351	556.8	.00371	.001973		
		90	.91540	566.5	.00321	.001727	0	.91351	553.1	.00279	.001484		
11.30		0	—	—	—	—	90	.91464	566.5	.00580	.003085		
		45	.90649	569.8	.00525	.002825	45	—	567.8	.00532	.002829		
		90	—	—	—	—	0	—	—	—	—		
11.59	1.90	0	.97050	608.8	.00457	.002459	90	.95563	598.5	.00777	.004132		
		45	.93543	596.8	.00685	.003686	45	.95114	600.1	.01060	.005638		
		90	.95937	621.1	.00987	.005311	0	.96799	611.8	.01094	.005818		
12.32		0	.95658	594.8	.00365	.001964	90	.94721	585.5	.00558	.002968		
		45	.93822	587.5	.00446	.002400	45	.95282	589.5	.00613	.003260		
		90	.95157	604.8	.00673	.003622	0	.95395	593.1	.00537	.002856		
13.82		0	.96438	591.1	.00213	.001146	90	.97136	579.1	.00085	.000452		
		45	.96326	588.8	.00192	.001033	45	.96293	575.1	.00139	.000739		
		90	.95046	589.1	.00324	.001744	0	.95058	571.8	.00165	.000878		
15.02	1.15	0	.99387	644.1	.01056	.005683	90	.98203	608.1	.00601	.003196		
		45	.95881	615.5	.00797	.004289	45	—	613.1	.00624	.003319		
		90	.98497	645.1	.01307	.007033	0	.99045	613.1	—	—		
15.12		180	—	—	—	—	180	.97697	621.5	.00467	.002484		
15.51		180	—	—	—	—	180	.98820	636.1	.00792	.004212		

^aRadius is listed only for hemispherical heat shield, step between parachute and radar canisters, and exit flat face.^bAccuracy depends on magnitude: $h > 0.015$, accuracy 10 percent; $0.001 \leq h \leq 0.015$, accuracy 15 percent; $h < 0.001$, accuracy 20 percent. (h measured in Btu/sq ft-sec-R°)

0319122A1030

40

TABLE VII. - HEAT-TRANSFER MEASUREMENTS ON ESCAPE CONFIGURATION - Continued

(a) M = 3.50 - Continued

x, in.	r, in. (a)	$\alpha = 50^\circ$ Leeward ($T_t = 711.8^\circ$)					$\alpha = -5^\circ$ Windward ($T_t = 714.2^\circ$)				
		θ , deg	T_e/T_t	T_w , deg (b)	h (b)	N _{St}	θ , deg	T_e/T_t	T_w , deg (b)	h (b)	N _{St}
-•.98	2.66	0	.94222	565.1	.00104	.000177	90	.94270	574.1	.00153	.000260
		45	.93829	565.1	.00140	.000238	45	.94548	575.5	.00153	.000260
		90	.93493	566.1	.00187	.000317	0	.93936	573.1	.00181	.000308
-.62	3.86	0	.94278	563.5	.00082	.000139	90	.93380	568.5	.00153	.000260
		45	.93549	561.5	.00114	.000193	45	.94493	576.1	.00168	.000286
		90	.92539	557.8	.00145	.000246	0	.94159	573.8	.00172	.000293
-.11	5.05	0	.92820	562.1	.00233	.000395	90	.93658	576.1	.00291	.000495
		45	.92595	569.8	.00329	.000558	45	.94103	588.8	.00542	.000922
		90	.92876	573.5	.00344	.000584	0	.92991	577.5	.00444	.000755
-.45		0	.92259	604.1	.01258	.002135	90	.94270	631.5	.01583	.002693
		45	.92932	611.1	.01511	.002565	45	.93380	641.1	.02440	.004151
		90	.92090	620.5	.02174	.003690	0	.91378	630.8	.02464	.004192
1.69		0	.92146	592.5	.00985	.001672	90	.93547	619.1	.01350	.002296
		45	.91586	591.5	.01127	.001913	45	.90599	613.5	.01952	.003321
		90	.89005	589.1	.01603	.002721	0	.89897	614.5	.02010	.003419
2.93		0	.91866	589.5	.00945	.001604	90	.93491	618.1	.01368	.002327
		45	.91866	593.8	.01106	.001877	45	.90043	610.1	.01898	.003229
		90	.88164	581.1	.01544	.002621	0	.88674	606.5	.02003	.003407
4.36		0	.92315	590.8	.00912	.001548	90	.95049	627.8	.01341	.002281
		45	.93156	601.1	.01067	.001811	45	.90209	610.8	.01872	.003184
		90	.89791	587.1	.01366	.002318	0	.88429	603.5	.01978	.003365
5.78		0	.92595	590.5	.00869	.001475	90	.92991	615.1	.01372	.002334
		45	.93212	599.8	.01005	.001706	45	.89598	605.5	.01755	.002985
		90	.89566	581.8	.01223	.002076	0	.87984	604.1	.01855	.003156
7.13		0	.93212	593.5	.00836	.001419	90	.92546	614.8	.01433	.002438
		45	.93100	599.1	.01022	.001735	45	.90043	610.8	.01887	.003210
		90	.91305	586.8	.01018	.001728	0	.88930	597.1	.01554	.002644
8.49		0	.93605	594.5	.00772	.001310	90	.92935	614.1	.01187	.002019
		45	.93044	602.5	.01103	.001872	45	.89319	607.8	.01498	.002548
		90	.91810	589.1	.00940	.001595	0	.89208	589.5	.01191	.002026
9.27		0	.93156	579.1	.00431	.000732	90	.91711	576.1	.00419	.000713
		45	.91249	570.1	.00577	.000979	45	.88263	564.1	.00723	.001230
		90	.91249	564.5	.00390	.000662	0	.88596	560.8	.00510	.000868
10.84		0	.91754	568.1	.00443	.000752	90	.89319	566.1	.00603	.001026
		45	.92427	581.8	.00657	.001115	45	.89598	580.1	.00955	.001625
		90	.90632	570.1	.00624	.001059	0	.88207	564.8	.00738	.001255
11.30		0	.93605	603.1	.00716	.001215	90	.90710	594.5	.01000	.001701
		90	.92876	602.5	.00811	.001377	0	.90043	598.8	.01297	.002206
12.32		0	.95961	607.1	.00549	.000932	90	.92991	599.8	.00833	.001417
		45	.95400	617.1	.00799	.001356	45	.93491	637.5	.01467	.002496
		90	.96017	623.1	.00871	.001478	0	.93324	604.5	.00825	.001403
13.82		0	.95063	597.8	.00665	.001129	90	.90543	598.1	.01178	.002004
		45	.93941	597.1	.00774	.001314	45	.88429	581.5	.01142	.001943
		90	.92707	591.5	.00857	.001455	0	.94715	613.8	.00975	.001659

^aRadius is listed only for hemispherical heat shield.^bAccuracy depends on magnitude: $h > 0.015$, accuracy 10 percent; $0.001 \leq h \leq 0.015$, accuracy 15 percent; $h < 0.001$, accuracy 20 percent. (h measured in Btu/sq ft-sec-R.)

I-1022

DECLASSIFIED

41

TABLE VII. - HEAT-TRANSFER MEASUREMENTS ON ESCAPE CONFIGURATION - Continued

(a) M = 3.50 - Continued

x, in.	r, in. (a)	$\alpha = 10^0$ Leeward ($T_t = 715.80$)					$\alpha = -10^0$ Windward ($T_t = 713.80$)				
		θ , deg	T_e/T_t	T_w , deg	h (b)	N_{St}	θ , deg	T_e/T_t	T_w , deg	h (b)	N_{St}
-•98	2•66	0	.93336	563•5	.00118	.000201	90	.93425	567•1	.00138	.000235
		45	.94064	567•5	.00135	.000230	45	.93480	566•5	.00144	.000245
		90	.94736	572•8	.00146	.000248	0	.93480	564•8	.00108	.000184
-•62	3•86	0	.93336	561•5	.00112	.000191	90	.92700	562•1	.00131	.000223
		45	.93448	564•5	.00141	.000240	45	.93592	568•1	.00144	.000245
		90	.93896	566•8	.00132	.000225	0	.93759	566•8	.00107	.000182
-•11	5•05	0	.92832	568•1	.00243	.000413	90	.92756	572•8	.00279	.000474
		45	.92608	579•1	.00374	.000636	45	.93759	583•5	.00512	.000871
		90	.93840	572•1	.00267	.000454	0	.93592	584•1	.00410	.000697
+•45		0	.91992	592•1	.00886	.001508	90	.92868	616•8	.01581	.002688
		45	.92552	621•1	.01371	.002333	45	.94205	644•1	.02552	.004339
		90	.94008	628•5	.01280	.002178	0	.94093	647•1	.02629	.004470
1•69		0	.91432	580•1	.00674	.001147	90	.92255	605•1	.01276	.002170
		45	.89808	583•8	.01077	.001833	45	.91698	619•8	.02078	.003533
		90	.93224	611•5	.01209	.002057	0	.93090	635•5	.02372	.004033
2•93		0	.91152	576•5	.00639	.001087	90	.92088	604•1	.01316	.002238
		45	.89304	578•8	.00999	.001700	45	.91029	616•1	.02032	.003455
		90	.92272	608•1	.01341	.002282	0	.92143	629•1	.02392	.004067
4•36		0	.91936	581•1	.00612	.001041	90	.93369	614•5	.01367	.002324
		45	.89920	580•5	.00912	.001552	45	.90973	615•8	.02104	.003578
		90	.92776	615•5	.01441	.002452	0	.91530	626•8	.02478	.004213
5•78		0	.92720	585•1	.00605	.001029	90	.90917	599•5	.01413	.002403
		45	.89304	573•5	.00821	.001397	45	.90082	610•1	.02063	.003508
		90	.89696	597•8	.01540	.002620	0	.90249	618•1	.02500	.004251
7•13		0	.93560	590•1	.00605	.001029	90	.90126	593•5	.01345	.002287
		45	.89248	574•8	.00853	.001451	45	.90305	612•1	.02131	.003623
		90	.88744	590•1	.01438	.002447	0	.89345	611•8	.02470	.004200
8•49		0	.93840	595•1	.00637	.001084	90	.88843	574•8	.00941	.001600
		45	.89416	573•5	.00806	.001371	45	.89847	609•1	.01935	.003290
		90	.88800	585•1	.00930	.001582	0	.90472	608•5	.01726	.002935
9•27		0	.93392	581•1	.00379	.000645	90	.89011	548•5	.00272	.000462
		45	.88016	550•5	.00500	.000851	45	.89513	576•8	.00943	.001603
		90	.89472	556•1	.00349	.000594	0	.89847	575•1	.00742	.001262
10•84		0	.92608	573•8	.00400	.000681	90	.86724	542•5	.000506	.000860
		45	.88632	556•1	.00526	.000895	45	.90416	586•8	.01100	.001870
		90	.87456	553•1	.00607	.001033	0	.89011	578•5	.01045	.001777
11•30		0	.93896	596•5	.00592	.001007	90	.88063	570•1	.00896	.001524
		90	.89304	584•5	.00985	.001676	0	.91530	621•8	.01986	.003377
12•32		0	.95128	605•5	.00532	.000905	90	.91586	585•5	.00777	.001321
		45	.92608	593•8	.00577	.000982	45	.93648	635•8	.01910	.003248
13•82		0	.95912	609•8	.00678	.001154	90	.91698	607•1	.01394	.002370
		45	.92832	587•8	.00628	.001069	45	.89513	588•5	.01212	.002061
		90	.91992	591•5	.00832	.001416	0	.95208	613•8	.00927	.001576

^aRadius is listed only for hemispherical heat shield.^bAccuracy depends on magnitude: $h > 0.015$, accuracy 10 percent; $0.001 \leq h \leq 0.015$, accuracy 15 percent; $h < 0.001$, accuracy 20 percent. (h measured in Btu/sq ft-sec^{-0.5}R.)

031912291030

42

TABLE VII. - HEAT-TRANSFER MEASUREMENTS ON ESCAPE CONFIGURATION - Continued

(a) $M = 3.50$ - Concluded

x, in.	r, in. (a)	Leeward ($T_t = 716.2^\circ$)						Windward ($T_t = 711.5^\circ$)					
		θ , deg	T_e/T_t	T_w , deg	h (b)	N_{St}	θ , deg	T_e/T_t	T_w , deg	h (b)	N_{St}		
-.98	2.66	0	.91902	555.8	.00125	.000123	90	.92948	559.8	.00102	.000173		
		45	.92740	557.5	.00072	.000122	45	.93283	562.1	.00113	.000192		
		90	.93354	563.1	.00104	.000177	0	.93843	563.5	.00082	.000139		
-.62	3.86	0	.91902	555.1	.00111	.000189	90	.92276	556.1	.00105	.000178		
		45	.91791	555.1	.00128	.000218	45	.93507	565.1	.00131	.000222		
		90	.92293	556.5	.00101	.000172	0	.94347	566.8	.00092	.000156		
-.11	5.05	0	.92628	566.8	.00177	.000301	90	.92220	566.5	.00255	.000433		
		45	.90841	559.1	.00260	.000442	45	.93787	582.1	.00494	.000838		
		90	.92461	569.1	.00269	.000458	0	.94291	587.1	.00417	.000708		
+.45		0	.92852	588.8	.00644	.001096	90	.92052	606.5	.01254	.002128		
		45	.91791	587.8	.00834	.001419	45	.94739	647.5	.02426	.004117		
		90	.92852	614.5	.01418	.002412	0	.95354	656.1	.02523	.004285		
1.69		0	.92852	584.8	.00575	.000978	90	.91604	595.8	.01021	.001733		
		45	.90506	572.8	.00671	.001142	45	.92556	628.1	.02244	.003811		
		90	.91567	600.5	.01223	.002081	0	.94571	646.1	.02331	.003956		
2.93		0	.92237	582.1	.00603	.001026	90	.91269	591.5	.00978	.001660		
		45	.89613	566.5	.00640	.001089	45	.91604	623.0	.02288	.003883		
		90	.90506	593.1	.01234	.002099	0	.93563	639.5	.02329	.003952		
4.36		0	.92070	583.1	.00646	.001099	90	.92388	599.1	.00980	.001663		
		45	.89110	562.1	.00618	.001051	45	.91045	620.0	.02312	.003923		
		90	.91902	598.1	.01095	.001863	0	.92892	636.5	.02423	.004112		
5.78		0	.91791	583.5	.00711	.001210	90	.90597	588.5	.01018	.001728		
		45	.88384	556.1	.00578	.000983	45	.89645	609.5	.02131	.003616		
		90	.90897	587.8	.00988	.001681	0	.91492	626.5	.02390	.004056		
7.13		0	.92293	588.1	.00744	.001266	90	.90541	588.1	.01012	.001717		
		45	.89389	563.8	.00607	.001033	45	.89590	604.1	.01891	.003209		
		90	.90841	588.5	.01005	.001710	0	.90261	618.5	.02347	.003983		
8.49		0	.91902	588.5	.00755	.001284	90	.87799	571.5	.00796	.001351		
		45	.90841	577.1	.00642	.001092	45	.89254	595.8	.01478	.002508		
		90	.88384	566.1	.00756	.001286	0	.90709	610.8	.01636	.002776		
9.27		0	.90506	562.5	.00361	.000614	90	.89142	549.1	.00302	.000512		
		45	.89613	554.8	.00368	.000626	45	.88022	565.8	.00834	.001415		
		90	.89669	554.8	.00308	.000524	0	.89645	577.5	.00821	.001393		
10.84		0	.89669	553.5	.00330	.000561	90	.87575	543.8	.00459	.000779		
		45	.85369	526.5	.00328	.000558	45	.88662	574.5	.00930	.001578		
		90	.88384	556.8	.00596	.001014	0	.88694	580.5	.01193	.001957		
11.30		0	.90953	577.8	.00472	.000803	90	.89030	573.8	.00830	.001408		
		90	.89724	592.1	.01173	.001996	0	.91380	618.0	.01671	.002836		
12.32		0	.91679	571.8	.00409	.000696	90	.90485	586.5	.00771	.001308		
		45	.90506	563.5	.00630	.001072	45	.93395	640.8	.02079	.003528		
		90	.91846	601.1	.01007	.001713	0	.94962	626.9	.02236	.002097		
13.82		0	.93410	593.5	.00668	.001136	90	.88470	599.8	.01550	.002630		
		45	.89278	566.5	.00629	.001070	45	.87519	596.1	.01253	.002126		
		90	.90339	583.1	.00879	.001495	0	.95354	622.5	.01033	.001753		

^aRadius is listed only for hemispherical heat shield.^bAccuracy depends on magnitude: $h > 0.015$, accuracy 10 percent; $0.001 \leq h \leq 0.015$, accuracy 15 percent; $h < 0.001$, accuracy 20 percent. (h measured in Btu/sq ft-sec- 0 R.)

L-1022

REF ID: A6492
~~REF ID: A6492~~
~~REF ID: A6492~~
REF ID: A6492
~~REF ID: A6492~~
~~REF ID: A6492~~

43

TABLE VII. - HEAT-TRANSFER MEASUREMENTS ON ESCAPE CONFIGURATION - Continued

(b) M = 4.44

$$\alpha = 0^\circ$$

L-1022

x, in.	r, in. (a)	Leeward ($T_t = 666.8^\circ$)				
		ϕ , deg	T_e/T_t	T_w , deg	h (b)	N_{St}
-.98	2.66	0	.95654	565.5	.00043	.000229
		45	.96049	567.5	.00033	.000175
		90	.94638	559.8	.00047	.000250
-.62	3.86	0	—	562.8	LOW	LOW
		45	.95315	562.8	.00032	.000170
		90	—	560.5	LOW	LOW
-.11	5.05	0	.91251	545.8	.00156	.000829
		45	.91985	551.5	.00209	.001111
		90	.93001	555.8	.00167	.000888
+.45		0	.87357	541.1	.00733	.003898
		45	.90066	556.5	.00651	.003462
		90	.92662	575.1	.00831	.004419
1.69		0	.86510	530.5	.00544	.002893
		45	.87526	534.1	.00446	.002372
		90	.90179	553.1	.00576	.003063
2.93		0	.85946	532.5	.00482	.002563
		45	.87695	534.1	.00400	.002127
		90	.89671	549.8	.00585	.003111
4.36		0	.87074	531.5	.00464	.002467
		45	.89219	547.8	.00380	.002021
		90	.90969	558.8	.00615	.003270
5.78		0	.88768	539.8	.00366	.001946
		90	.88881	546.5	.00623	.003313
7.13		0	.89671	543.1	.00325	.001728
		45	.90969	552.5	.00395	.002100
		90	.89050	550.8	.00571	.003036
8.49		0	.91420	551.5	.00243	.001292
		45	.92775	564.1	.00386	.002052
		90	.93227	565.1	.00364	.001935
9.27		0	.92154	548.5	.00112	.000596
		45	.90969	547.8	.00181	.000962
		90	.92888	552.8	.00081	.000431
10.84		0	.91759	549.1	.00174	.000925
		45	.91815	553.1	.00272	.001446
		90	.90404	543.1	.00221	.001175
11.30		0	.94130	566.8	.00235	.001250
		90	.92380	563.5	.00388	.002063
12.32		0	.95879	576.8	.00221	.001175
		45	.95710	580.8	.00317	.001686
		90	.95146	578.5	.00356	.001893
13.82		0	.93791	571.5	.00287	.001526
		45	.92323	557.8	.00295	.001569
		90	.92098	557.5	.00335	.001781

^aRadius is listed only for hemispherical heat shield.^bAccuracy depends on magnitude: $h > 0.015$, accuracy 10 percent; $0.001 \leq h \leq 0.015$, accuracy 15 percent; $h < 0.001$, accuracy 20 percent. (h measured in Btu/sq ft-sec-R.)

TABLE VII. - HEAT-TRANSFER MEASUREMENTS ON ESCAPE CONFIGURATION - Continued

(b) M = 4.44 - Continued

x, in.	r, in. (a)	$\alpha = 5^\circ$					$\alpha = -5^\circ$					
		Leeward ($T_t = 677.2^\circ$)				Windward ($T_t = 674.2^\circ$)						
		θ , deg	T_e/T_t	T_w , deg	h (b)	N_{St}		θ , deg	T_e/T_t	T_w , deg	h (b)	N_{St}
-.98	2.66	0		567.8 563.5 559.5	LOW .00053 .00054	LOW .000283 .000288	90 45 0	.95877 .96668 .96272	565.1 571.5 568.5	.00036 .00058 .00052	.000194 .000313 .000281	
		45	.95587 .94795									
		90										
-.62	3.86	0		566.1 556.8 556.8	LOW .00032 .00045	LOW .000171 .000240	90 45 0	.96046	564.5 567.1 568.5	LOW .00050 LOW	LOW .000270 LOW	
		45	.94569 .94399									
		90										
-.11	5.05	0	.93777 .91797 .93041	556.8 546.1 557.1	.00114 .00134 .00201	.000609 .000716 .001073	90 45 0	.93787 .93731 .92827	559.8 565.5 558.1	.00132 .00245 .00216	.000712 .001322 .001165	
		45										
		90										
+.45		0	.92815 .90383 .92702	566.8 552.5 582.8	.00402 .00453 .00970	.002147 .002419 .005180	90 45 0	.94013 .93110 .90343	579.8 584.1 566.5	.00654 .01103 .01066	.003528 .005950 .005751	
		45										
		90										
1.69		0	.93041 .89760 .90043	563.5 542.5 557.8	.00311 .00318 .00678	.001661 .001698 .003620	90 45 0	.93449 .90343 .89439	570.5 559.5 555.5	.00470 .00805 .00829	.002535 .004343 .004472	
		45										
		90										
2.93		0	.92306 .90326 .89195	558.1 546.5 551.8	.00298 .00332 .00681	.001591 .001773 .003636	90 45 0	.93336 .89608 .88422	569.1 555.1 548.5	.00467 .00787 .00796	.002519 .004245 .004294	
		45										
		90										
4.36		0	.92759 .91514 .90383	560.1 554.8 556.8	.00275 .00345 .00601	.001468 .001842 .003209	90 45 0	.94860 .89608 .88479	577.1 554.5 547.8	.00427 .00748 .00762	.002303 .004035 .004111	
		45										
		90										
5.78		0	.93211 .91062 .88912	562.1 552.8 545.8	.00256 .00347 .00541	.001367 .001853 .002889	90 45 0	.92658 .88084 .89044	564.1 544.1 548.5	.00442 .00699 .00641	.002384 .003771 .003458	
		45										
		90										
7.13		0	.93890 .91797 .89704	565.8 557.1 548.1	.00256 .00361 .00447	.001367 .001928 .002387	90 45 0	.92263 .88310 .90399	562.5 545.8 552.1	.00442 .00724 .00495	.002384 .003906 .002670	
		45										
		90										
8.49		0	.94343 .93720 .92532	567.5 567.5 558.5	.00227 .00304 .00281	.001212 .001623 .001501	90 45 0	.94691 .90512 .91077	571.5 553.1 550.8	.00297 .00482 .00318	.001602 .002600 .001715	
		45										
		90										
9.27		0	.94682 .92532 .92702	564.1 552.1 551.1	.00125 .00140 .00106	.000667 .000748 .000566	90 45 0	.93562 .88887 .91472	556.1 532.1 544.8	.00099 .00174 .00118	.000534 .000939 .000637	
		45										
		90										
10.84		0	.93890 .92815 .92136	560.1 555.1 550.8	.00135 .00185 .00174	.000721 .000988 .000929	90 45 0	.91585 .89721 .90964	547.8 541.8 543.8	.00186 .00308 .00173	.001003 .001662 .000933	
		45										
		90										
11.30		0	.95644 .93890	574.1 565.5	.00176 .00232	.000940 .001239	90 0	.92940 .93223	561.8 562.1	.00303 .00255	.001035 .001376	
		45										
		90										
12.32		0	.96153 .95417 .95644	572.8 574.5 576.1	.00127 .00218 .00231	.000678 .001164 .001234	90 45 0	.94804 .94691 .94635	572.1 578.1 568.8	.00280 .00429 .00222	.001510 .002314 .001198	
		45										
		90										
13.82		0	.95644 .95474 .95135	572.8 576.1 574.1	.00210 .00263 .00288	.001121 .001404 .001538	90 45 0	.91585 .91754 .95312	553.1 557.1 576.8	.00304 .00359 .00287	.001640 .001937 .001548	
		45										
		90										

^aRadius is listed only for hemispherical heat shield.^bAccuracy depends on magnitude: $h > 0.015$, accuracy 10 percent; $0.001 \leq h \leq 0.015$, accuracy 15 percent; $h < 0.001$, accuracy 20 percent. (h measured in Btu/sq ft-sec⁻²R.)

DECLASSIFIED

45

TABLE VII. - HEAT-TRANSFER MEASUREMENTS ON ESCAPE CONFIGURATION - Continued

(b) M = 4.44 - Continued

x, in.	r, in. (a)	$\alpha = 10^\circ$					$\alpha = -10^\circ$				
		Leeward ($T_t = 576.2^\circ$)					Windward ($T_t = 660.2^\circ$)				
		θ , deg	T_e/T_t	T_w , deg	h (b)	N _{St}	θ , deg	T_e/T_t	T_w , deg	h (b)	N _{St}
- .98	2.66	0 45 90	.96327 — —	566.1 567.8 569.5	.00032 LOW LOW	.000171 LOW	90 45 0	.95137 .96098 —	560.5 565.8 565.8	.00040 .00036 LOW	.000213 .000191 LOW
- .62	3.86	0 45 90	.95253 — —	563.5 561.8 569.8	.00035 LOW LOW	.000187 LOW	90 45 0	.95477 — —	559.8 562.8 564.1	LOW .00042 LOW	LOW .000223 LOW
- .11	5.05	0 45 90	.94010 .92484 .93388	557.1 553.5 557.1	.00073 .00173 .00121	.000389 .000922 .000645	90 45 0	.92989 .93215 .93272	552.5 561.5 559.1	.00105 .00233 .00186	.000558 .001238 .000988
.45		0 45 90	.93332 .91693 .92597	560.8 568.8 573.1	.00173 .00522 .00495	.000922 .002783 .002639	90 45 0	.92989 .93215 .92989	570.5 582.8 581.5	.00620 .01101 .01081	.003294 .005850 .005744
1.69		0 45 90	.94462 .88981 .93049	568.1 543.8 569.1	.00153 .00370 .00369	.000816 .001973 .001967	90 45 0	.92084 .90840 .92254	560.5 562.1 573.1	.00463 .00840 .00917	.002460 .004463 .004872
2.93		0 45 90	.93897 .88359 .92936	563.1 539.5 569.8	.00154 .00343 .00399	.000821 .001829 .002127	90 45 0	.91632 .90162 .91067	558.5 557.8 566.8	.00536 .00792 .00972	.002848 .004208 .005164
4.36		0 45 90	.94236 .89490 .93558	566.1 544.1 576.8	.00172 .00295 .00474	.000917 .001573 .002527	90 45 0	.92876 .90162 .90332	570.1 557.8 563.1	.00518 .00793 .01026	.002752 .004213 .005451
5.78		0 45 90	.94292 .89546 .89942	567.1 542.8 557.8	.00182 .00266 .00551	.000970 .001418 .002938	90 45 0	.90219 .88918 .88862	552.8 550.8 553.5	.00486 .00819 .00984	.002582 .004352 .005228
7.13		0 45 90	.94575 .90902 .88359	570.1 548.8 547.8	.00212 .00230 .00550	.001130 .001226 .002932	90 45 0	.89257 .89201 .88466	550.1 552.8 550.1	.00496 .00839 .00936	.002635 .004458 .004973
8.49		0 45 90	.94518 .92767 .91354	572.8 555.8 555.1	.00222 .00150 .00282	.001184 .000800 .001504	90 45 0	.91519 .91293 .91406	547.8 561.5 560.5	.00207 .00672 .00588	.001100 .003570 .003124
9.27		0 45 90	.94575 .91128 .91919	563.8 543.1 547.1	.00094 .00111 .00084	.000501 .000592 .000448	90 45 0	.92141 .89710 .91180	544.5 539.1 545.5	.00064 .00257 .00196	.000340 .001365 .001041
10.84		0 45 90	.94349 .90846 .89942	563.1 542.1 541.8	.00123 .00132 .00205	.000656 .000704 .001093	90 45 0	.89710 .90105 .89653	534.1 545.1 540.1	.00150 .00394 .00285	.000797 .002093 .001514
11.30		0 90	.95988 .91015	577.8 556.8	.00164 .00291	.000874 .001552	90 0	.90614 .92141	546.8 563.5	.00250 .00494	.001328 .002625
12.32		0 45 90	.95649 .93727 .92823	572.1 561.5 569.1	.00126 .00129 .00283	.000672 .000688 .001509	90 45 0	.92706 .93611 .94742	556.5 577.1 574.1	.00251 .00653 .00368	.001334 .003470 .001955
13.82		0 45 90	.95988 .94066 .93388	581.8 568.1 565.8	.00229 .00219 .00259	.001221 .001168 .001381	90 45 0	.92310 .90388 .94685	563.1 549.8 570.5	.00476 .00444 .00283	.002529 .002359 .001504

^aRadius is listed only for hemispherical heat shield.^bAccuracy depends on magnitude: $h > 0.015$, accuracy 10 percent; $0.001 \leq h \leq 0.015$, accuracy 15 percent; $h < 0.001$, accuracy 20 percent. (h measured in Btu/sq ft-sec-°R.)

TABLE VII. - HEAT-TRANSFER MEASUREMENTS ON ESCAPE CONFIGURATION - Concluded

(b) M = 4.44 - Concluded

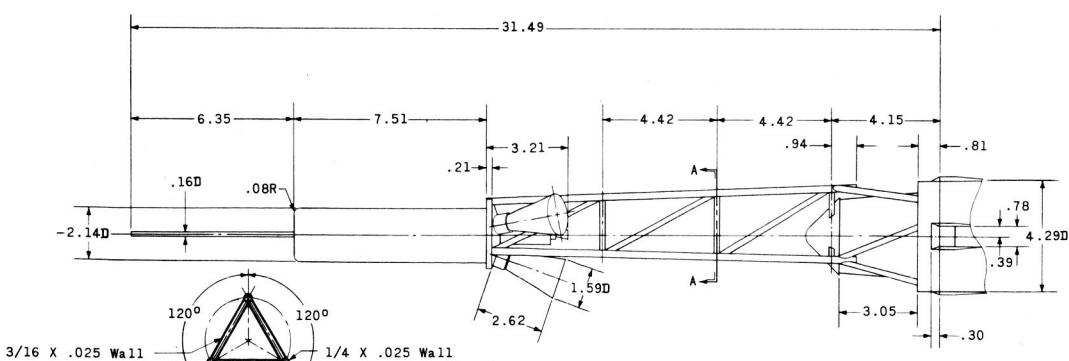
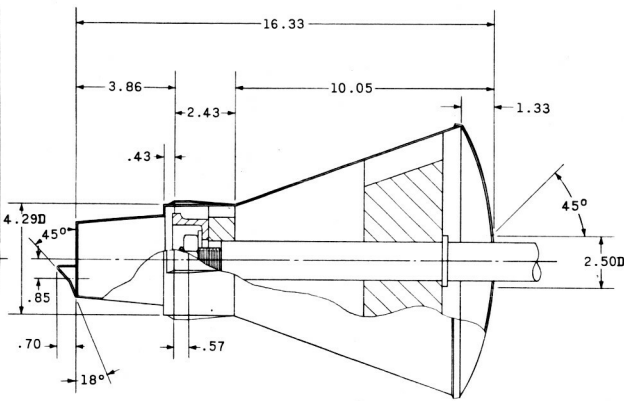
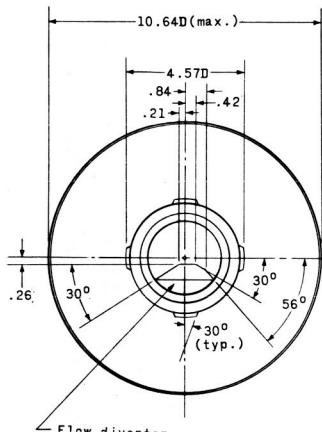
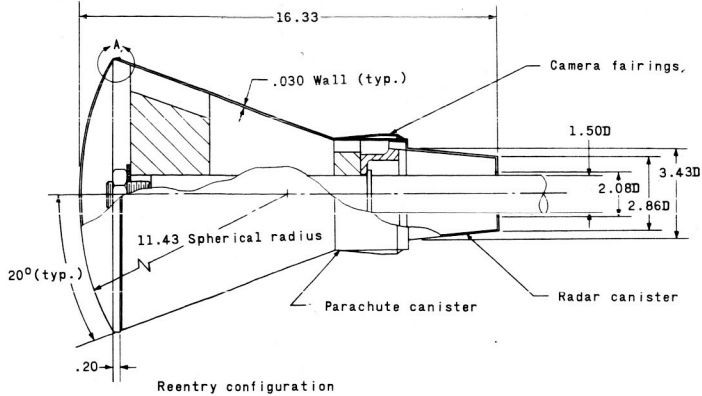
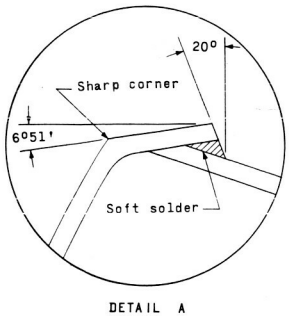
I-1022

x, in.	r, in. (a)	$\alpha = 15^\circ$					$\alpha = -15^\circ$				
		Leeward ($T_t = 682.5^\circ$)			Windward ($T_t = 664.8^\circ$)						
		θ , deg	T_e/T_t	T_w , deg	h (b)	N _{St}	θ , deg	T_e/T_t	T_w , deg	h (b)	N _{St}
-0.98	2.66	0	—	555.5	LOW	LOW	90	.94525	557.1	.00030	.000159
		45	—	558.8	LOW	LOW	45	.95992	566.1	.00031	.000165
		90	—	558.1	LOW	LOW	0	—	567.1	LOW	LOW
-0.62	3.86	0	—	553.1	LOW	LOW	90	—	555.8	LOW	LOW
		45	—	555.5	LOW	LOW	45	—	562.1	LOW	LOW
		90	—	558.5	LOW	LOW	0	—	564.1	LOW	LOW
-0.11	5.05	0	.92779	551.5	.00069	.000370	90	.91477	546.1	.00128	.000680
		45	.91143	543.8	.00109	.000584	45	.92436	560.5	.00315	.001673
		90	.92441	552.8	.00138	.000740	0	.93114	562.8	.00251	.001333
+0.45		0	.92384	558.1	.00179	.000959	90	.91477	562.8	.00722	.003834
		45	.89169	547.5	.00292	.001565	45	.93339	590.8	.01642	.008719
		90	.93118	581.1	.00466	.002498	0	.93904	591.1	.01426	.007572
1.69		0	.93005	562.8	.00173	.000927	90	.91138	556.5	.00531	.002820
		45	.87589	529.8	.00204	.001093	45	.91420	572.8	.01257	.006674
		90	.92723	575.8	.00429	.002299	0	.93565	587.5	.01352	.007179
2.93		0	.91933	556.1	.00214	.001147	90	.90630	552.8	.00532	.002825
		45	.86969	525.1	.00204	.001093	45	.90743	569.1	.01241	.006589
		90	.91200	565.8	.00497	.002664	0	.92323	580.1	.01401	.007439
4.36		0	.91764	556.5	.00219	.001174	90	.91928	560.1	.00505	.002681
		45	.87307	527.1	.00156	.000836	45	.90461	567.5	.01240	.006584
		90	.92159	568.1	.00420	.002251	0	.91477	575.8	.01471	.007811
5.78		0	.91538	555.5	.00223	.001195	90	.89947	548.5	.00492	.002612
		45	.87025	523.8	.00139	.000745	45	.88140	553.1	.01255	.006664
		90	.90353	556.8	.00391	.002096	0	.89501	563.8	.01495	.007938
7.13		0	.92328	559.5	.00213	.001142	90	.89270	543.8	.00474	.002517
		45	.88774	533.8	.00151	.000809	45	.87632	546.1	.01106	.005873
		90	.90015	554.8	.00396	.002123	0	.88197	555.8	.01458	.007742
8.49		0	.92666	563.5	.00197	.001056	90	.90122	544.1	.00320	.001699
		45	.93061	555.5	.00098	.000525	45	.88874	549.5	.00853	.004529
		90	.90297	550.1	.00230	.001233	0	.90404	560.8	.00880	.004673
9.27		0	.93174	555.5	.00081	.000434	90	.90179	538.5	.00119	.000632
		45	—	—	—	—	45	.87180	533.5	.00343	.001821
		90	.91594	546.5	.00090	.000482	0	.89834	541.8	.00291	.001545
10.84		0	.93287	556.1	.00087	.000466	90	.89665	536.5	.00188	.000998
		45	.91312	543.1	.00088	.000472	45	.87357	532.8	.00532	.002825
		90	.90297	545.8	.00222	.001190	0	.88705	539.8	.00456	.002421
11.30		0	.94866	568.1	.00108	.000579	90	.90969	551.8	.00303	.001609
		90	.91369	563.8	.00236	.001265	0	.91533	566.5	.00826	.004386
12.32		0	.94076	561.5	.00090	.000482	90	.91477	555.1	.00362	.001922
		45	.92666	559.1	.00141	.000756	45	.93339	586.1	.01165	.006186
		90	.92892	572.1	.00262	.001404	0	.94750	587.5	.00501	.002660
13.82		0	.93230	565.1	.00213	.001142	90	.89439	550.8	.00614	.003260
		45	.90748	549.1	.00202	.001083	45	.87914	538.1	.00570	.003027
		90	.93230	566.5	.00252	.001351	0	.95089	580.5	.00596	.003165

^aRadius is listed only for hemispherical heat shield.^bAccuracy depends on magnitude: $h > 0.015$, accuracy 10 percent; $0.001 \leq h \leq 0.015$, accuracy 15 percent; $h < 0.001$, accuracy 20 percent. (h measured in Btu/sq ft-sec^{-0.5}R.)

DECLASSIFIED

47

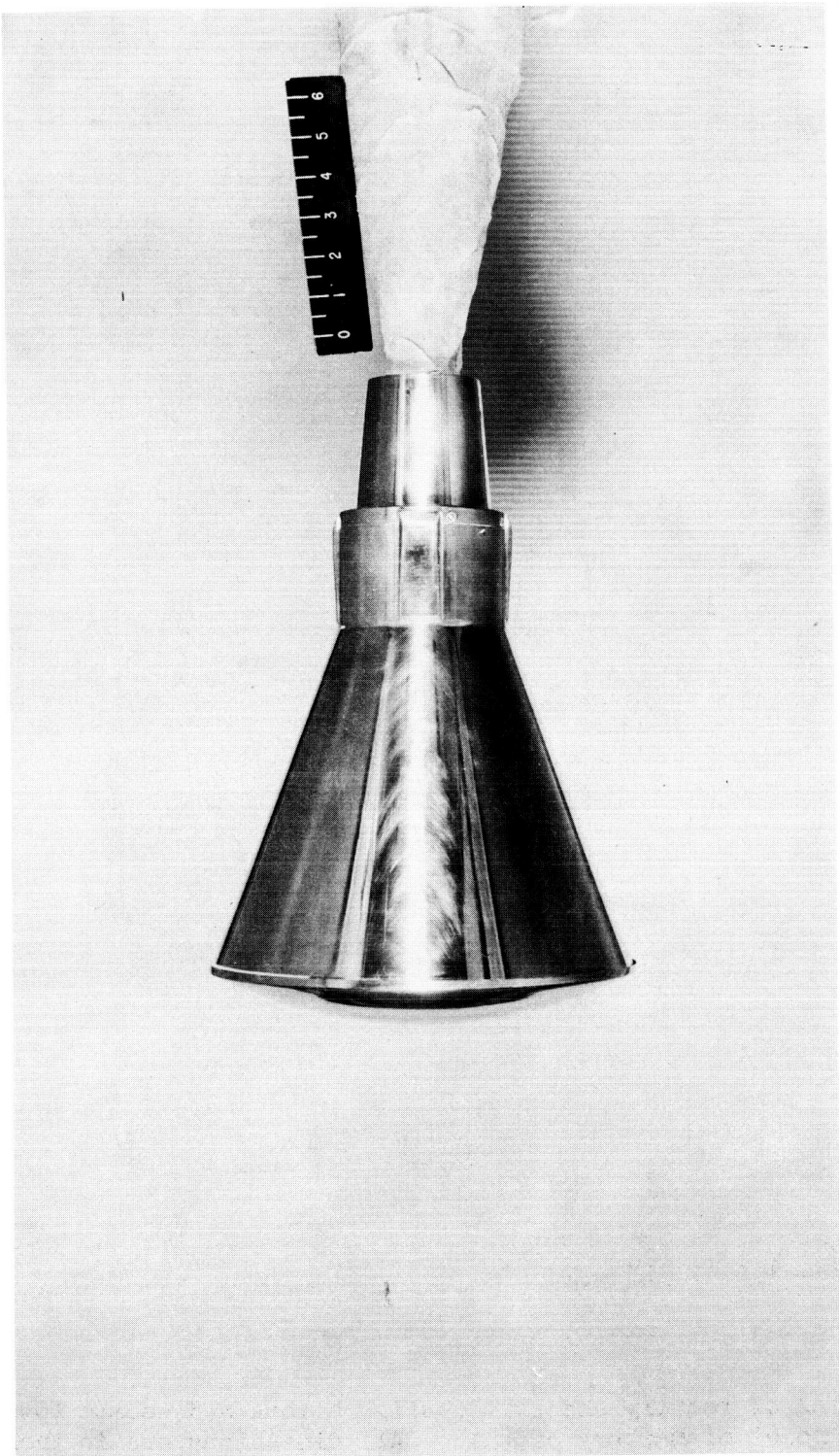


Escape tower

Figure 1.- Drawing of reentry and exit configurations and escape tower of 1/7-scale model of Mercury capsule. All dimensions are in inches unless otherwise noted.

0317122AJS30

48



(a) Reentry configuration.
L-59-3730

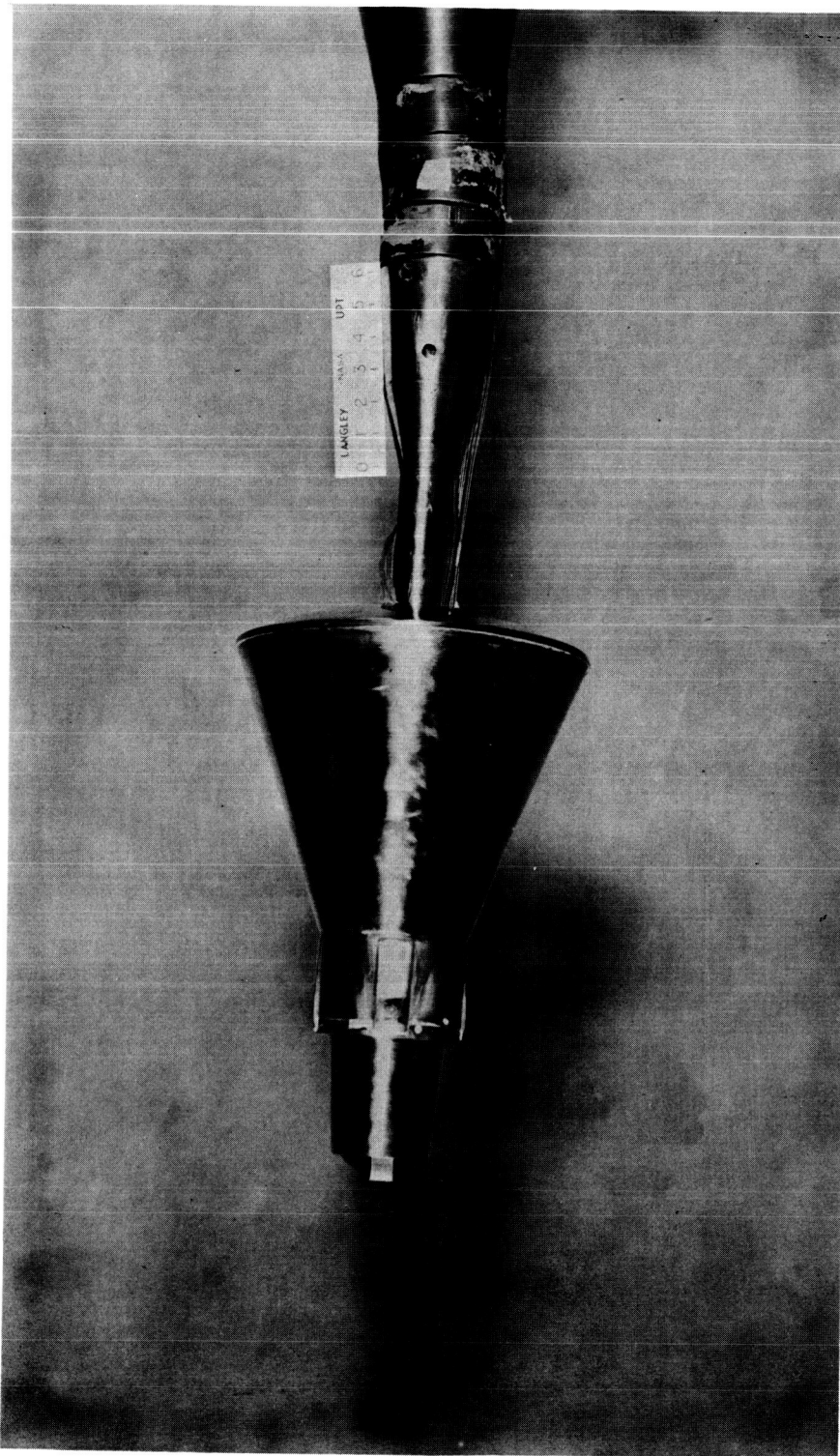
Figure 2.- Photographs of model of Mercury capsule.

L-1022

4G

DECLASSIFIED

49



(b) Exit configuration.

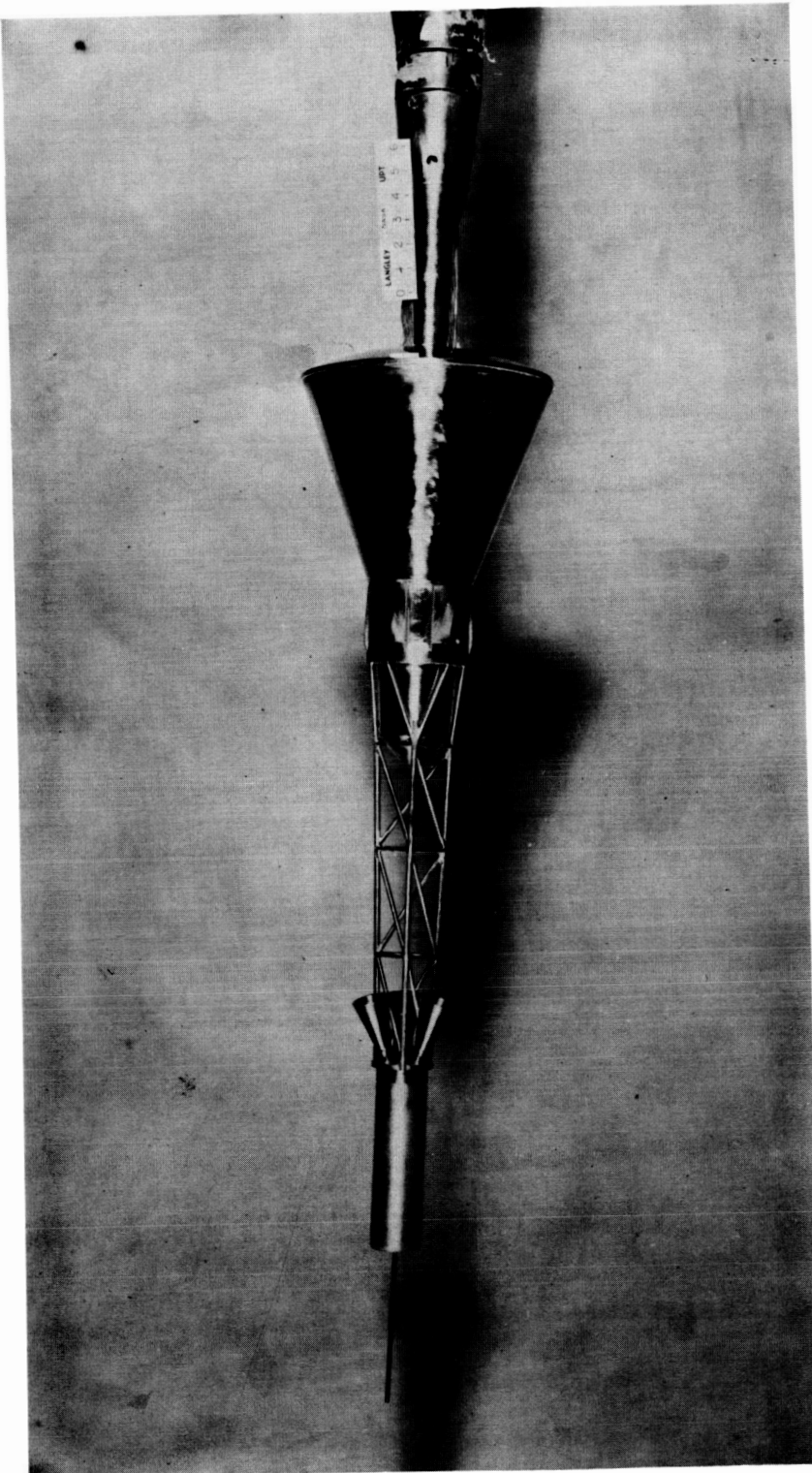
L-59-3876

Figure 2.- Continued.

L-1022

031912201030

50



L-59-3874

(c) Escape configuration.

Figure 2.- Concluded.

L-1022

DECLASSIFIED

Thermocouple	Orifice #, in.	r_x , in.	Thermocouple	Orifice #, in.	r_x , in.	Thermocouple	Orifice #, in.	r_x , in.	Thermocouple	Orifice #, in.	r_x , in.
1	1	-0.98	2.66	17	-0.98	2.66	33	-1.28	0.53		
2	2	-0.62	5.66	18	-0.63	5.66	34	-0.63	5.66		
3	3	-0.11	5.05	19	-0.11	5.05	35	-0.62	5.05		
4	4	0.45	5.16	20	0.45	5.16	36	-0.11	5.05		
5	5	1.69	4.71	21	1.69	4.71	37	0.45	5.16		
6	6	2.92	4.29	22	2.92	4.29	38	1.69	4.71		
7	7	5.15	3.74	23	5.15	3.74	39	2.92	4.29		
8	8	7.38	3.22	24	7.38	3.22	40	4.17	3.74		
9	9	7.13	2.73	25	7.13	2.73	41	5.38	2.22		
10	10	6.19	2.23	26	6.19	2.23	42	7.13	2.22		
11	11	9.27	2.17	27	9.27	2.17	43	6.49	2.25		
12	12	10.64	2.28	28	10.64	2.28	44	9.27	2.17		
13	13	11.30	2.21	29	11.30	2.21	45	10.84	2.28		
14	14	11.59	1.98	30	11.59	1.98	46	11.30	2.21		
15	15	12.32	1.65	31	12.32	1.65	47	11.59	1.98		
16	16	13.82	1.53	32	13.82	1.53	48	12.32	1.65		

X Location of thermocouples
● Location of orifices

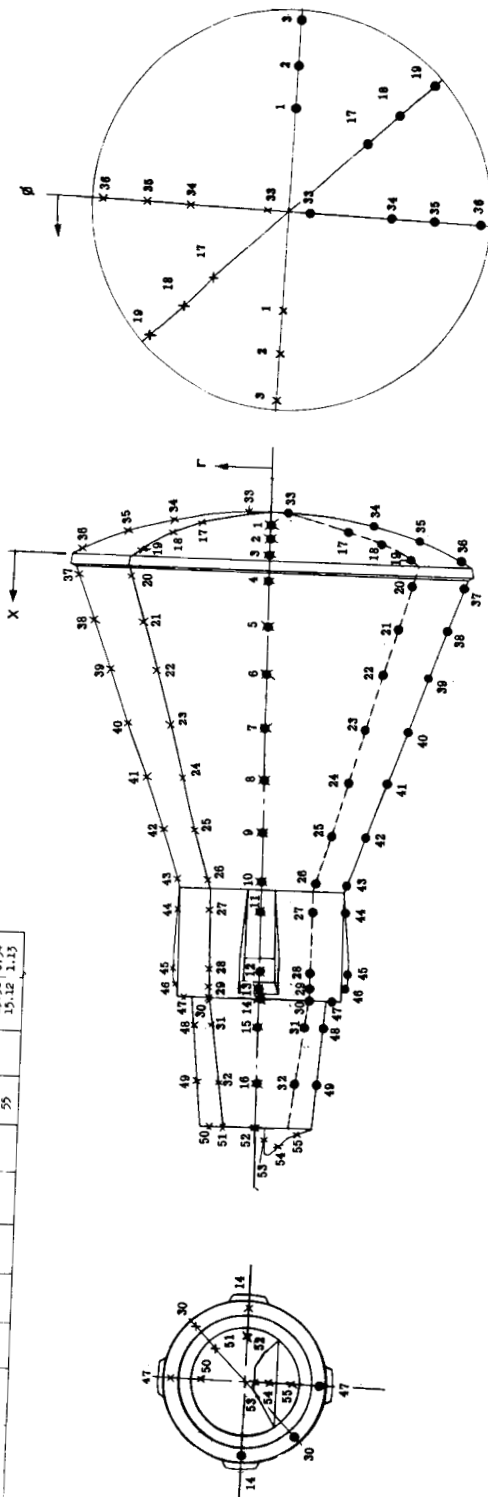


Figure 3.- Location of pressure orifices and heat-transfer thermocouples on 1/7-scale model of Mercury capsule.

031312201030

52

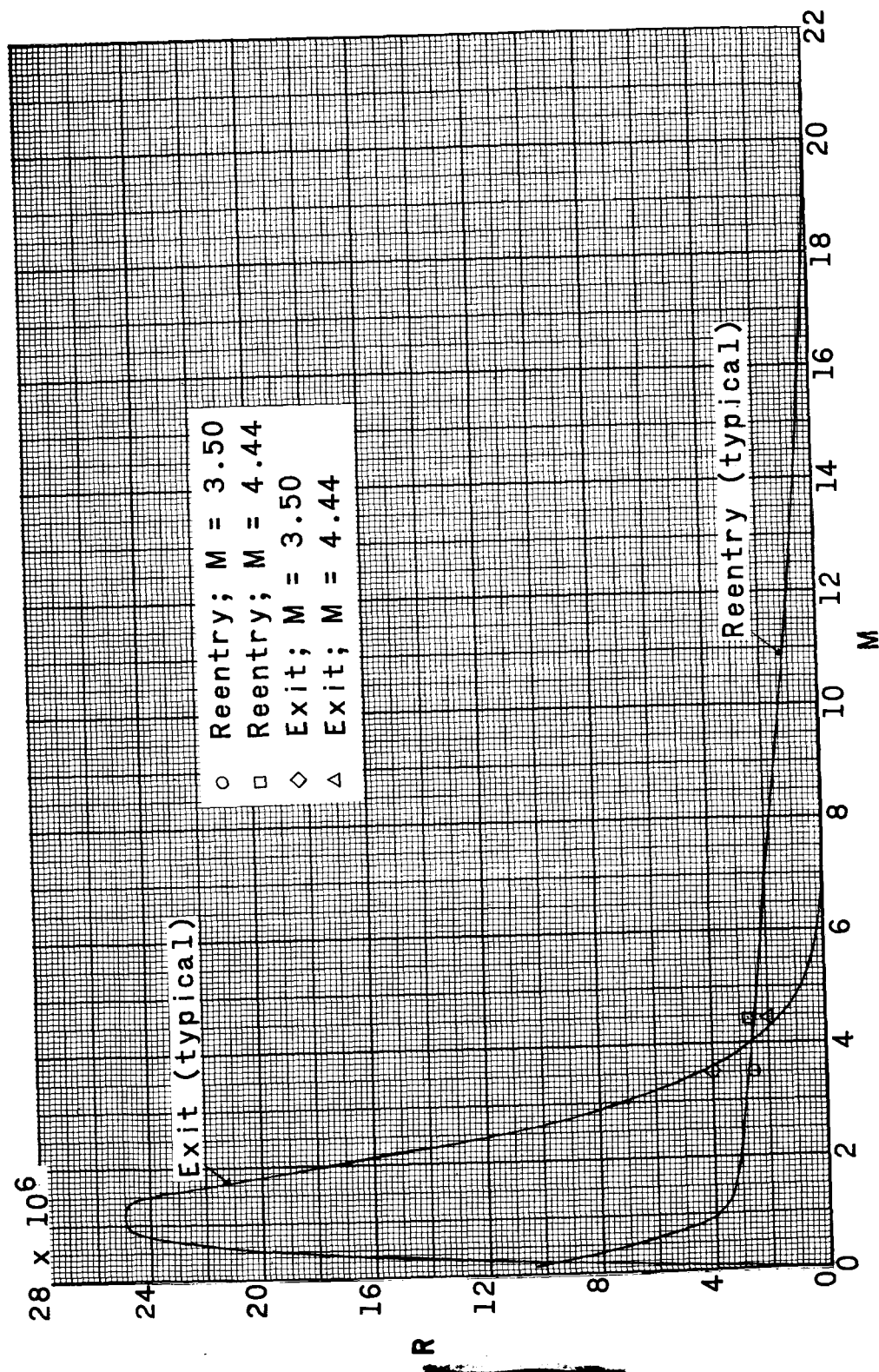
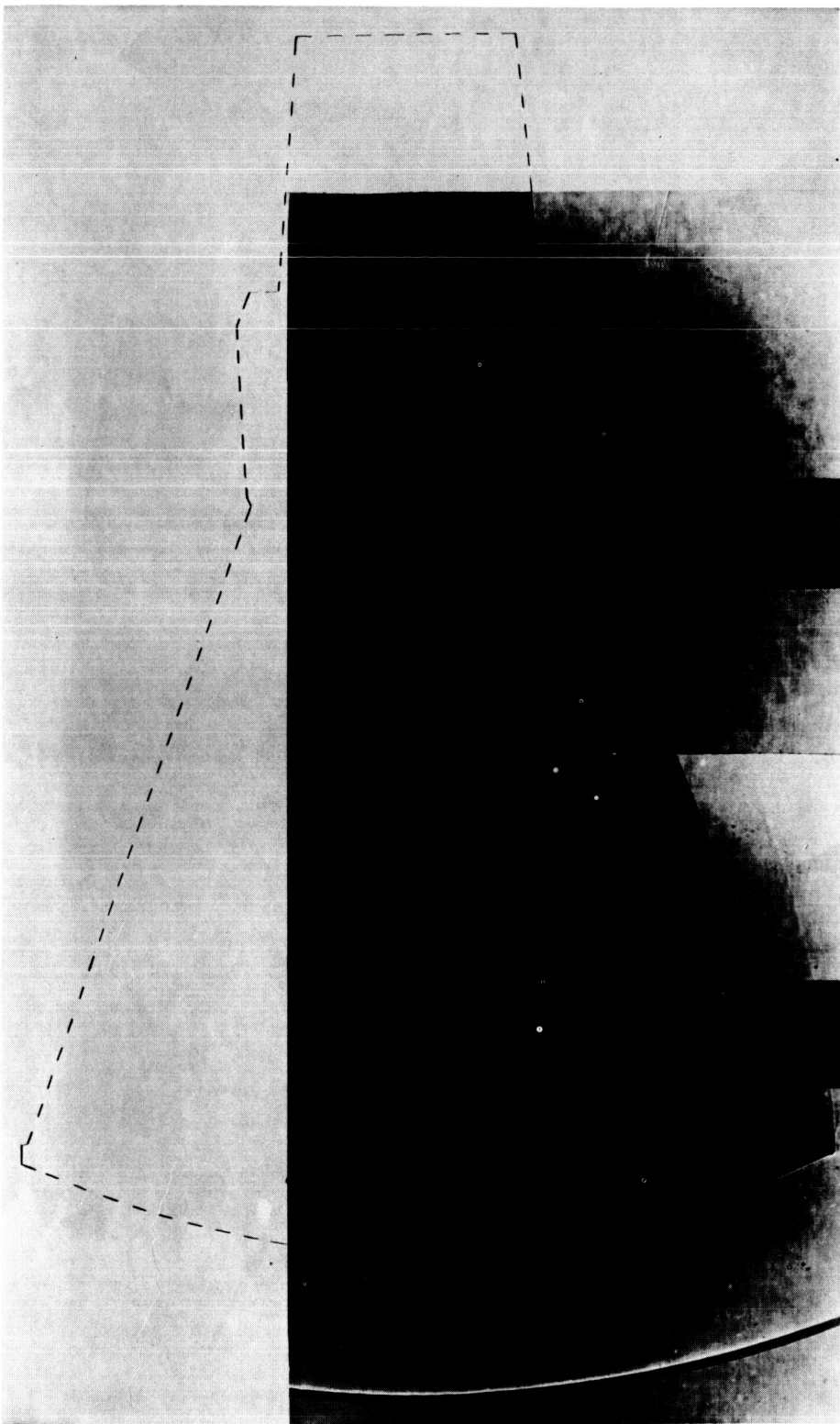


Figure 4.- Typical Mercury capsule trajectory and tunnel test conditions.

L-1022

DECLASSIFIED

53



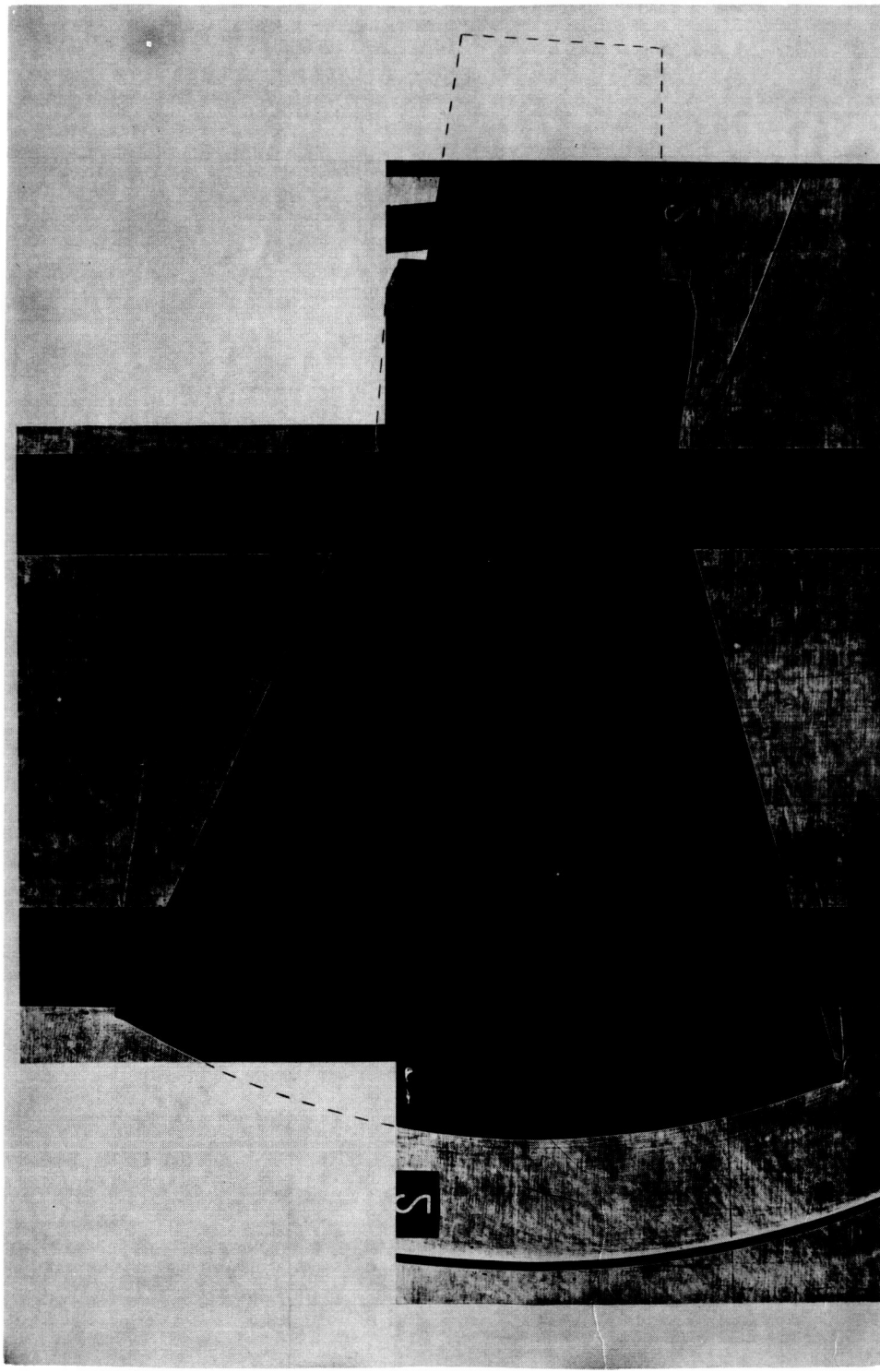
(a) Reentry configuration; $M = 3.50$; $\alpha = 0^\circ$. L-61-62

Figure 5.- Shadowgraphs of Mercury capsule model.

L-1022

0319122A1030

54



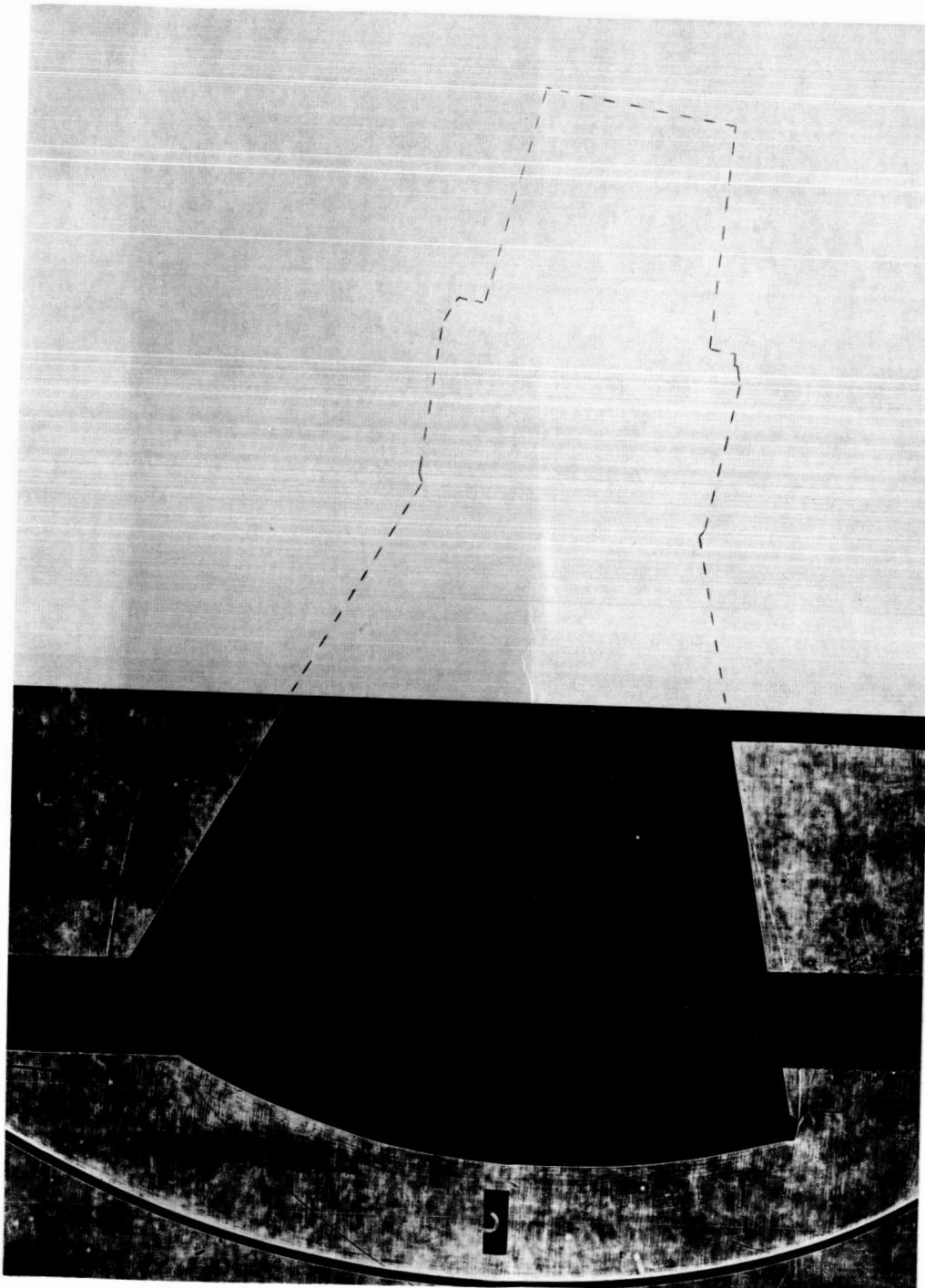
(b) Reentry configuration; $M = 3.50$; $\alpha = 5^\circ$. L-61-63

Figure 5.- Continued.

L-1022

DECLASSIFIED

55



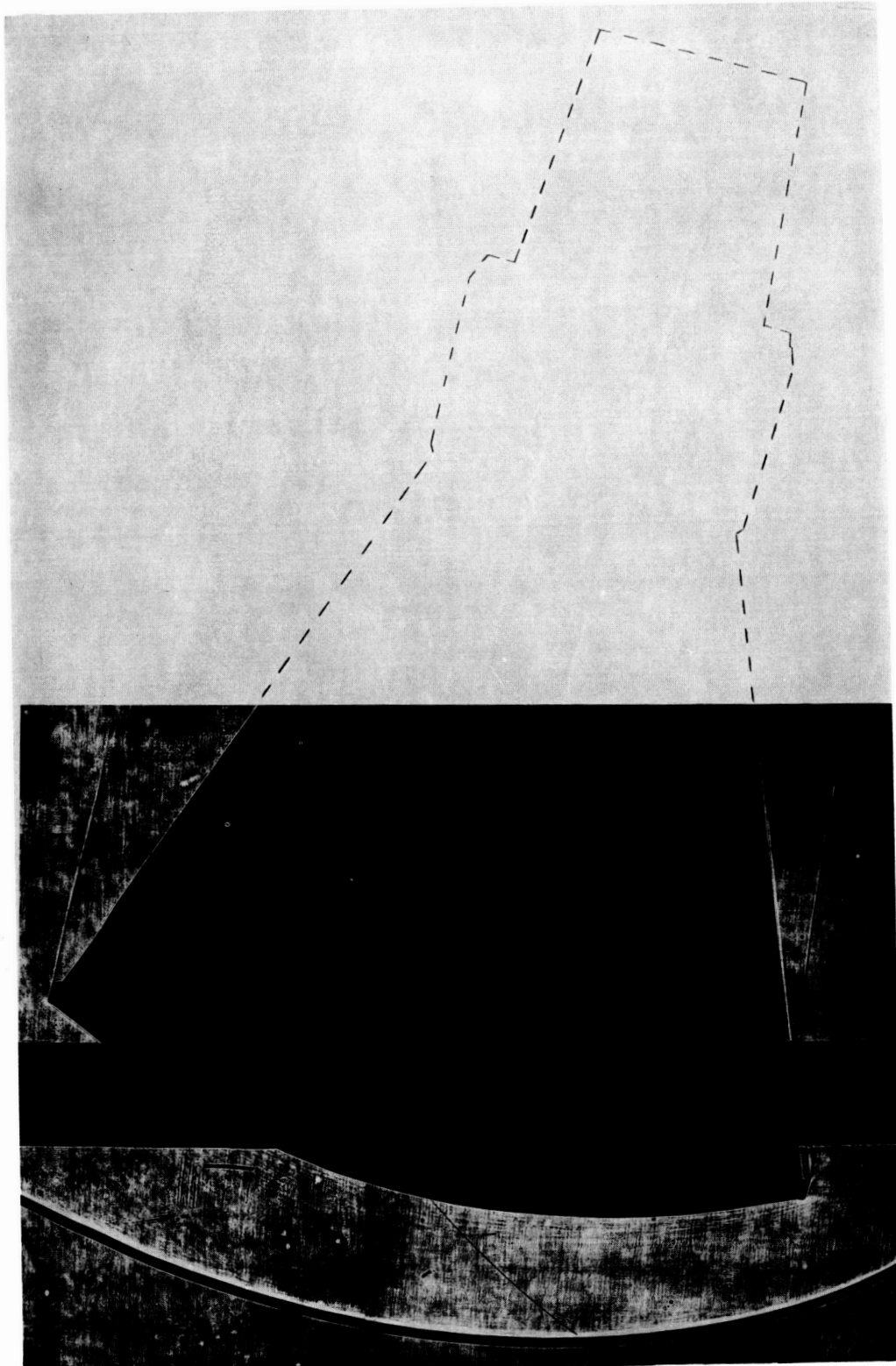
(c) Reentry configuration; $M = 3.50$; $\alpha = 10^\circ$. L-61-64

Figure 5.- Continued.

L-1022

031912201030

56

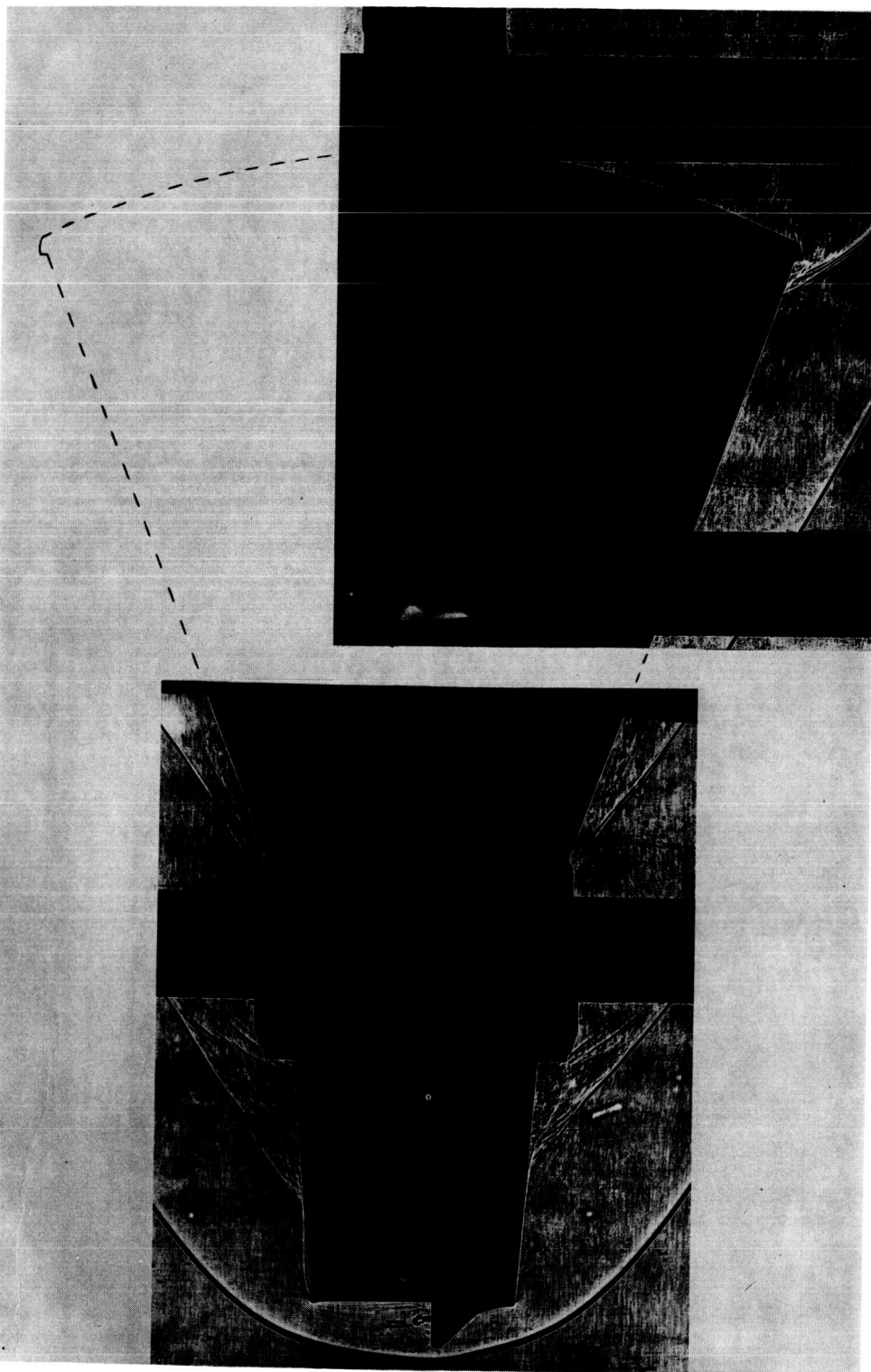


(d) Reentry configuration; $M = 3.50$; $\alpha = 15^\circ$. L-61-65

Figure 5.- Continued.

DECLASSIFIED

57



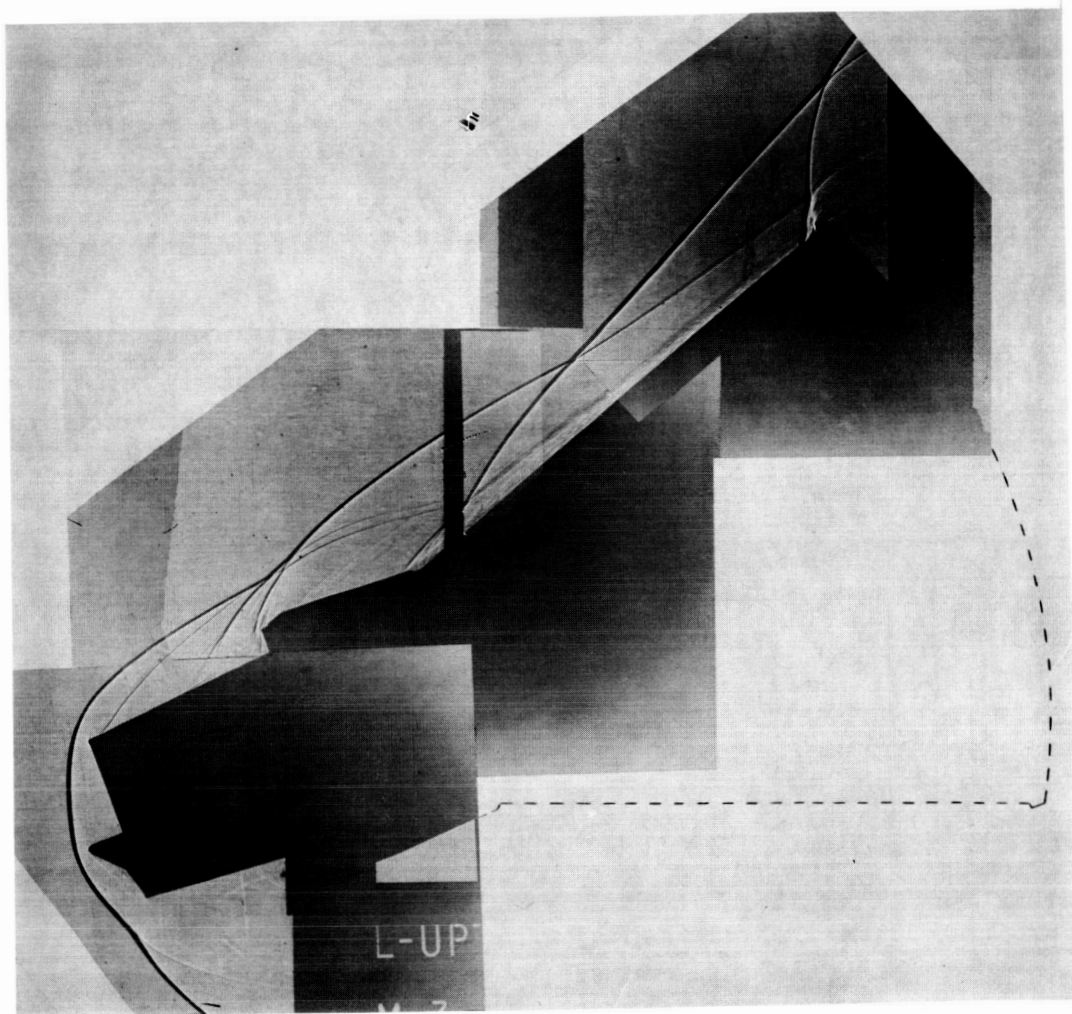
(e) Exit configuration; $M = 3.50$; $\alpha = 0^\circ$. L-61-66

Figure 5.- Continued.

L-1022

001122A1030

58



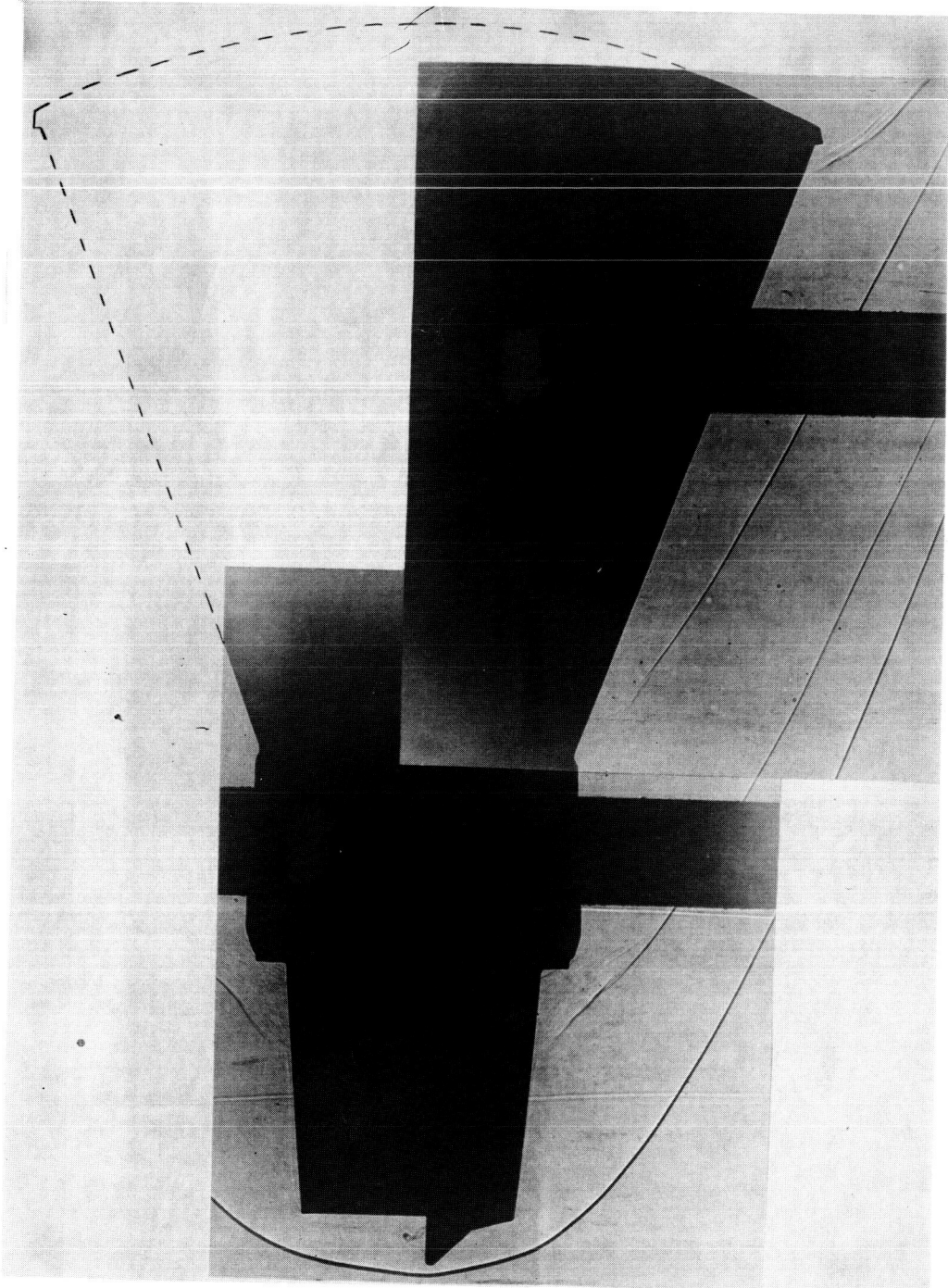
(f) Exit configuration; $M = 3.50$; $\alpha = -20^\circ$. L-61-67

Figure 5.- Continued.

L-1022

DECLASSIFIED

59



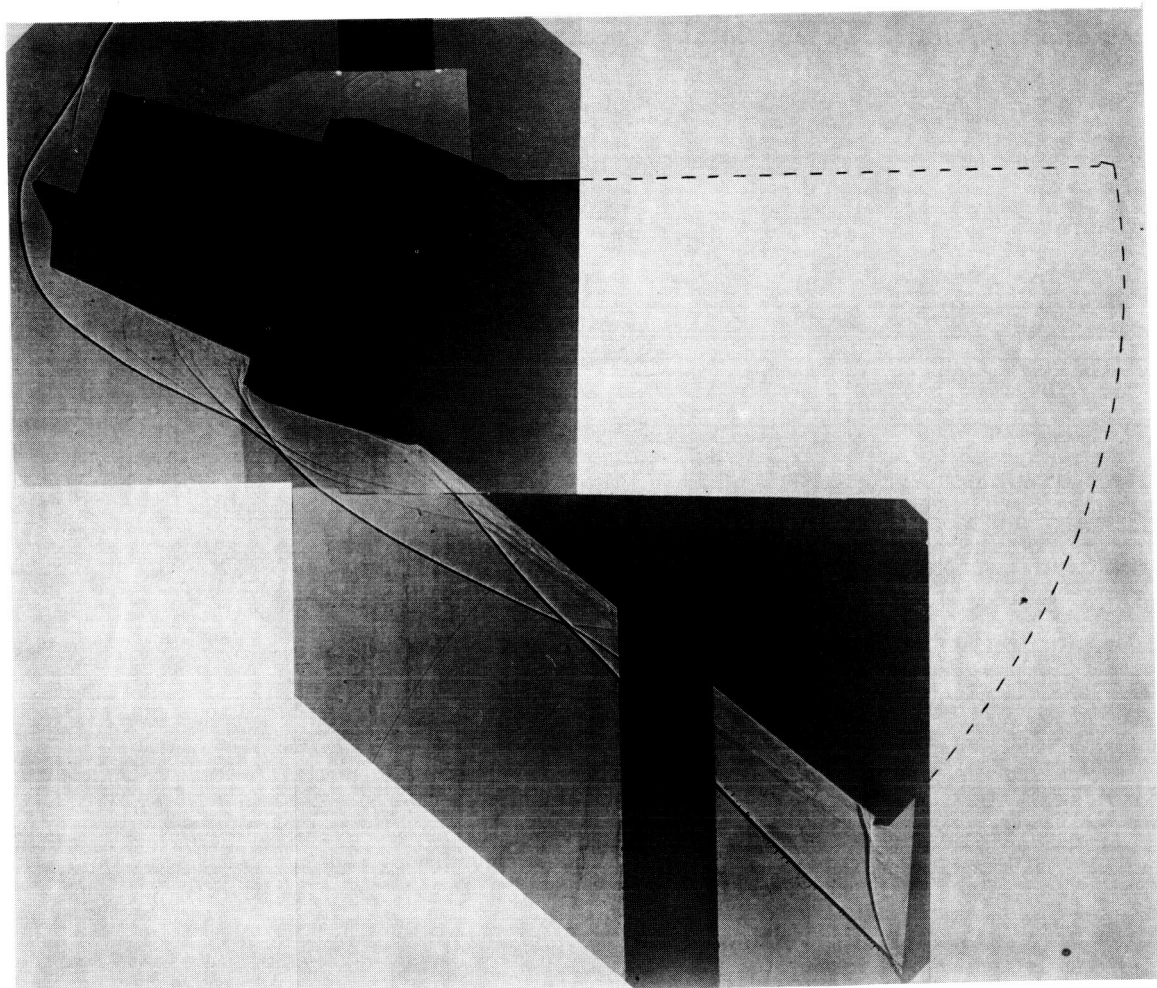
(g) Exit configuration; $M = 4.44$; $\alpha = 0^\circ$. L-61-68

Figure 5.- Continued.

L-1022

0319122A1030

60



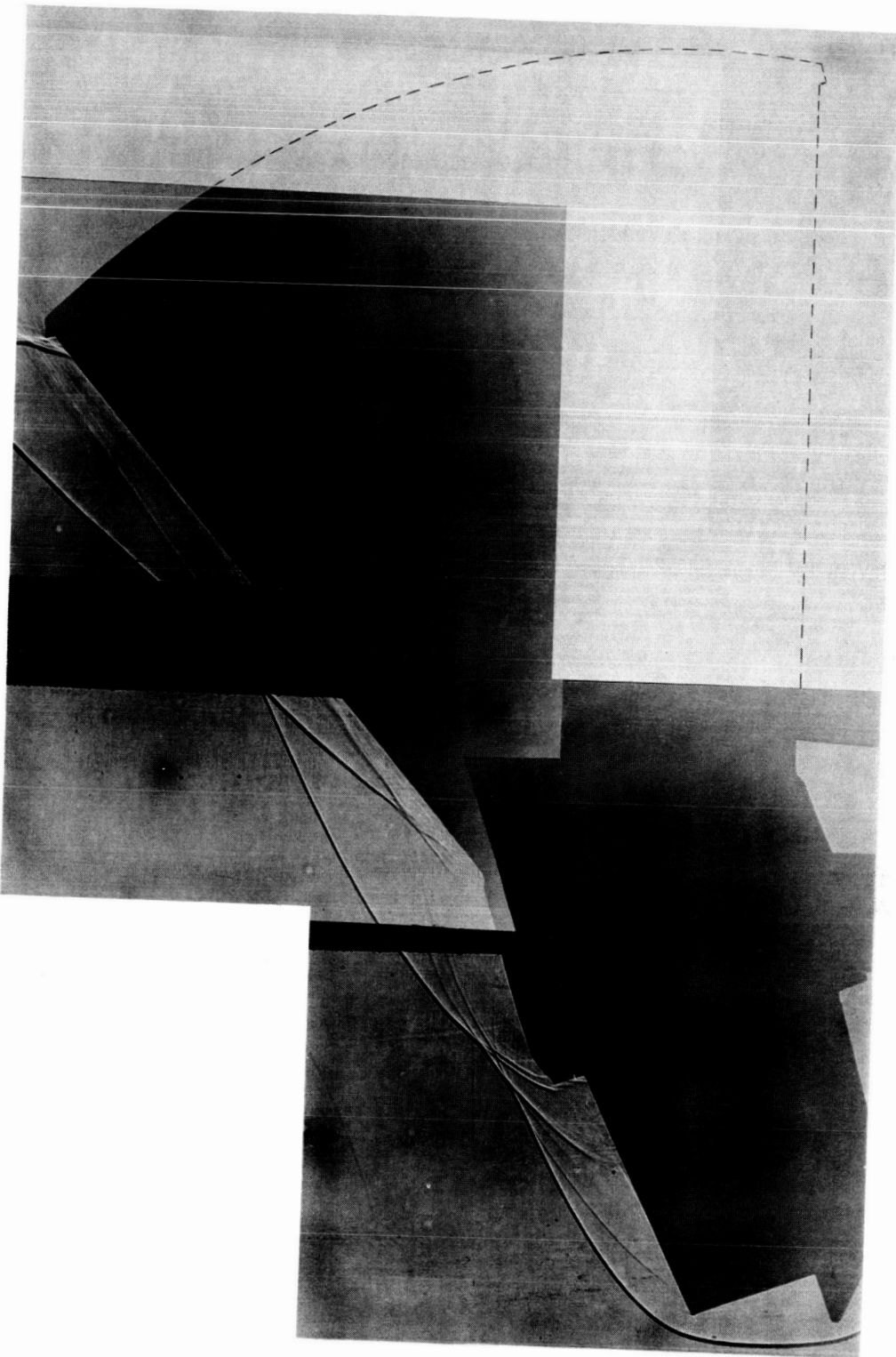
(h) Exit configuration; $M = 4.44$; $\alpha = 20^\circ$. L-61-69

Figure 5.- Continued.

L-1022

DECLASSIFIED

61



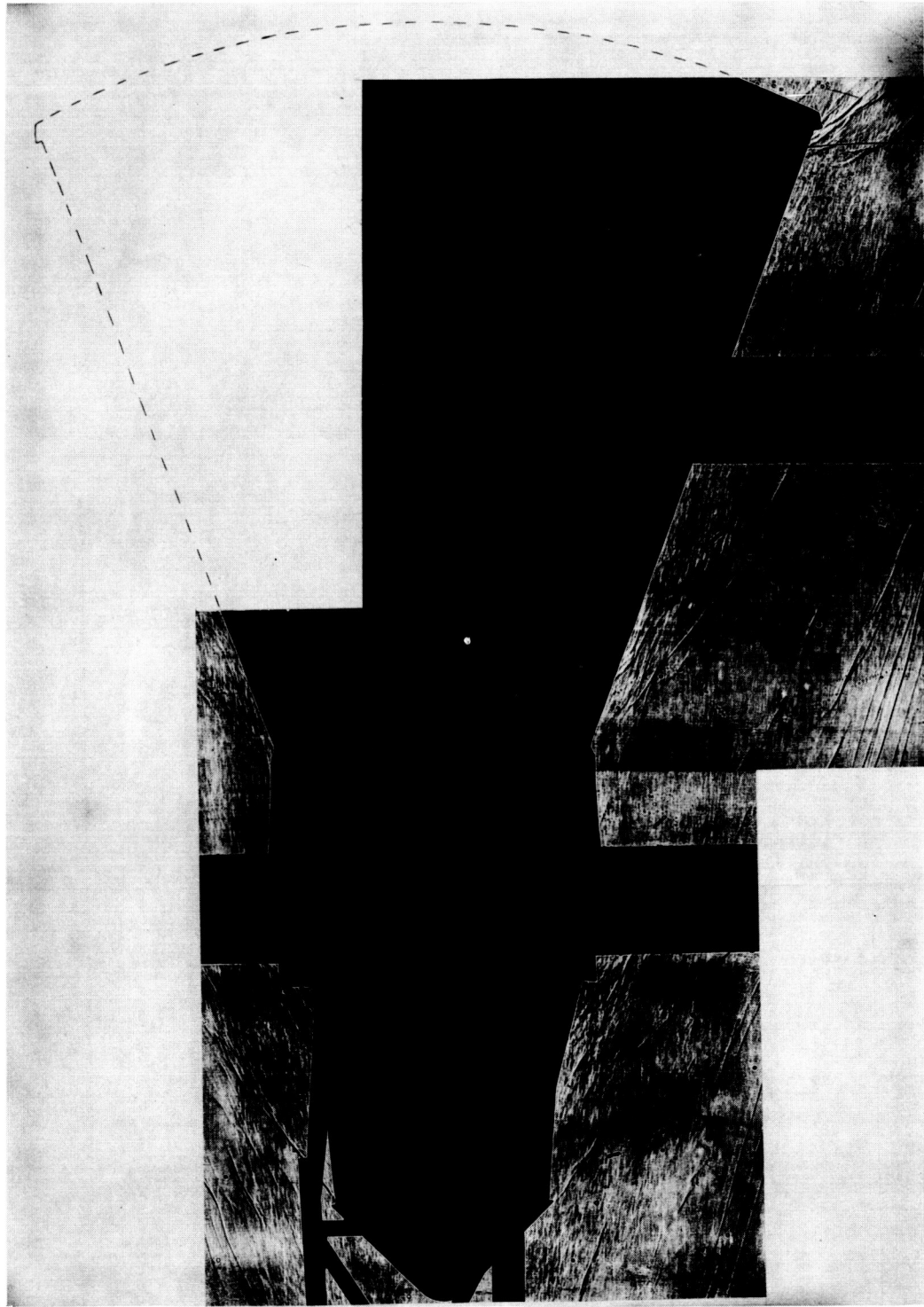
(1) Exit configuration; $M = 4.44$; $\alpha = -20^\circ$. L-61-70

Figure 5.- Continued.

L-1022

0319122A1030

62



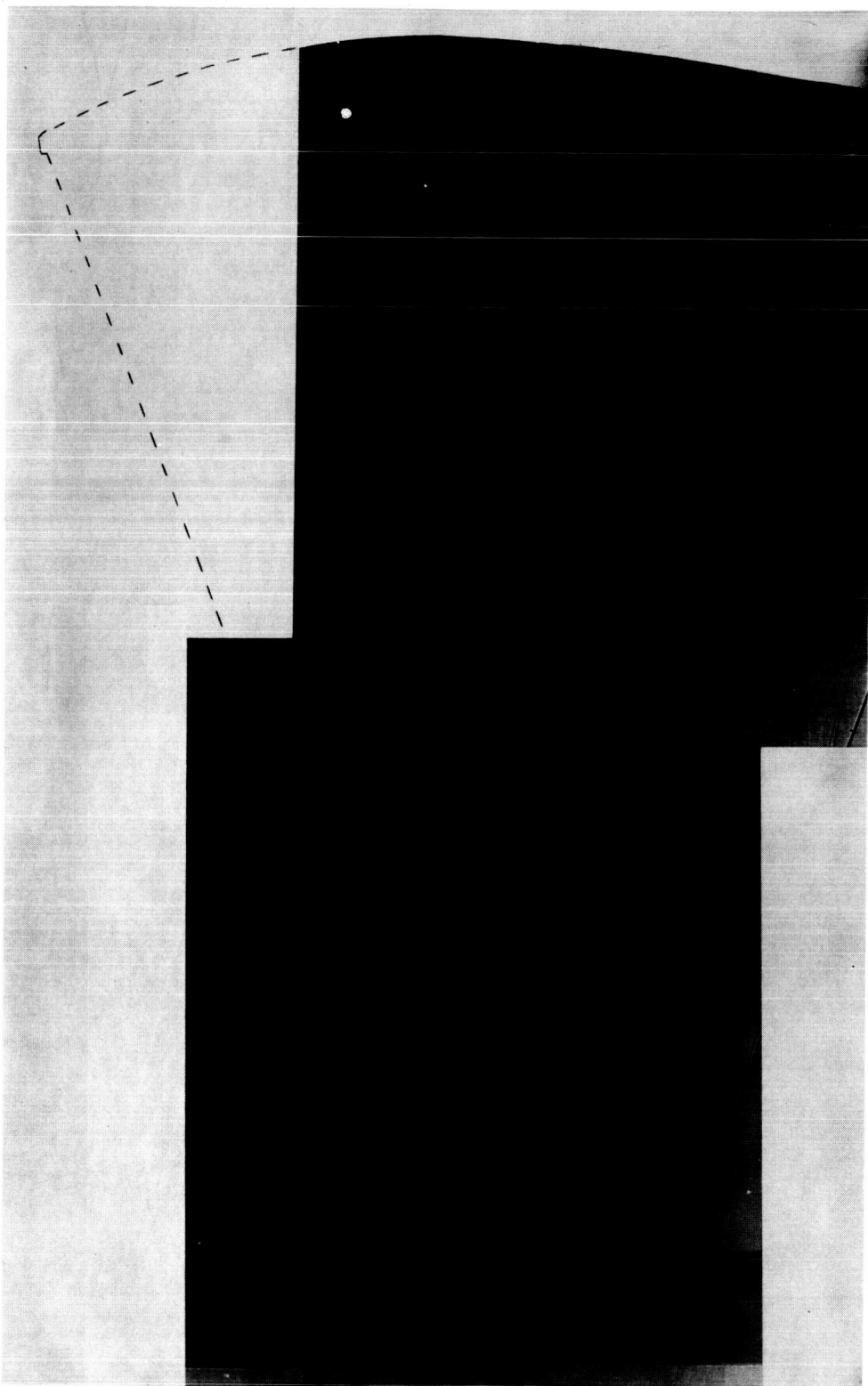
(j) Escape configuration; $M = 3.50$; $\alpha = 0^\circ$. I-61-71

Figure 5.- Continued.

I-1022

DECLASSIFIED

[REDACTED]
63



L-1022

(k) Escape configuration; $M = 4.44$; $\alpha = 0^\circ$. L-61-72

Figure 5.- Concluded.

031312201030

64



$\alpha = 0^\circ$



$\alpha = 10^\circ$



$\alpha = 15^\circ$

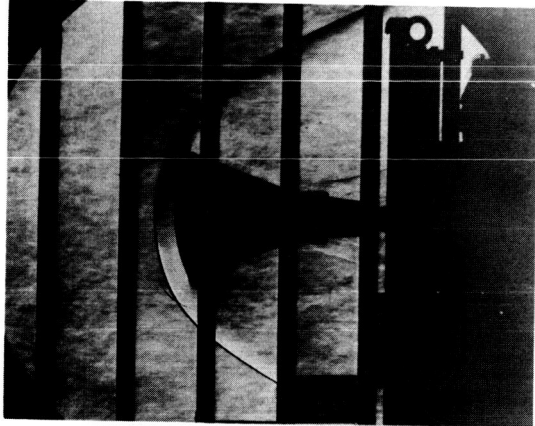
(a) Reentry configuration; $M = 3.50$.

L-61-73

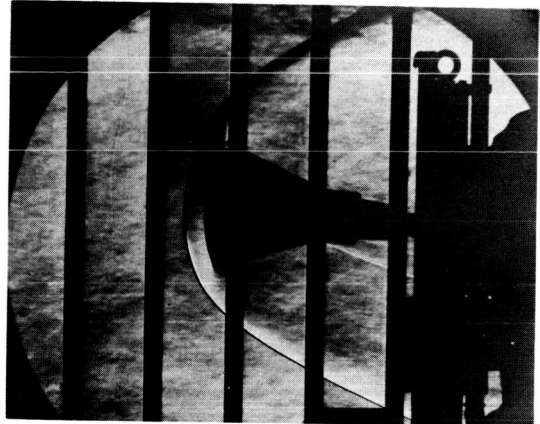
Figure 6.- Schlieren photographs of Mercury capsule model.

L-1022

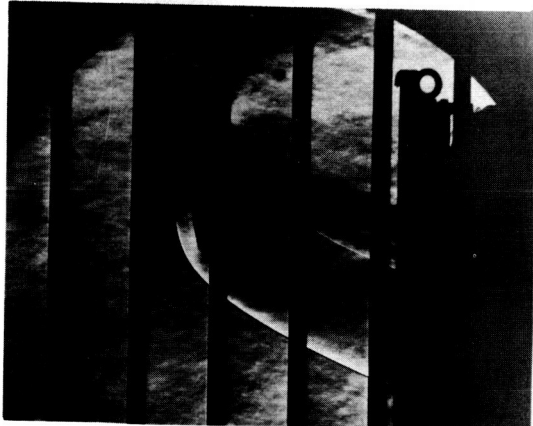
DECLASSIFIED



$\alpha = 0^\circ$



$\alpha = 5^\circ$



$\alpha = 10^\circ$



$\alpha = 15^\circ$

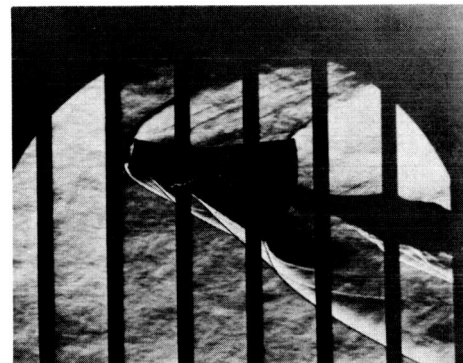
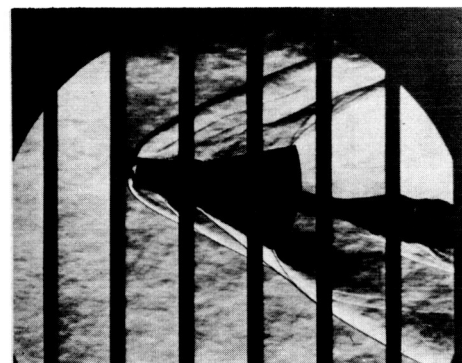
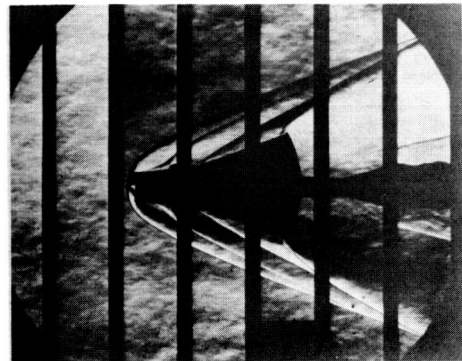
(b) Reentry configuration; $M = 4.44$.

L-61-74

Figure 6.- Continued.

0010201000

66



(c) Exit configuration; $M = 3.50$.

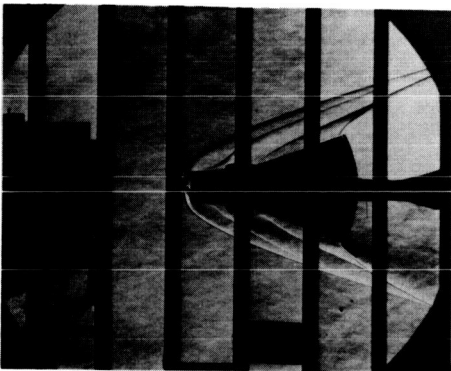
L-61-75

Figure 6.- Continued.

L-1022

DECLASSIFIED

67



$\alpha = 0^\circ$



$\alpha = 5^\circ$



$\alpha = 10^\circ$



$\alpha = 15^\circ$



$\alpha = 20^\circ$

(d) Exit configuration; $M = 4.44$.

L-61-76

Figure 6.- Continued.

031712201030

68

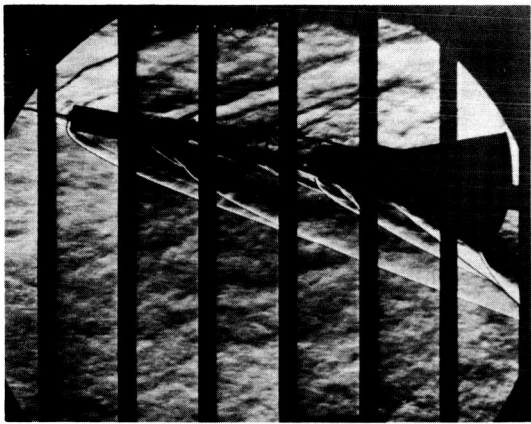
L-1022



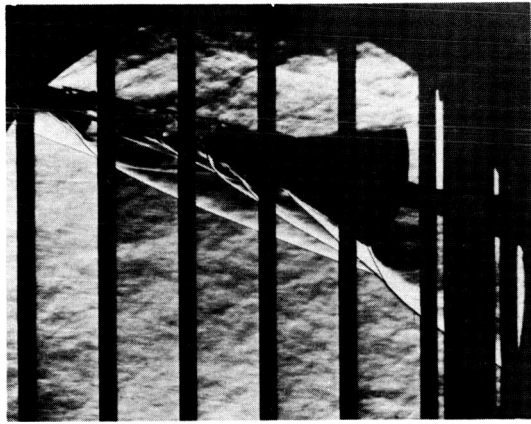
$\alpha = 0^\circ$



$\alpha = 5^\circ$



$\alpha = 10^\circ$



$\alpha = 15^\circ$

(e) Escape configuration; $M = 3.50$.

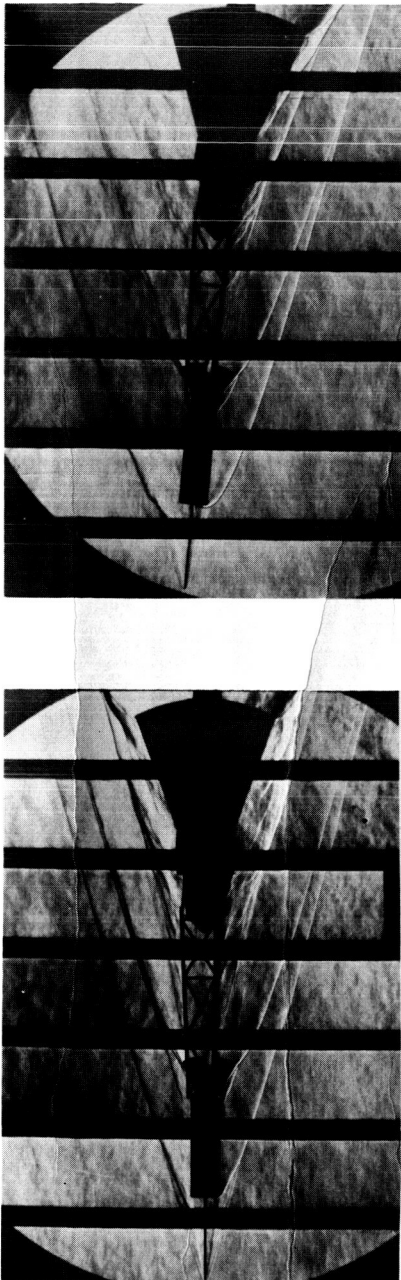
L-61-77

Figure 6.- Continued.

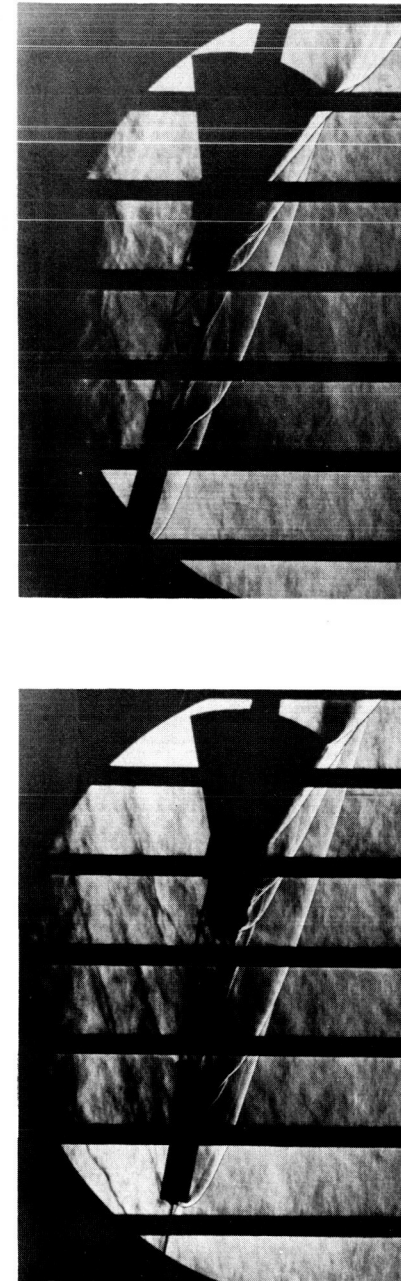
DECLASSIFIED

69

I-1022



$\alpha = 0^\circ$

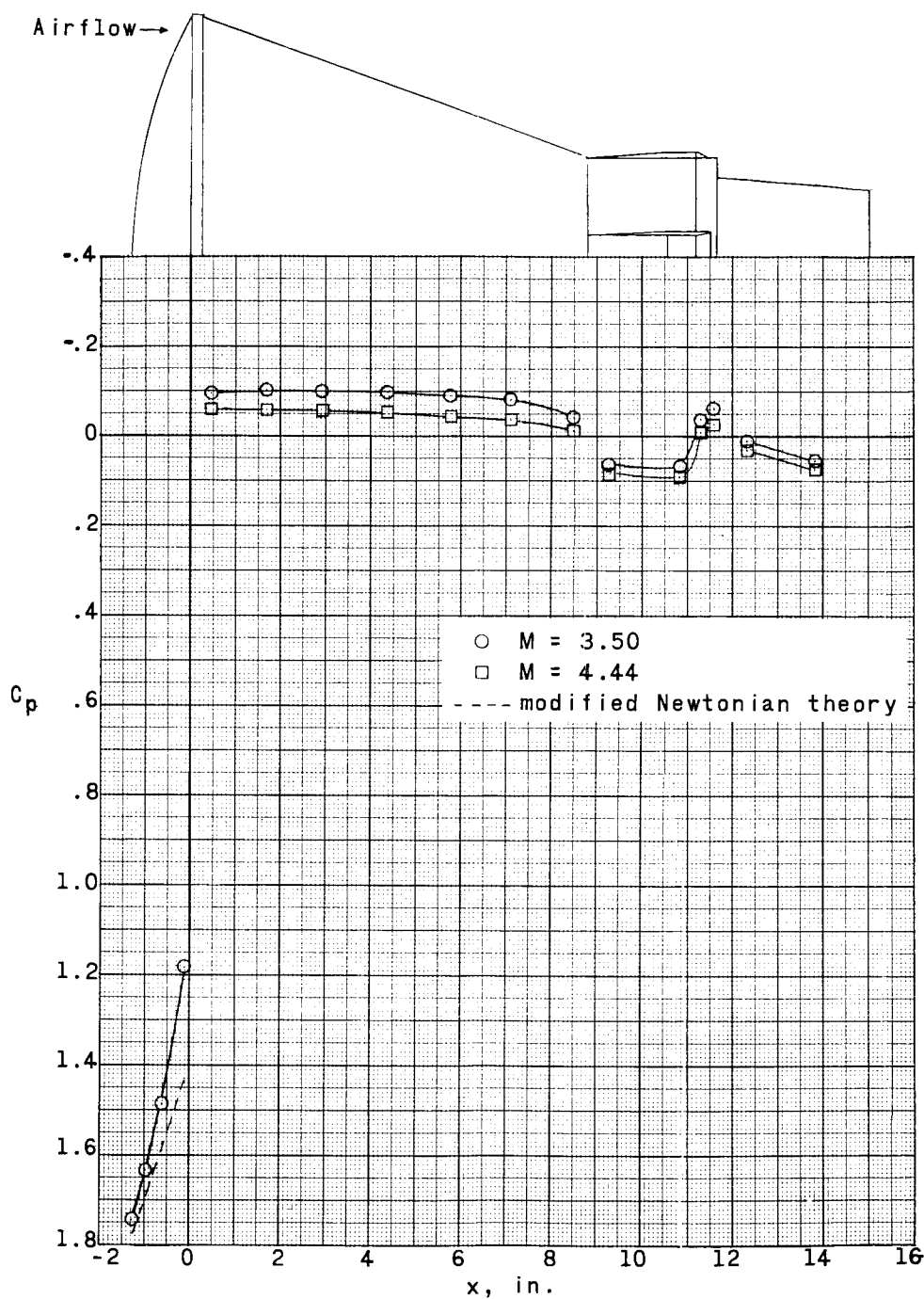


$\alpha = 5^\circ$

$\alpha = 15^\circ$

(f) Escape configuration; $M = 4.44$. L-61-78

Figure 6.- Concluded.



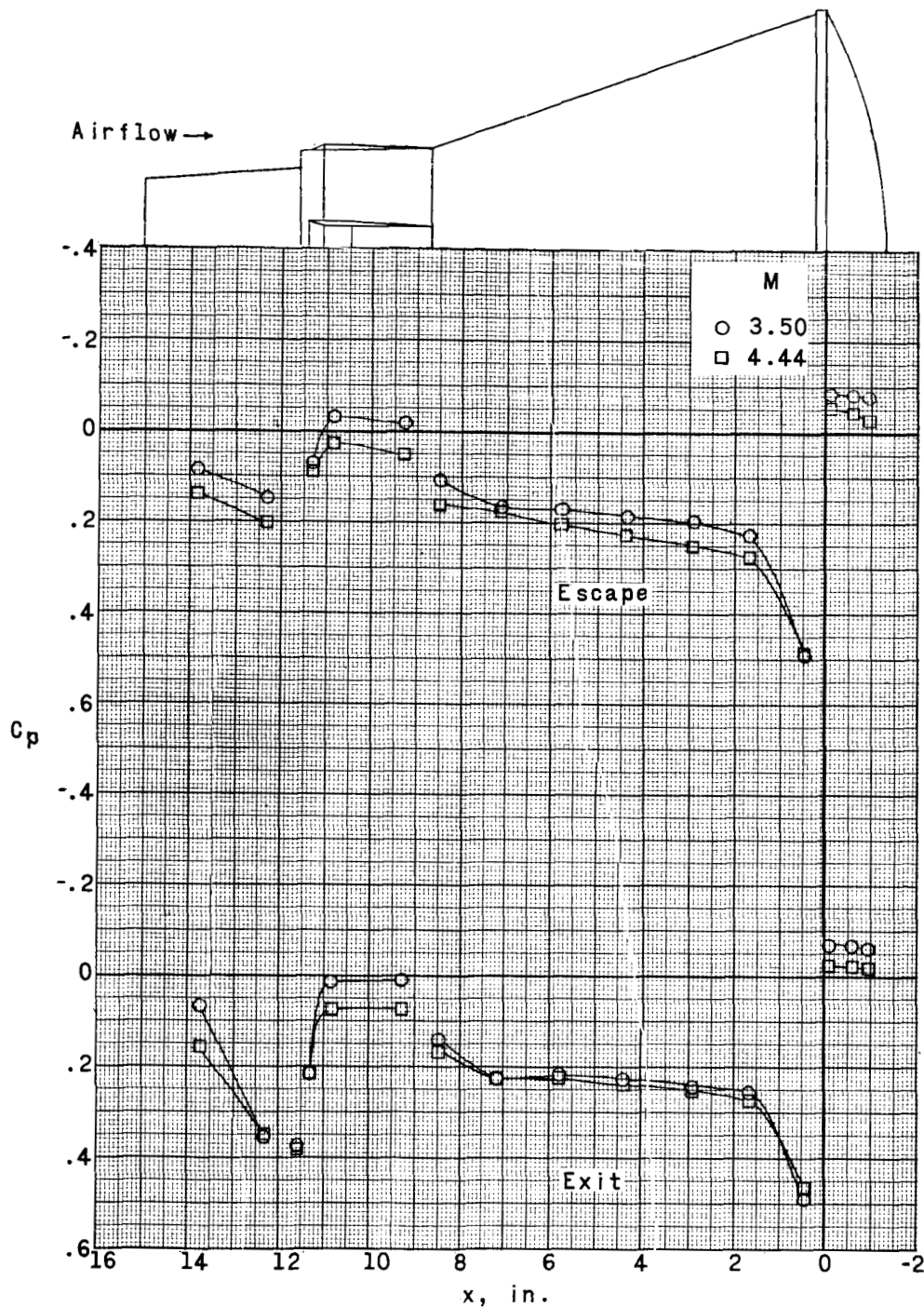
(a) Reentry configuration.

Figure 7.- Effect of Mach number on pressure distribution. $\phi = 180^\circ$;
 $\alpha = 0^\circ$.

DECLASSIFIED

71

I-1022



(b) Escape and exit configurations.

Figure 7.- Concluded.

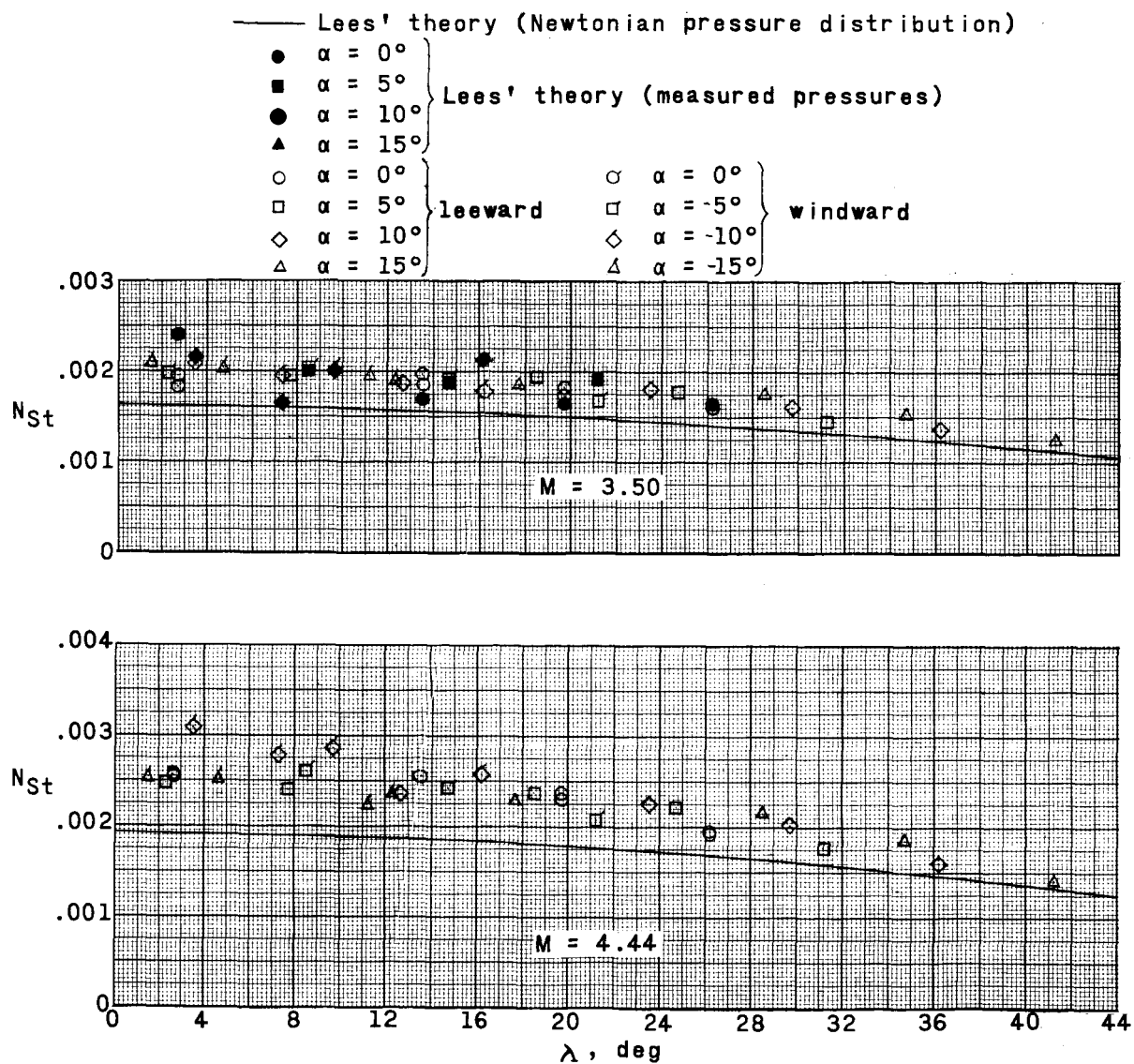
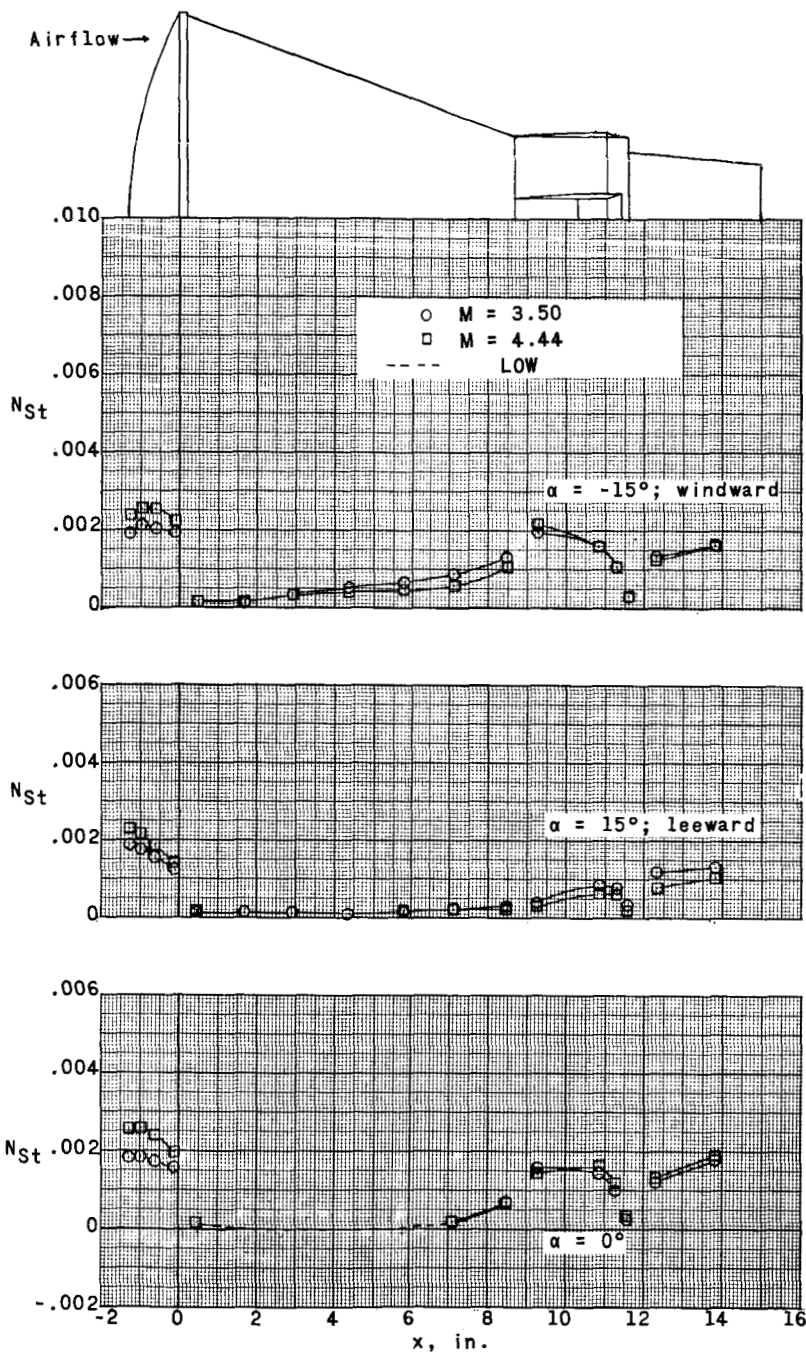


Figure 8.- Variation of Stanton number on the hemispherical heat shield of the reentry configuration for Newtonian flow angle.

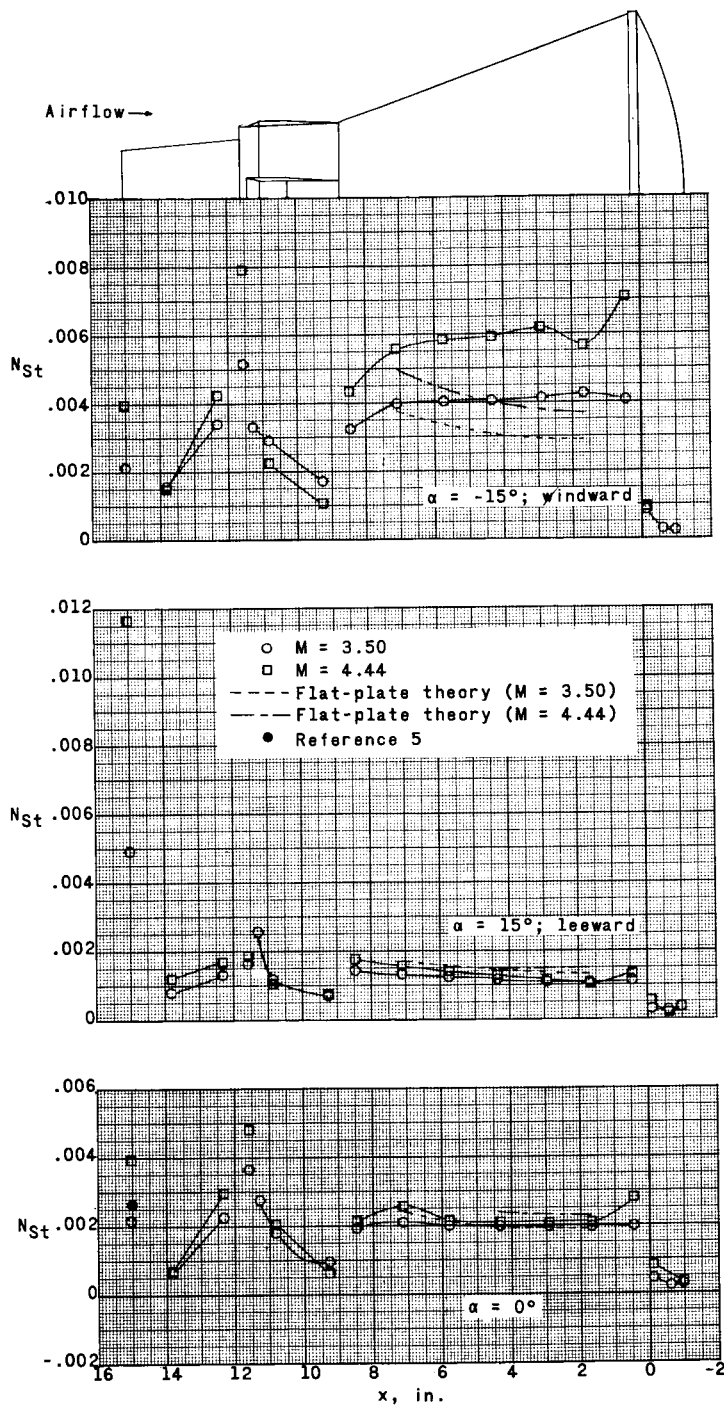
DECLASSIFIED

73



(a) Reentry configuration.

Figure 9.- Effect of Mach number on Stanton number distribution at $\phi = 0^\circ$ and angles of attack of 0° and $\pm 15^\circ$.

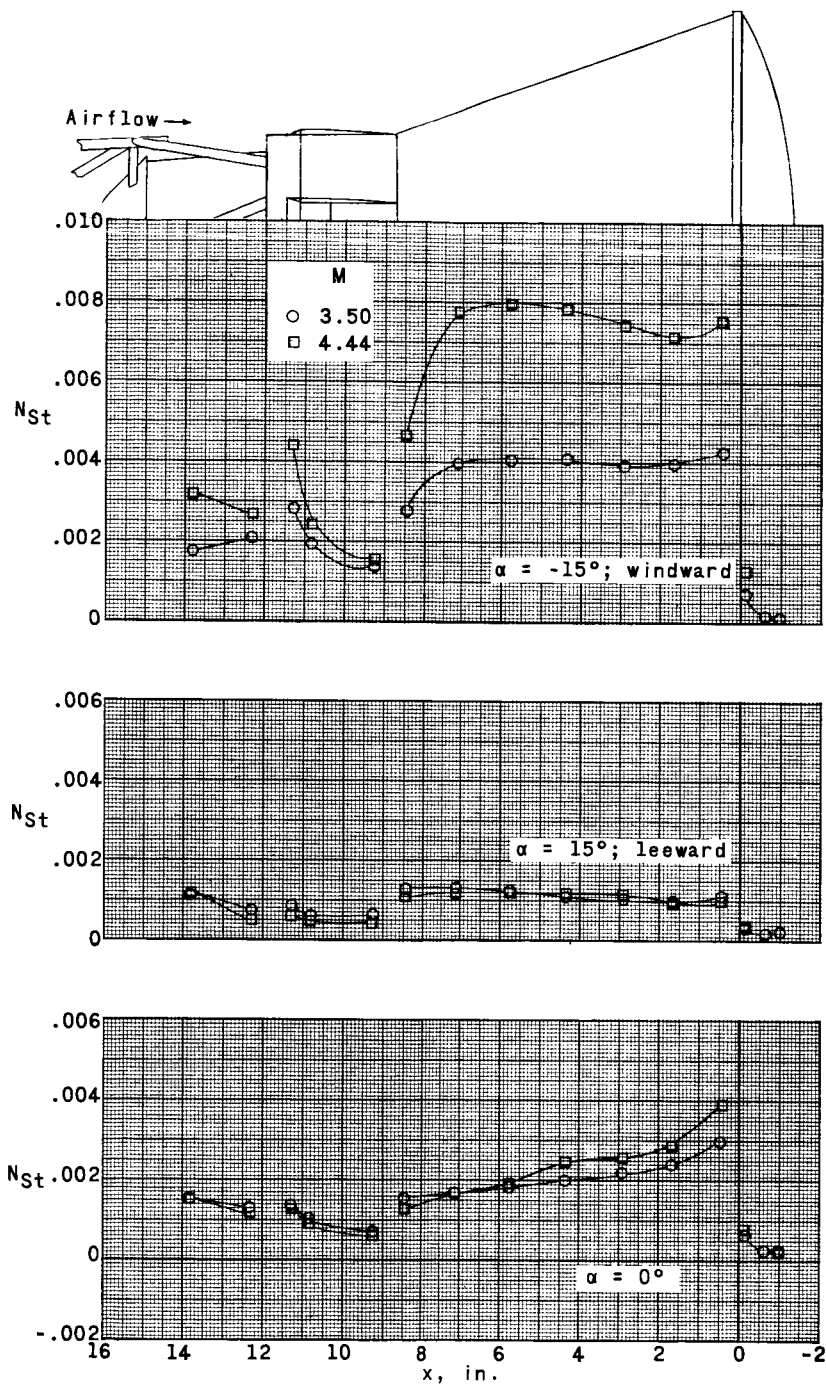


(b) Exit configuration.

Figure 9.- Continued.

REF CLASSIFIED

75



(c) Escape configuration.

Figure 9.- Concluded.

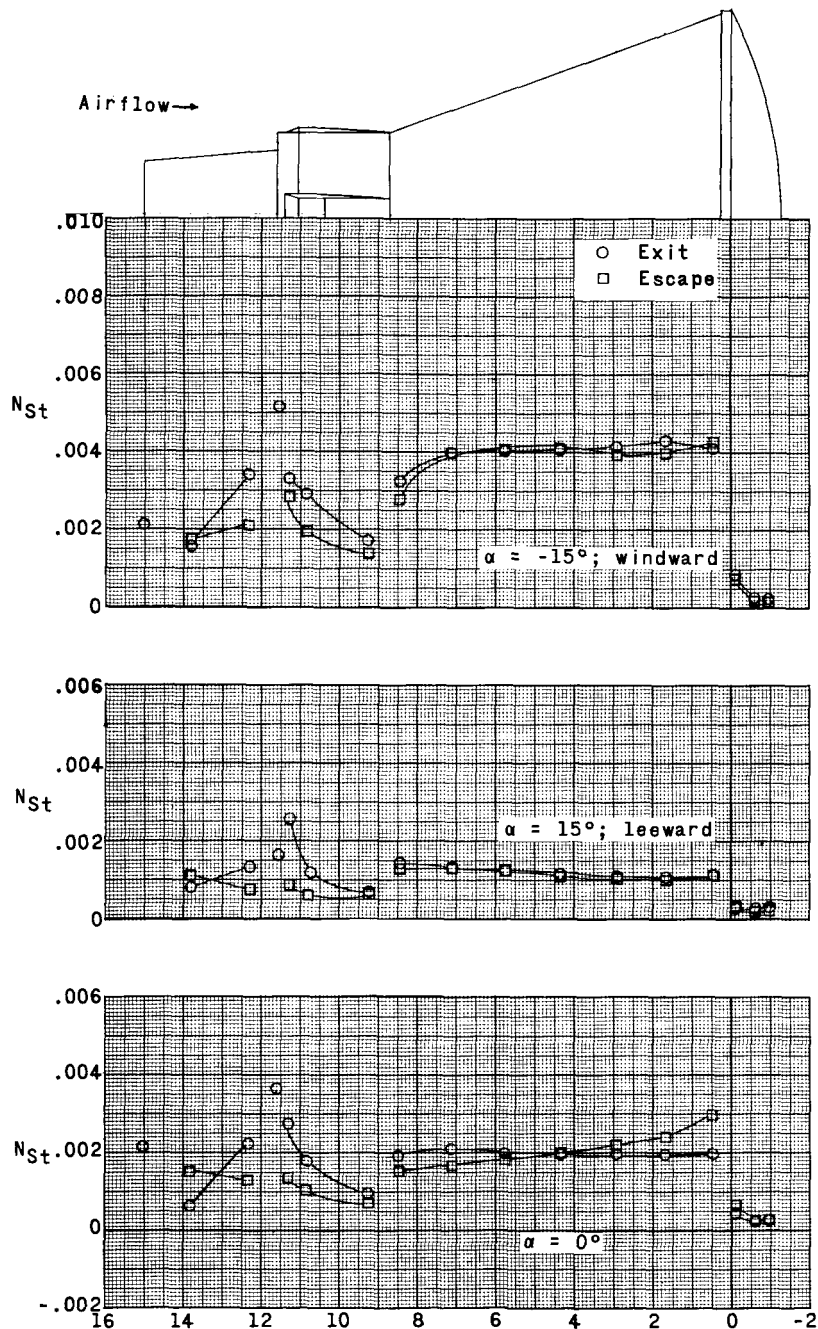
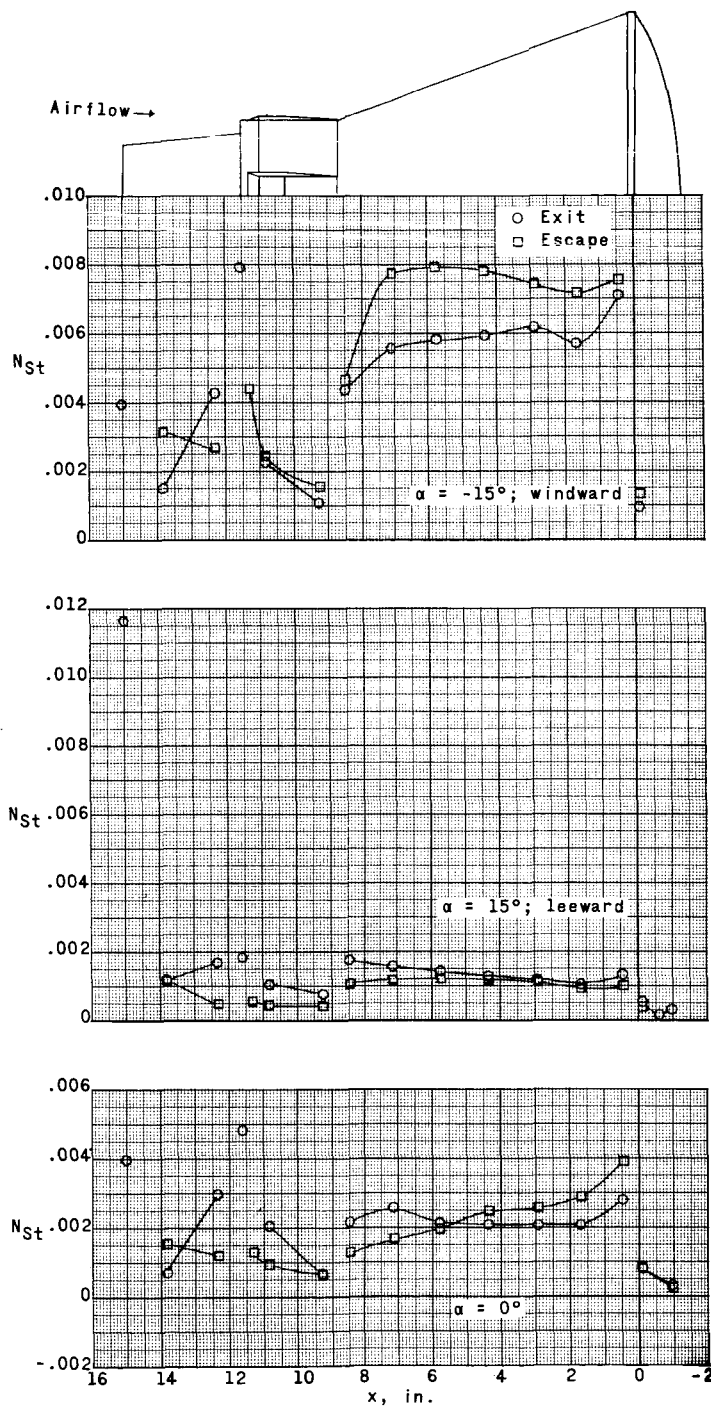
(a) $M = 3.50$.

Figure 10.- Effect of tower on Stanton number distribution at $\phi = 0^\circ$ and angles of attack of 0° and $\pm 15^\circ$.

DECLASSIFIED

77



(b) $M = 4.44$.

Figure 10.- Concluded.

L-1022